TAP2 - PAT2

PROGRAMME TO STIMULATE
KNOWLEDGE TRANSFER
IN AREAS OF STRATEGIC IMPORTANCE

Innovative joining of critical aluminium structures with the friction stir welding technique

CASSTIR

W. VAN HAVER (BWI)
B. DE MEESTER (UCL)
A. GEURTEN (CEWAC)
J. DEFRANCQ (UGENT)

STANDARDISATION

TELECOMMUNICATIONS

SPACE SECTOR

CLEAN TECHNOLOGIES

NEW MATERIALS

.be

PROGRAMME TO STIMULATE KNOWLEDGE TRANSFER IN AREAS OF STRATEGIC IMPORTANCE

TAP2

FINAL REPORT

INNOVATIVE JOINING OF CRITICAL ALUMINIUM STRUCTURES WITH THE FRICTION STIR WELDING TECHNIQUE

CASSTIR

P2/00/02

Promoters

Wim Van Haver
Belgian Welding Institute (BWI)
Sint-Pietersnieuwstraat 41, B-9000 Ghent

Bruno de Meester
Université catholique de Louvain (UCL)
Place de l'Université 1, B-1348 Louvain-La-Neuve

Alban Geurten
Centre d'études wallon de l'assemblage et du contrôle des matériaux (CEWAC)
Rue Bois St. Jean 8, B-4102 Ougrée-Seraing

Jacques Defrancq
Ghent University (UGent)
Sint-Pietersnieuwstraat 41, B-9000 Ghent

Authors

Wim Van Haver (BWI)
Bruno de Meester (UCL)
Alban Geurten (CEWAC)
Jacques Defrancq (UGent)

D/2010/1191/13
Published in 2010 by the Belgian Science Policy
Avenue Louise 231
Louizalaan 231
B-1050 Brussels
Belgium
Tel: +32 (0)2 238 34 11 – Fax: +32 (0)2 230 59 12
http://www.belspo.be

Contact person: *Anna Calderone*
Secretariat: +32 (0)2 238 34 80

W. Van Haver, B. de Meester, A. Geurten, J. Defrancq, ***Innovative joining of critical aluminium structures with the friction stir welding technique - CASSTIR***, Final Report, Belgian Science Policy (Programme to stimulate knowledge transfer in areas of strategic importance – TAP2), Brussels, 2010, 110 p.

TABLE OF CONTENTS

1 RESUME

A. Contexte

Le soudage est généralement considéré comme une étape critique majeure dans la production d'une structure métallique. La rentabilité doit être associée à des propriétés optimales d'assemblage. En outre, et à juste titre, une attention de plus en plus grande est accordée à l'impact environnemental des procédés de soudage.
Le **soudage par friction-malaxage** ("Friction stir welding" - FSW), inventé et breveté par "The Welding Institute" (Royaume-Uni) au début des années 1990 [1], est une technique d'assemblage qui fournit une solution à ces préoccupations, parfaitement adaptée pour le soudage des alliages d'aluminium. Cette méthode d'assemblage a déjà trouvé de nombreuses applications à l'étranger et a démontré ses capacités dans des domaines parfois très pointus, tels que l'aérospatiale et l'aviation, les domaines du transport, le secteur nucléaire et l'industrie automobile.
A travers le monde, beaucoup de recherches sont menées sur cette technique d'assemblage très prometteuse. Cependant, la quantité de données expérimentales disponibles en termes de paramètres de soudage pour la réalisation de véritables applications est relativement limitée par rapport à l'énorme quantité de publications sur le FSW à l'échelle expérimentale. De plus, seul un nombre limité de publications de soudage par friction-malaxage est disponible au sujet de l'analyse des coûts, des études sur l'environnement et de la comparaison avec d'autres techniques d'assemblage pour des applications réelles. En outre, il faut tenir compte du fait que les grandes entreprises internationales disposent généralement de fonds suffisants pour mener des recherches confidentielles et des travaux de développement, contrairement à beaucoup d'entreprises belges.
En raison de l'investissement relativement important et des coûts de licence, un seul fabricant belge a investi dans cette technique à ce jour. En Belgique, plus de 440 entreprises sont directement liées au traitement de l'aluminium, correspondant à un revenu annuel total de 20 milliards € et plus de 15.000 emplois. Il est essentiel que le FSW puisse s'introduire plus encore dans ces sociétés: il existe de nombreuses applications dans cette branche industrielle qui s'avèrent prometteuses pour souder à l'aide du FSW. Il s'agit entre autres : des pièces de suspension de véhicule, des structures d'ailes pour l'aviation, de structures pour les wagons de chemin de fer, des soudures longitudinales de tubes pour les industries chimiques. Le projet de 3 ans CASSTIR (débuté fin 2006), financé par la Politique scientifique fédérale, est une étroite collaboration entre l'IBS, UCL, CEWAC et UGent. Le projet visait à stimuler et à introduire la technique innovante par FSW appliquée aux alliages d'aluminium en Belgique, mais aussi à obtenir une connaissance approfondie de ce procédé de soudage par l'étude des caractéristiques des joints de friction-malaxage, et ce dans les moindres détails.

B. Objectifs

Le projet CASSTIR avait le but de renforcer le potentiel scientifique et technique des entreprises belges actives dans le domaine de l'aluminium, ce qui leur permet de faire face à la concurrence internationale avec une compétitivité accrue. Les objectifs principaux étaient les suivants:

- Indication des possibilités du procédé, mais aussi de ses limites;
- Démonstration et optimisation du FSW, appliqué aux alliages d'aluminium, qui sont pertinentes pour les sociétés participantes;
- Caractérisation détaillée des soudures par friction-malaxage;
- Recherche sur le transfert des paramètres de soudage d'une machine de soudage par friction-malaxage à une autre;
- Réalisation de joints soudés préindustriels de grande longueur, soumis à des essais mécaniques, de corrosion et de fatigue pertinents;
- Simulation numérique du FSW;
- Comparaison de la technique FSW et de la technique d'assemblage actuellement utilisée, tant en terme de faisabilité économique qu'en terme d'impact environnemental;
- Participation à l'élaboration de règles de bonnes pratiques et de lignes directrices, sur base des principaux résultats expérimentaux obtenus, pour les normes FSW en cours d'élaboration et/ou en création;
- Diffusion des résultats vers un public plus large (publications, présentations, newsletters, pages Web, organisation de workshop).

C. Conclusions

Dans la première phase du projet, trois applications à la fois techniquement pointues et pertinentes d'un point de vue industriel ont été sélectionnées pour être étudiées dans le projet CASSTIR, sous l'impulsion du Comité de Suivi CASSTIR:

- Application 1: FSW de profilés extrudés creux en 6082-T6 pour le transport;
- Application 2: soudage par recouvrement par friction-malaxage sur tôles en 2124 pour le secteur aérospatial;
- Application 3: soudage bout à bout par friction-malaxage de tôles minces en 5754-H111 pour l'aérospatiale et l'automobile.

Ces applications représentent un large spectre en termes de géométrie d'assemblage, d'épaisseur de matériau de base et de composition de l'alliage.

L'**application 1** concernait l'assemblage bout à bout de profils creux rectangulaires relativement peu compliqués. Après l'optimisation des paramètres initiaux sur profil plat, le soudage par friction-malaxage a été appliqué au profil creux avec une épaisseur de paroi verticale (qui agit comme un support reprenant les efforts générés par le FSW) de plus en plus petite, en s'efforçant de trouver un optimum entre la soudabilité par friction-malaxage, la facilité d'extrusion de la matière première et la limitation en poids. Cela a finalement abouti à la réalisation de profils d'extrusion soudés par friction-malaxage de 4 m de longueur, avec une épaisseur de paroi verticale sensiblement réduite et une vitesse de soudage de 2 m/min. Le soudage par friction-malaxage peut être appliqué soit en contrôle de position soit en mode de contrôle de force. Pour la réalisation de joints soudés de grande longueur, où la variation d'épaisseur et de hauteur le long du joint soudé devient possible, seul le FSW piloté en force a abouti à des soudures sans défaut; par conséquent c'est l'approche privilégiée pour ce type d'application. Des soudures optimisées de soudage en friction-malaxage de l'application 1 ont été soumises à des procédures d'essai élaborées par l'IBS et UGent, y compris les essais dynamiques de pliage sur quatre points et les essais de corrosion sous atmosphère saline. Le FSW a été comparé au soudage laser hybride (HLW) en termes de coût et de consommation d'énergie.

Une étude approfondie a été consacrée à l'optimisation de l'utilisation de matière pour la production de pièces aéronautiques fortement usinées dans un alliage d'aluminium de haute résistance non soudable par fusion (**application 2**). Le but de cette étude était de <u>souder</u> à deux reprises des plats dans une configuration par recouvrement sur une embase épaisse plutôt que de l'<u>usiner</u> hors masse, ce qui réduirait les pertes en matière due à l'usinage de 40 à 50%. Par conséquent, dans ce cas, le FSW a été utilisé en tant que technique alternative et complémentaire à l'usinage – une approche encore peu connue et peu documentée. Le défi principal de cette recherche, pour réaliser des soudures sans défauts avec une productivité raisonnable, était de trouver un optimum entre l'état thermique initial du matériau et les paramètres de soudage par friction-malaxage incluant la géométrie d'outil et le traitement thermique après soudage. Les pièces résultantes ont été soumises à des essais métallographiques, de micro dureté, des essais mécaniques de la rupture, et des essais de corrosion.

L'**application 3** concernait le soudage par friction-malaxage de tôles minces (< 1 mm d'épaisseur). C'est un sujet qui est toujours en phase de développement au niveau international. Au sein de CASSTIR, des joints de bonne qualité ont été produits avec le FSW à une vitesse acceptable de soudure (jusqu'à 1 m/min) en employant des outils de géométries "non conventionnelles". Des phénomènes qui ne sont pas importants pour le soudage d'alliages épais, tels que la perte d'épaisseur due au passage de l'outil sous l'effort de forgeage, peuvent avoir un impact significatif sur les propriétés mécaniques de matériau de faible épaisseur. En plus du FSW, des processus par fusion conventionnels (TIG et MIG) et d'autres plus avancés (laser LBW et soudage MIG CMT) ont été appliqués, ce qui a permis de comparer tous les processus en termes d'économie et d'efficacité énergétique.

Le projet CASSTIR a permis au partenaire de recherche UCL d'acquérir encore plus d'expérience dans les mesures de contraintes résiduelles au moyen de la méthode "crack compliance", une technique relativement rapide et économe comparé à d'autres méthodes. Cette technique a été appliquée aux soudures choisies - réalisées aussi bien par FSW que par les méthodes alternatives citées ci-dessus – pour les applications 1 et 3.

Le sous-traitant CENAERO a développé des modèles des assemblages par friction-malaxage pour les applications 1 et 2, qui ont été validés par des résultats expérimentaux tels que des mesures de la température. De manière générale, les résultats expérimentaux et la simulation ont montré une bonne corrélation, ce qui indique que la tâche très délicate de modéliser le processus de FSW est aujourd'hui de mieux en mieux connue. L'intérêt spécifique de la modélisation est de prévoir des paramètres optimaux pour le soudage pour une application donnée, plutôt que de se baser sur l'optimisation de paramètres de soudure par essai et erreur.

La comparaison économique du FSW avec d'autres procédés de soudage, effectuée pour les applications 1 et 3, a montré que le FSW peut être très rentable, bien qu'un coût important de licence soit associé au procédé. Cependant, il est clair que le FSW est particulièrement intéressant lorsque des joints de haute qualité et avec un bon aspect visuel sont exigés, pour des produits réalisés en grandes séries et/ou des longueurs de soudure importantes. Chaque procédé de soudage a son propre domaine d'application, et cela vaut certainement aussi pour la technique de soudage par friction-malaxage. Par exemple, le FSW appliqué à l'application 3 a donné de bons résultats en termes de propriétés dans le joint soudé - cependant, comme l'alliage 5754 a une bonne soudabilité par fusion, d'autres procédés de soudage peuvent être considérés comme plus rentables pour l'application donnée. D'autre part, cette recherche a également montré qu'une fraiseuse conventionnelle adaptée pour le FSW peut effectuer avec succès le soudage des alliages d'aluminium (qui peuvent ne pas être soudables par fusion) pour des épaisseurs en-dessous de 5 millimètres. Basé sur ce rapport, on peut déclarer que le FSW est une technologie d'assemblage sûre et favorable à l'environnement: il n'y a pas besoin de produits chimiques, de gaz de protection ou d'autres consommables, et le procédé ne génère pas de rayonnement UV, de projections ni de fumée de soudage. De plus, les courants électriques utilisés et les champs magnétiques en résultant sont bien plus faibles en comparaison aux procédés conventionnels. En outre, le procédé FSW offre un haut rendement énergétique, pour autant que la machine de FSW soit bien dimensionnée pour l'application en question.

D. Apport du projet dans un contexte d'appui scientifique au transfert des connaissances et à l'innovation

Ce projet, coordonné par l'Institut Belge de la Soudure, fut une réussite grâce à la combinaison du savoir-faire et de l'équipement expérimental des différents partenaires de recherches: soudage par FSW des alliages d'aluminium par UCL et CEWAC, métallurgie du soudage et caractérisation par l'IBS, propriétés de corrosion par UGent et modélisation par le sous-traitant CENAERO. Il est clair que la technique de soudage par friction-malaxage est fortement innovante, étant donné ses caractéristiques uniques, et un intérêt significatif dans cette technologie est bien présent en Belgique. Ceci se révèle par la participation très active du Comité de Suivi de CASSTIR composé de 17 membres différents (membres industriels, représentants d'établissements publics, d'associations et de centres de recherches).
Les applications choisies permettaient de démontrer entièrement les possibilités de la technique dans les secteurs qui parfois ont été à peine documentés auparavant. Ceci a permis aux partenaires de recherches d'entreprendre un grand nombre d'actions de valorisation, allant de la vulgarisation de présentations et d'articles, jusqu'à la contribution à des congrès et à des journaux renommés au niveau international.
Il est clair que l'innovation est le maître mot pour des compagnies dans le secteur métallurgique afin de maintenir voire d'augmenter plus encore leurs activités en Belgique. Les avantages offerts par le soudage en friction-malaxage convaincront certainement de nombreuses compagnies orientées vers l'innovation à investir dans les cinq prochaines années dans le soudage par FSW. Une forte croissance est particulièrement prévue à partir de 2014, quand le deuxième brevet de TWI expirera. Dans le cadre de la mise en application de la technique dans la production, ces compagnies peuvent compter sur l'expertise recueillie au sein du projet CASSTIR par les partenaires de recherche: même si un nombre limité d'applications a été étudié au sein de CASSTIR, les résultats de ce projet peuvent être extrapolés à d'autres produits, et la plupart des directives de bonnes pratiques qui peuvent être dérivées implicitement de la recherche restent valides pour d'autres applications.
En attendant, les partenaires de recherche tâchent de continuer à développer leur compétence dans le domaine du soudage par friction-malaxage (entre autres le micro-soudage par FSW, le soudage FSW par points et le soudage FSW des aciers) à travers des projets communs pour l'industrie et des projets de recherche publics.

E. Mots-clés

Assemblage, Soudage, Soudage à l'état solide, Soudage par friction-malaxage, Alliages non- ferreux, Aluminium, Alliage d'aluminium, Technologie verte, Analyse économique.

2 SAMENVATTING

A. Context

Lassen wordt algemeen erkend als één van de meest kritische stappen in het productieproces van een metalen structuur. Rentabiliteit dient steeds gekoppeld te worden aan optimale laseigenschappen. Verder gaat er, met recht en reden, steeds meer aandacht uit naar de milieuvriendelijkheid van lasprocessen.

Friction stir welding (FSW – ook nog soms aangeduid als "wrijvingsroerlassen"), begin jaren 1990 uitgevonden en gepatenteerd door The Welding Institute (UK) [1], is een verbindingstechniek die een oplossing biedt aan deze bekommernissen – bovendien is FSW perfect geschikt voor het lassen van aluminiumlegeringen. Deze methode kent reeds talrijke toepassingen in het buitenland, en wordt in soms zeer kritische domeinen toegepast, zoals lucht- en ruimtevaart, massatransport, de nucleaire sector en de automobielindustrie.

Wereldwijd wordt op grote schaal onderzoek gevoerd naar deze zeer veelbelovende verbindingstechniek. Desalniettemin is er slechts een beperkte hoeveelheid experimentele gegevens beschikbaar inzake lasparameters voor de realisatie van echte toepassingen – dit in tegenstelling tot de gigantische hoeveelheid publicaties over FSW uitgevoerd in labo-omgeving. Verder worden in de gespecialiseerde literatuur terzake slechts uitzonderlijk gegevens verstrekt over kosten-baten analyses, milieustudies of vergelijking met alternatieve verbindingsmethodes voor concrete toepassingen. Er moet hierbij ook rekening gehouden worden met het feit dat grote internationale bedrijven voldoende middelen hebben voor onderzoek en ontwikkeling met vertrouwelijk karakter – dit in tegenstelling tot veel Belgische bedrijven.

Door de relatief hoge investerings- en licentiekosten beschikt op dit moment slechts één Belgisch bedrijf over deze techniek. In België zijn meer dan 440 bedrijven direct betrokken bij de verwerking van aluminium, wat een totale jaarlijkse omzet van 20 miljard euro en meer dan 15.000 arbeidsplaatsen vertegenwoordigt. Het is essentieel dat FSW verdere toepassing kent in deze bedrijven: er zijn talrijke toepassingen in deze industrietak waarvoor FSW zeker veelbelovend is, zoals ophangingsonderdelen voor voertuigen, vleugelstructuren voor de luchtvaart, panelen voor treinwagons, langslassen van buizen voor de chemische industrie…

Het driejarig project CASSTIR (dat eind 2006 werd opgestart), gesubsidieerd door het Federaal Wetenschapsbeleid, betreft een samenwerking tussen het BIL, UCL, CEWAC en UGent. Het project was erop gericht om in België het gebruik van de innovatieve FSW techniek toegepast op aluminiumlegeringen te stimuleren, alsook om diepgaande kennis te ontwikkelen door een gedetailleerde studie van de eigenschappen van friction stir gelaste verbindingen.

B. Doelstellingen

Project CASSTIR had als doel de mogelijkheden van Belgische aluminiumverwerkende bedrijven te versterken op wetenschappelijk en technisch vlak, wat hen toelaat om hun concurrentiepositie internationaal te versterken. De belangrijkste doelstellingen hiertoe waren:

- Aangeven van de mogelijkheden van het proces, alsook de beperkingen ervan;
- Demonstratie en optimalisatie van FSW toegepast op aluminiumlegeringen die direct relevant zijn voor de deelnemende bedrijven;
- Gedetailleerde karakterisatie van friction stir lassen;
- Onderzoek naar de overdraagbaarheid van lasparameters tussen friction stir lasmachines;
- Uitvoeren van grootschalige prototypelassen, die onderworpen worden aan relevante mechanische, corrosie- en vermoeiingsproeven;
- Numerieke simulatie van FSW;
- Vergelijking van de FSW techniek met actueel gebruikte verbindingsprocessen op gebied van economische haalbaarheid en impact op het milieu;
- Formuleren van regels van de goede praktijk, die samen met de belangrijkste experimentele bevindingen worden verspreid naar relevante FSW normen die onder voorbereiding zijn of nog moeten opgestart worden;
- Verspreiding van de resultaten naar de grote doelgroep (door middel van publicaties, presentaties, nieuwsbrieven, organisatie van een workshop).

C. Besluiten

In the beginstadium van het project werden drie technisch uitdagende en industrieel relevante toepassingen ter studie binnen project CASSTIR gekozen, op aangeven het CASSTIR Opvolgingscomité:

- Toepassing 1: friction stir stomplassen van 6082-T6 holle profielen voor de transportsector;
- Toepassing 2: friction stir overlaplassen van 2124 gewalste plaat voor de luchtvaart;
- Toepassing 3: friction stir stomplassen van dunne 5754-H111 plaat voor de luchtvaart en automobielsector.

Deze toepassingen omvatten een breed spectrum inzake lasgeometrie, basismateriaaldikte en legeringssamenstelling.

Toepassing 1 betrof het stomplassen van relatief eenvoudige, rechthoekige holle extrusieprofielen. Na de aftastende parameteroptimalisatie op vlakke profielen werd FSW toegepast op holle profielen met steeds verder verdunde verticale wanddikte (die als steun dient voor de hoge drukkracht tijdens het proces), teneinde een optimum te vinden tussen friction stir lasbaarheid, extrudeerbaarheid van het basismateriaal en gewichtsbeperking. Dit resulteerde uiteindelijk in de realisatie van 4 meter lange friction stir gelaste extrusieprofielen met significant gereduceerde verticale wanddikte, gelast aan 2 m/min. FSW kan ofwel verplaatsingsgestuurd, ofwel krachtgestuurd uitgevoerd worden. Voor de realisatie van grote laslengtes, waarbij dikte- of hoogtevariatie langsheen de las mogelijk wordt, bleek enkel krachtgestuurd FSW foutvrije lassen op te leveren – dit is dus de te verkiezen aanpak voor dit type toepassing. Geoptimaliseerde friction stir lassen van toepassing 1 werden onderworpen aan beproevingsprocedures ontwikkeld door het BIL en UGent, zoals dynamische vierpuntsbuiging en dooizoutcorrosieproeven. FSW werd vergeleken met het hybride laserlassen inzake kost en energieverbruik.

Een uitgebreide studie werd gewijd aan de optimalisatie van het materiaalgebruik voor de productie van diepgemachineerde luchtvaartonderdelen in een niet-smeltlasbare aluminiumlegering (**toepassing 2**). Het doel van deze studie betrof het oplassen van flenzen in twee opeenvolgende laspassen op een dikke basisplaat, als alternatief voor het machineren van deze flenzen – dit zou materiaalverliezen door machineren verminderen met 40-50%. In dit geval wordt FSW dus gebruikt als een "neat-net shape" proces – een aanpak die tot dusver nog relatief onbekend is en waarover weinig gepubliceerd werd. De belangrijkste uitdaging bij dit onderzoek om foutvrije lassen te verkrijgen met aanvaardbare productiviteit bestond erin om een optimum te vinden tussen de uitgangstoestand van het basismateriaal, de FSW parameters (met inbegrip van toolgeometrie), en de warmtebehandeling na lassen. De resulterende flenzen werden onderworpen aan metallografie, microhardheids-onderzoek, breukmechanische beproeving en corrosieproeven.

Toepassing 3 betrof FSW van dunne (< 1 mm dikke) plaat. Dit is een onderwerp dat zich internationaal nog in de ontwikkelingsfase bevindt. Binnen CASSTIR konden, met behulp van FSW, kwalitatieve lasverbindingen worden geproduceerd met een aanvaardbare lassnelheid (1 m/min), gebruik makend van "niet-conventionele" toolgeometrieën. Er werd vastgesteld dat fenomenen die bij legeringen met hogere dikte niet belangrijk zijn, zoals lokale vermindering van de sectie door de indruk van de tool, een significante invloed kunnen hebben op de mechanische eigenschappen van lagere materiaaldiktes. Naast FSW werden ook conventionele (TIG, MIG) en meer geavanceerde (laserlassen, Cold Metal Transfer) smeltlasprocessen toegepast, wat toeliet om alle processen onderling te vergelijken op economisch vlak en op gebied van energetisch rendement.

Project CASSTIR liet de onderzoekspartner UCL toe om zich te bekwamen inzake het meten van restspanningen met behulp van de "crack compliance" methode, een relatief vlugge en goedkope techniek in vergelijking met andere methodes. Deze techniek werd toegepast op geselecteerde lassen – zowel gerealiseerd met FSW als met andere lasprocessen – van toepassingen 1 en 3.

De onderaannemer CENAERO ontwikkelde friction stir modellen voor de toepassingen 1 en 2, die gevalideerd werden tegen experimentele resultaten zoals temperatuursmetingen. Over het algemeen werd een goede overeenstemming gevonden tussen de experimentele gegevens en de simulaties, wat aangeeft dat de zeer uitdagende taak (die het modelleren van FSW is) in de juiste richting evolueert. Deze specifieke interesse in modelleren bestaat erin om optimale lasparameters voor een gegeven toepassing te voorspellen, eerder dan deze door trial-and-error te bepalen.
De vergelijking op economisch vlak van FSW met andere lasprocessen, uitgevoerd voor toepassingen 1 en 3, toonde aan dat FSW zeer kostenefficiënt kan zijn, zelfs al gaat de toepassing van het proces gepaard met een aanzienlijke licentiekost. Het is echter duidelijk dat FSW vooral interessant is wanneer lassen met <u>hoge kwaliteit</u> en <u>goed visueel aspect</u> worden vereist, voor producten die <u>aanzienlijke seriegrootte</u> en/of <u>grote laslengtes</u> gemeenschappelijk hebben. Elk lasproces heeft een eigen toepassingsdomein, en dit is zeker ook geldig voor de FSW techniek. Zo leverde bijvoorbeeld friction stir welding bij toepassing 3 goede resultaten op het vlak van mechanische eigenschappen – echter, aangezien legering 5754 een goede smeltlasbaarheid bezit, kunnen andere lasprocessen meer kostenefficiënt geacht worden voor de toepassing in kwestie. Anderzijds heeft dit onderzoek ook aangetoond dat een conventionele freesbank, aangepast voor FSW, succesvol (al dan niet smeltlasbare) aluminiumlegeringen met dikte kleiner dan 5 mm kan friction stir lassen. Op basis van de discussie opgenomen in het rapport, is het gerechtvaardigd te stellen dat FSW een veilige en milieuvriendelijke verbindingstechniek betreft: er is geen nood aan chemische reinigingsmiddelen, beschermgassen of andere verbruiksmiddelen, het proces gaat niet gepaard met UV straling, lasspatten, lasrook, hoge elektrische stromen of hoge elektromagnetische velden. Verder biedt het proces een hoog energetisch rendement wanneer een FSW machine wordt gebruikt die aangepast is aan de toepassing in kwestie.

D. Bijdrage van het project in een context van wetenschappelijke ondersteuning aan transfer van kennis en innovatie

Dit project, gecoördineerd door het BIL, was succesvol door de bundeling van kennis en experimentele apparatuur beschikbaar bij de verschillende onderzoekspartners, namelijk op het vlak van FSW van aluminiumlegeringen (UCL en CEWAC), lasmetallurgie en –karakterisatie (BIL), corrosie-eigenschappen (UGent) en modelleren (de onderaannemer CENAERO). Er is duidelijk gebleken dat de FSW techniek hoogst innovatief mag genoemd worden, gezien de unieke eigenschappen ervan, en deze techniek mag in België op een belangrijke interesse rekenen. Dit wordt weerspiegeld door de actieve betrokkenheid van het CASSTIR

Opvolgingscomité dat bestond uit 17 verschillende organisaties (industriële leden, vertegenwoordigers van publieke instellingen, koepelorganisaties en onderzoekscentra).
De geselecteerde toepassingen lieten toe ten volle de mogelijkheden van de techniek aan te tonen in gebieden die tot dusver soms amper gedocumenteerd waren. Dit liet de onderzoekspartners toe om een groot aantal valorisatie-acties te ondernemen, gaande van populariserende presentaties en artikels, tot bijdragen aan internationaal vermaarde congressen en tijdschriften.
Het is zonder meer duidelijk dat innovatie het sleutelwoord vormt voor bedrijven uit de metaalverwerkende sector om hun activiteiten in België te behouden, laat staan uit te breiden. De voordelen geboden door FSW zullen zeker meerdere innovatiegerichte bedrijven in de komende vijf jaar overtuigen om in deze techniek te investeren. Een grote groei wordt vooral verwacht vanaf 2014, wanneer het tweede TWI patent verstrijkt. Bij de concrete toepassing van de techniek in productie kunnen deze bedrijven rekenen op de expertise van de onderzoekspartners opgebouwd binnen CASSTIR: ook al werd een beperkt aantal toepassingen bestudeerd binnen CASSTIR, toch kunnen de resultaten van het project worden geëxtrapoleerd naar andere producten, en de meeste richtlijnen voor goede praktijk die impliciet uit het onderzoek kunnen afgeleid worden blijven geldig voor andere toepassingen.
In de tussentijd streven de onderzoekspartners ernaar hun competentie op het vlak van FSW uit te breiden (bvb. micro-FSW, friction stir puntlassen, FSW van staal) door middel van industriële of door de overheden gesubsidieerde onderzoeksprojecten.

E. Trefwoorden

Verbinden, Lassen, Vaste-toestandslassen, Wrijvingsroerlassen, Friction stir welding, Non-ferrolegeringen, Aluminium, Aluminiumlegeringen, Groene technologie, Kosten-baten analyse.

3 SUMMARY

A. Context

Welding is generally recognised as a major critical step in the production of a metallic structure. Profitability needs to be coupled to optimum joint properties. Moreover, with good reason, larger attention goes out to the environmental soundness of the welding processes.

Friction stir welding (FSW), invented and patented by The Welding Institute (UK) in the early 1990's [1], is a joining technique with provides a solution to these concerns, and it is perfectly suited for welding of aluminium alloys. This joining method has already found numerous applications abroad, and has demonstrated its capabilities in sometimes highly critical areas, such as aerospace and aviation, mass transportation, the nuclear sector and the automotive industry.

Worldwide, a great deal of research is conducted on this very promising joining technique. However, the amount of available experimental data in terms of welding parameters for the realisation of <u>true applications</u> is relatively limited compared to the vast amount of publications about FSW on a laboratory scale. Furthermore, only a limited amount of friction stir welding publications is available about cost analysis, environmental studies and comparison with other joining techniques for actual applications. Also, one must take into account that large international companies have sufficient funds to conduct <u>confidential</u> research and development work, contrary to many Belgian companies.

Due to the relatively large investment and license costs, only one Belgian manufacturer has invested in this technique up to this point. In Belgium, more than 440 companies are directly related to aluminium processing, corresponding with a total annual revenue of 20 billion € and more than 15.000 jobs. It is essential that FSW finds further entrance into these companies: there are numerous applications in this industry branch which are found at least promising for joining with FSW. These include, amongst others: vehicle suspension parts, wing structures for aviation, hulls for railway wagons, longitudinal welding of tubes for the chemical process industry…

The three-year project CASSTIR (started up at the end of 2006), funded by the Belgian Science Policy, is a collaboration between BWI, UCL, CEWAC and UGent. The project aimed at stimulating and introducing the innovative friction stir welding technique applied to aluminium alloys in Belgium, as well as obtaining a profound knowledge in this welding process by studying the friction stir joint characteristics into great detail.

B. Objectives

The aim of project CASSTIR was to strengthen the scientific and technical potential of Belgian aluminium-processing companies, which allows them to face the international concurrence with increased competitiveness. The main objectives to achieve this were the following:

- Indicating the capabilities of the process, but also its limitations;
- Demonstration and optimisation of FSW applied to aluminium alloys which are relevant to the participating companies;
- Detailed characterisation of friction stir welds;
- Investigation of the transferability of welding parameters from one friction stir welding machine to another;
- Performing large scale pre-industrial welds, which are subjected to the relevant mechanical, corrosion and fatigue testing;
- Numerical modelling of FSW;
- Comparing the FSW technique and the currently used joining technique, both in terms of economical feasibility as in terms of environmental impact;
- Drafting good practice rules and guidelines, which are disseminated together with the principal experimental findings to relevant FSW standards which are under preparation or that still need to be started up;
- Dissemination of the results towards a greater audience (publications, presentations, newsletters, webpages, organisation of a workshop).

C. Conclusions

In the first stage of the project, three technically challenging and industrially relevant applications were selected for study within project CASSTIR, based on input from the CASSTIR Follow-up Committee. These were the following:

- Application 1: friction stir butt welding of 6082-T6 hollow extrusion profiles for transportation;
- Application 2: friction stir overlap welding of 2124 rolled plate for aerospace;
- Application 3: friction stir butt welding of thin 5754-H111 sheet for aerospace and automotive.

These applications represent a broad spectrum in terms of joint geometry, base material thickness and alloy composition.

Application 1 concerned butt joining of relatively uncomplicated rectangular hollow profiles. After initial parameter optimisation on flat profile, friction stir welding was applied to the hollow profile with increasingly smaller vertical wall thickness (which acts as a support for the high downforce during FSW), striving to find an optimum between friction stir weldability, extrudability of the base material and weight limitation. This finally resulted in the realisation of 4 m long friction stir welded extrusion profiles with significantly reduced vertical wall thickness, produced at a welding speed of 2 m/min. Friction stir welding can be applied in either displacement control or force control mode. For the realisation of long weld lengths, where thickness or height variation along the weld joint becomes possible, only FSW in force control mode yielded defect-free welds, hence this is the preferred approach for this type of application. Optimised friction stir welds of application 1 were subjected to testing procedures developed by BWI and UGent, including dynamic four-point bend tests and de-icing salt corrosion tests. The FSW process was compared to hybrid laser welding (HLW) in terms of cost and energy consumption.

An elaborate study was dedicated to optimisation of material consumption for the production of deeply-machined aerospace parts in a non-fusion weldable high-strength aluminium alloy (**application 2**). The aim of this study was to weld flanges in an overlap configuration onto a thick base plate in two consecutive passes rather than to machine them, which would reduce material losses by machining by 40-50%. Hence, in this case FSW was used as a near-net shape processing technique – an approach which is still fairly unknown and undocumented. The main challenge in this investigation in order to achieve defect-free welds with reasonable productivity was to find an optimum between the initial base material temper, the friction stir welding parameters including tool geometry, and the post-weld heat treatment. The resulting flanges were subjected to metallography, microhardness testing, fracture mechanical testing and corrosion testing.

Application 3 concerned FSW of thin (< 1 mm thick) sheet. This is a topic which is internationally still in a development phase. Within CASSTIR, good quality joints were produced with FSW at an acceptable welding speed (up to 1 m/min) by using "non-conventional" tool geometries. It was found that phenomena which are not as important in high thickness alloys, such as thinning due to the tool imprint, may have a significant effect on the mechanical properties in lower thickness material. Besides FSW, also conventional (TIG, MIG) and more advanced (laser beam welding, Cold Metal Transfer) fusion welding processes were applied, which made it possible to compare all processes in terms of economy and energy efficiency.

Project CASSTIR allowed the research partner UCL to become experienced in the measurement of residual stresses by means of the crack compliance method, a relatively fast and cheap technique compared to other methods. This technique was applied to selected welds – both realised with FSW and alternative welding methods – from applications 1 and 3.

The subcontractor CENAERO developed friction stir welding models for applications 1 and 2, which were validated against experimental results such as temperature evolutions. Generally, good correlation was obtained between the experimental results and the simulations, which indicates that the very challenging task of modelling the FSW process is moving into the right direction. The specific interest in modelling is to predict optimum welding parameters for a given application, rather than basing the welding parameter optimisation on trial-and-error.

The economic comparison of FSW with other welding processes, carried out for applications 1 and 3, proved that FSW can be highly cost-effective, even though an important license cost is associated to the process. However, it is clear that FSW is especially interesting when joints with high quality and good visual aspect are demanded, for products which have large production series and/or large weld length in common. Every welding process has its own domain of application, and this is certainly also true for the friction stir welding technique. For instance, FSW applied to application 3 yielded good results in terms of weld properties – however, as alloy 5754 has good fusion weldability, other welding processes can be considered more cost-effective for the given application. On the other hand, this investigation has also proven that a conventional milling machine adapted for FSW can successfully friction stir weld aluminium alloys (which may not be fusion weldable) with thicknesses below 5 mm. Based on the discussion included in the report, it is justified to state that FSW corresponds to safe and environmental friendly joining technology: there is no need for chemical agents, shielding gases or other consumables, and the process does not involve UV radiation, spatter, weld fume, high electric current or electromagnetic fields. Furthermore, the process offers a high energy efficiency when applying a well-dimensioned FSW machine for the application in question.

D. Contribution of the project in a context of scientific support to transfer of knowledge and innovation

This project, coordinated by the Belgian Welding Institute, was successful by the combination of the know-how and experimental equipment of the different research partners, namely in terms of friction stir welding of aluminium alloys (UCL and CEWAC), welding metallurgy and characterisation (BWI), corrosion properties (UGent) and modelling (subcontractor CENAERO). It is clear that the friction stir welding technique is highly innovative, given its unique characteristics, and significant interest into this technology is present in Belgium. This is reflected by the very active involvement of the CASSTIR Follow-up Committee that consisted of 17 different organisations (industrial members, representatives from public institutions, associations and research centres).

Based on the input of the Follow-up Committee, very appealing applications were selected for the experimental work in CASSTIR, covering significantly different aluminium alloys, thicknesses and joint geometries, in order to fully demonstrate the capabilities of the technique in areas that were sometimes hardly documented previously. This allowed the research partners to undertake a large amount of valorisation actions, ranging from popularizing presentations and articles, to contributions to internationally renowned congresses and journals.

It is clear that innovation is the key word for companies in the metalworking sector in order to maintain, let alone expand their activities in Belgium. The benefits offered by friction stir welding will most certainly convince multiple innovation-minded companies within the next five years to invest in friction stir welding. A large growth is especially expected as from 2014, when the second TWI patent expires. In the course of implementing the technique in production, these companies can count on the expertise gathered within project CASSTIR by the research partners: even though a limited number of applications was studied within CASSTIR, the results of this project can be extrapolated to other products, and most of the good practice guidelines that can be derived implicitly from the research remain valid for other applications.

In the meantime, the research partners strive to continue to develop their competence in the field of friction stir welding (e.g. micro-friction stir welding, friction stir spot welding, friction stir welding of steels) through both projects for industry and publicly funded research projects.

E. Keywords

Joining, Welding, Solid-state welding, Friction stir welding, Non-ferrous alloys, Aluminium, Aluminium alloys, Green technology, Economical analysis.

1. INTRODUCTION

It should be noted that the items described below – intended to generate a better understanding of project CASSTIR to companies and institutions that weren't directly involved in the project – are treated into a much more detailed extent in the literature review that was prepared by the research partners within the framework of CASSTIR.

1.1. Aluminium alloys

Aluminium and its alloys belong to the light metals, given their approximate density of 2,70 kg/dm³. For comparison: steel has a density of typically 7,85 kg/dm³. Aluminium has the largest field of application of the light metals. In 2005, the worldwide annual production of aluminium was 31 Mt.

This is due to the versatility of this metal [2]-[5]:

- Aluminium is **ductile**; it can be hot rolled or cold rolled down to thicknesses of 6-7 µm (foil). It can be extruded down to wall thicknesses of 0,5 mm. It can also be pressed, drawn, forged, stamped or cast by traditional methods.
- Aluminium is **corrosion resistant**, and its surface can be further protected from corrosion by anodising, painting or lacquering.
- Aluminium can be **joined** by most well-known joining methods, including welding, brazing, soldering, gluing and riveting.
- The **tensile strength** of aluminium can be varied from 70 to 700 MPa, depending on the alloying elements added and the processing. Its ductility and strength can be altered during the working process to give the material the desired degree of strength. If aluminium is used in structural components that are subject to stress or bending however, it must be borne in mind that the metal's rigidity (modulus of elasticity) is <u>not</u> altered significantly by alloying or hardening. It will always remain about one-third that of steel (E_{Al} = 70 GPa, E_{Fe} = 210 GPa).
- Aluminium is **light-weight**. Used in vehicles, it reduces deadweight and energy consumption while increasing load capacity. Aluminium has only one-third the density of steel.
- Aluminium is a good **conductor of heat**. This property is exploited in products such as cooking utensils and heat-exchange systems.
- Aluminium is an excellent **conductor of electricity**: its thermal coefficient per weight unit is twice that of copper. This has made aluminium the most commonly used material in major power transmission lines.
- Aluminium **does not have a ductile-to-brittle transition temperature** (contrary to steels), which explains their use for cryogenic applications.

- Aluminium is **non-toxic, impervious and odourless**, which justifies its use in packaging for food and pharmaceuticals.
- Aluminium is **non-combustible** and practically **non-magnetic**.
- Aluminium is a **good reflector** of visible light as well as heat (applications: reflectors in light fittings, rescue blankets).
- Aluminium has an excellent **recyclability**; only 5% of the energy required for the primary production is needed to produce equally usable metal. Therefore, aluminium products also have a high scrap value.

Aluminium alloys can be subdivided in wrought alloys and cast alloys. All aluminium alloys under investigation with CASSTIR are wrought alloys (rolled or extruded) – see §2.1. Based on the presence or absence of certain alloying elements, the wrought aluminium alloys are subdivided into 8 series in total. Only the series directly relevant to the experimental work within CASSTIR are described very briefly in the paragraphs below, ranked in the order of the respective applications [6]-[8].

1.1.1. 6xxx series – alloy 6082-T6 (application 1)

The 6xxx series of alloys widely used in transport, engineering and architecture primarily contain magnesium (< 2%) and silicon (< 2%), which form a strengthening constituent, magnesium silicide (Mg_2Si). The application of fusion welding processes without the introduction of an appropriate filler metal often results in hot cracking (see §1.2). 6xxx series alloys generally have a good extrudability.

EN AW-6082 aluminium alloy, also indicated in the EN 573-3 standard by means of chemical symbols as EN AW-Al Si1MgMn, is a heat treatable wrought alloy, with Mg_2Si being the main precipitation hardening component. For the investigation of application 1, the alloy was delivered by Sapa RC Profiles as extrusion profiles in the T6-temper according to EN 515. This temper corresponds to a solution heat treatment followed by artificial ageing. The geometry of the profile, shown in Figure 9 on the left, shows that the horizontal part has a thickness of 4 mm, while the vertical is 6 mm. The chemical composition of the 6082 alloy in this investigation is shown in Table 1 (together with the EN 573-3 requirements for 6082 alloy), and the mechanical properties are given in Table 2 (compared with the EN 755-2 requirements for 6082-T6 extrusion profiles).

Table 1: Chemical composition of 6082 base material compared to EN 573-3

	Si	Fe	Cu	Mn	Mg	Cr	Zn	Ti	Other
EN 573-3	0,7-1,3	0,50 max.	0,10 max.	0,40-1,0	0,6-1,2	0,25 max.	0,20 max.	0,10 max.	0,15 max.
Certificate	1,02	0,24	0,03	0,50	0,63	0,02	0,01	0,02	/

Table 2: Mechanical properties of 6082-T6 base material compared to EN 755-2

	Yield strength $R_{p0,2}$ [MPa]	Tensile strength R_m [MPa]	Elongation A_{50} [%]
EN 755-2	≥ 240	≥ 295	≥ 6
Longitudinal	282 ± 3	309 ± 2	10,9 ± 0,1
Transverse	283 ± 4	312 ± 4	7,5 ± 0,4

1.1.2. 2xxx series – alloy 2124 (application 2)

The 2xxx series alloys primarily contain copper as alloying element, up to 7%. They are very strong in age hardened condition and are therefore used for structural purposes (mostly aerospace applications), but the additional strength achieved is at the detriment of their durability. Copper in aluminium alloys generally decreases the resistance to general corrosion and pitting. With proper heat-treatment, quenching, and ageing, these alloys can achieve moderately good resistance to stress-corrosion cracking (SCC) and other forms of intergranular corrosion (IGC). The resistance to general and pitting corrosion is strongly influenced by the copper content regardless of the thermal processing control. These alloys are significantly affected in heavily polluted industrial or marine environments. Therefore this group of alloys requires protection in aggressive environments. Moreover, the majority of 2xxx series alloys are considered unweldable by means of conventional fusion welding processes, due to a high tendency to hot cracking (see §1.2).

EN AW-2124 aluminium alloy is in the EN 573-3 standard also indicated by means of chemical symbols as EN AW-Al Cu4Mg1(A). It is a heat treatable wrought alloy, with Al_2CuMg as the main precipitation hardening component. 2124 alloy was delivered by Aleris Aluminum Koblenz GmbH as large rolled plates with a thickness of 44 mm (used as "base plate" – see Figure 25) and 26 mm (used for the build-up of "flanges" – Figure 25), in the T851 temper according to EN 515. Table 3 gives the chemical composition of the parent materials.

Table 3: Chemical composition of 26 and 44 mm 2124 material (base material certificate) compared to EN 573-3

	Si	Fe	Cu	Mn	Mg	Cr	Zn	Ti	Other
EN 573-3	0,20 max.	0,30 max.	3,8 - 4,9	0,30 - 0,9	1,2 - 1,8	0,10 max.	0,25 max.	0,15 max.	0,15 max.
Certificate 26 mm	0,03	0,07	4,00	0,56	1,28	0,00	0,01	0,02	0,02
Certificate 44 mm	0,03	0,07	4,11	0,61	1,28	0,00	0,02	0,03	0,02

The T851 temper designation applies to material which has been solution heat treated, stress relieved by stretching to a controlled amount (permanent set 1,5 to 3% for plate) and then artificially aged. Products receive no further straightening after stretching. 2124 alloy is mostly used in this temper, as it then possesses good toughness and strength and optimum machinability.

In a later stage of the project, the 2124-T851 was subjected to a T4 heat treatment, which corresponds to solution heat treating and water quenching (performed in accordance with the specifications in AMS 2772C), followed by natural ageing during at least 1 month. Tensile properties of both base plate and flange plate material in T851 and T4 material (performed according to EN 485-2) are given in Table 4. Clearly, the T4 heat treatment has a large influence in terms of yield strength and elongation after fracture; the tensile strength on the other hand is only marginally affected.

Table 4: Tensile test results of 2124-T851 and 2124-T4 parent material

	Yield strength $R_{p0,2}$ [MPa]	Tensile strength R_m [MPa]	Elongation A_{50} [%]
2124-T851 (26 mm, certificate)	449 ± 6	486 ± 5	11,2 ± 0,3
2124-T851 (26 mm, BWI test result)	454 ± 2	495 ± 1	12,8 ± 0,8
2124-T851 (44 mm, certificate)	448 ± 1	491 ± 1	10,8 ± 0,2
2124-T851 (44 mm, BWI test result)	450 ± 1	494 ± 2	10,6 ± 1,0
2124-T4 (26 mm, BWI test result)	291 ± 1	450 ± 1	28,5 ± 0,9
2124-T4 (44 mm, BWI test result)	306 ± 2	473 ± 2	24,5 ± 0,3

1.1.3. 5xxx series – alloy 5754-H111 (application 3)

The 5xxx series alloys primarily contain magnesium, up to 6%. Several of these alloys also contain manganese. Magnesium is a powerful solid solution strengthening element. The 5xxx series of alloys are the strongest non-heat treatable aluminium alloys, and can only be further strengthened by cold work. 5xxx series aluminium alloys are considered to have good weldability with conventional techniques. The magnesium additions generally improve the corrosion resistance of these alloys, especially in saltwater. The high-Mg alloys (3 to 6%) possess the highest strength and outstanding corrosion resistance in saltwater environments. The only drawback is that these can be susceptible to intergranular forms of corrosion, including exfoliation and SCC, due to the selective precipitation of Mg_5Al_8 along the grain boundaries. This can be avoided by using particular tempers and by limiting the maximum service temperature to 65°C. The 5xxx series have a better corrosion resistance than the 6xxx series. Unlike the 6xxx series, the 5xxx series can be used in marine conditions where total immersion in sea water is required.

EN AW-5754 aluminium alloy is a non-heat treatable wrought alloy, that can only be strengthened by cold deformation. Typical applications of this alloy are welded structures in nuclear, chemical and food industries, marine and offshore applications, vehicle bodywork and pressure vessels. The base material was supplied as 0,8 mm thick rolled sheet in H111 condition produced by the Aleris Aluminium Duffel. According to EN 515, H111 temper applies to alloys which are strain-hardened less than the amount required for a controlled H11 temper. It can therefore be stated that the amount of strain hardening in the base material is marginal compared to the O ("dead soft" or "fully annealed") condition. The chemical composition of EN AW-5754 alloy (also referred to as EN AW-Al Mg3) is shown in Table 5, and the base material tensile properties (measured transverse to the rolling direction) are given in .

Table 5: Base material chemical composition, compared with EN 573-3 specifications for EN AW-5754 alloy

	Si	Fe	Cu	Mn	Mg	Cr	Ti	Zn	Mn+Cr
EN 573-3	≤ 0,40	≤ 0,40	≤ 0,10	≤ 0,50	2,6 - 3,6	≤ 0,30	≤ 0,15	≤ 0,20	0,1 - 0,6
Base material	0,24	0,29	0,02	0,42	2,7	0,02	0,01	0,02	0,44

Table 6: Base material transverse tensile properties, compared with EN 485-2 specifications for EN AW-5754-O/H111 sheet with thickness over 0,5 mm up to 1,5 mm

	Yield strength at 0,2 %, $R_{p0,2}$ [MPa]	Ultimate tensile strength, R_m [MPa]	Elongation at fracture, A_{50} [%]
EN 485-2	≥ 80	190 - 240	≥ 14
Base material	118	228	21

1.2. Weldability of aluminium alloys

Before discussing the weldability of aluminium alloys, it is interesting to define "welding". Welding can be described as the joining of two components by a coalescence of the surfaces in contact with each other. This coalescence can be achieved by melting the two parts together – fusion welding – or by bringing the two parts together under pressure, perhaps with the application of heat, to form a metallic

bond across the interface. The latter is known as solid phase bonding; the friction stir welding process belongs to this category of welding processes (see §1.3).
Welding that involves the melting and fusion of the parent metals only is known as autogenous welding, but many processes involve the addition of a filler metal (also often addressed to as consumable, which is a more general term) which is introduced in the form of a wire or rod and melted into the joint. Together with the melted parent metal, this forms the weld metal. The use of filler metal is depending on the welding process (e.g. metal inert gas – MIG – welding cannot be executed without filler metal), the joint geometry and – especially true for aluminium alloys – metallurgical reasons (e.g. avoidance of hot cracking).

There is a multitude of possible welding processes for aluminium alloys, most of which are described publicly accessible on [9]. For structural applications, MIG and tungsten inert gas (TIG) welding are the most commonly used fusion welding techniques for aluminium and its alloys, although (hybrid) laser welding is also gaining importance.

The main potential welding problems with aluminium and its alloys are [10]-[11]:

- Weld metal **porosity** (see Figure 1, left). The main reason for weld metal porosity in aluminium alloys is hydrogen porosity, arising from hydrogen dissolved in the molten weld metal becoming trapped as it solidifies, thus forming bubbles in the solidified weld. Weld metal porosity can only occur either when the weld metal has been in fluid state (as in fusion welding processes), or when the base material itself contains porosity. As no fusion takes place in friction stir welding (hereafter "FSW"), porosity cannot occur and a different terminology is used for addressing "absence of material in the joint" (e.g. voids, tunnel defects...).
  Small pores only have limited influence on static strength, and, as they are generally globular, they are less detrimental for fatigue strength than cracks, inclusions or lack of fusion. Larger pores have an increasingly negative influence on fatigue strength. However, the pore distribution is also very important: a small amount of larger pores is less dangerous than linearly scattered small pores.
- **Lack of fusion** due to inappropriate execution of the weld. The oxide skin, always apparent on aluminium and its alloys, needs to be removed mechanically and/or chemically prior to fusion welding. Lack of fusion is generally detrimental for both static and fatigue strength.
- **Inclusions** of oxide or slag due to inappropriate weld seam preparation, excessive oxidation due to too slow welding speed, shielding gas turbulence or dirty seam edges. Other possibilities are tungsten inclusions with the TIG process, and flux residues in e.g. shielded metal arc welding or oxyfuel welding (the latter are not recommended for Al alloys). Inclusions are especially

detrimental for the dynamic strength of the structure, as they can easily act as fatigue crack initiation sites.

- The most feared welding defect in aluminium alloys is perhaps the occurrence of **hot cracking** (see Figure 1, right). This type of cracking develops by the occurrence of shrinkage stresses at the moment (in a certain temperature interval) where the weld metal or the heat affected zone (HAZ) possess a low strength and/or very limited ductility. Hot cracking can occur in the weld metal itself or in the HAZ.

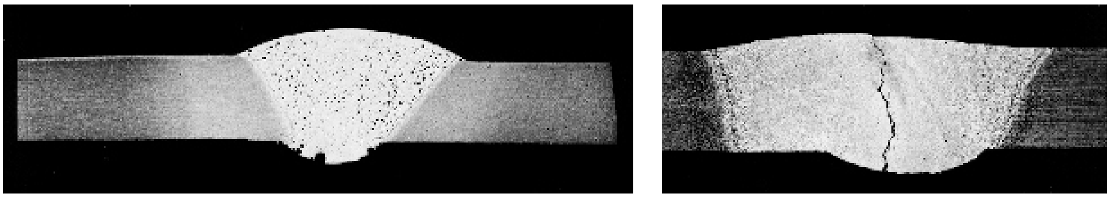

Figure 1: Porosity (left) and hot cracking (right) in aluminium welds [12].

  - Hot cracking in the HAZ can be avoided by using filler material with a solidus temperature lower than that of the base material (in practice: by choosing a filler material with higher alloying content). This way, the formation of tensile stresses in the HAZ caused by shrinkage of the weld metal is moved to the time where the low-melting phases in the HAZ have already solidified.
  - Hot cracks in the weld metal itself can be avoided by an appropriate selection of the composition of the filler metal. The resulting composition of the weld metal (parent metal diluted with filler metal) should be such that it falls outside the range of maximum hot crack sensitivity.
  - In some alloys (2xxx series, Cu-containing 7xxx series), which are tragically in many cases also the strongest aluminium alloys available, hot cracking can hardly be prevented in production by fusion welding due to the unavailability of suitable filler material which guarantees avoidance of hot cracking in combination with sufficient weld metal strength. Therefore, these alloys were mostly joined by riveting before friction stir welding became established.
  - Hot cracks generally have a very significant influence on both static and dynamic strength of welded structures. The attention should be drawn to the fact that there are no reported cases of hot cracking in optimised aluminium friction stir welds, which is not surprising given the fact that no liquid phase should be present during this process.
- **Reduction in mechanical properties** in the HAZ and the weld metal compared to the base material. In practice, the mechanical properties of the weld metal can be optimised by appropriate filler metal selection. The degree of softening in the HAZ on the other hand is depending on the heat input of the welding process. In the case of precipitation hardenable alloys, performing a suitable post-weld heat

treatment can improve the mechanical properties of the weld zone. The degree of softening can be very significant. This also has an important influence on the dynamic behaviour of welded structures.

As will be indicated in §1.3, there are no problems with the occurrence of hydrogen porosity or hot cracking when friction stir welding aluminium alloys, due to the fact that it is a solid-state joining process. However, this does not mean that defects aren't possible at all in friction stir welds: for each alloy and thickness, parameter windows which guarantee good joint properties are to be determined experimentally. Outside these parameter windows, specific defects may occur [13].

1.3. The friction stir welding technique

In the ISO 9000 series, welding is considered a “special process”, which means that even if 100% non-destructive testing is possible for the welded product, the quality is still not guaranteed. Generally, welding is recognised as one of the most critical steps in the production process of a metallic structure. For demanding structures, economic factors need to be combined with optimum joint properties, both in terms of mechanical, fatigue and corrosion properties. With good reason, in the last years greater attention goes out to the environmental friendliness of welding processes. **Friction stir welding (FSW)**, invented and patented by The Welding Institute (UK) in the early 1990's [1], is a joining technique which provides a solution to all these concerns, especially when applied to aluminium alloys. The basic principle of FSW is to soften the material by frictional heat generated between the material surfaces and a rotating tool (Figure 2).

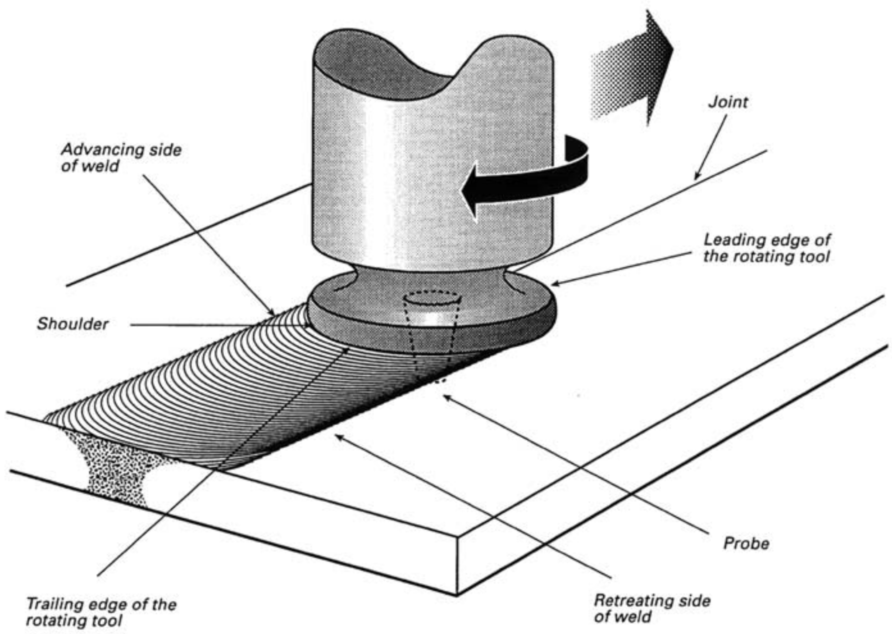

Figure 2: Schematic representation of the friction stir welding process [14].

In the classic butt joint set-up, the components to be joined are rigidly clamped on a backing plate. A rotating tool, consisting of a profiled pin and a shoulder, is forced down into the material until the shoulder meets the surface of the workpieces. The material in the close surrounding of the tool is thereby frictionally heated to temperatures where it is easily plasticised. As the tool moves forward, material is stirred from the leading to the trailing edge of the pin. Behind the pin, the solid state joint is formed. A distinction is made between the advancing side of the weld (AS – the side where the tool rotation direction is the same as the welding direction), and the retreating side (RS – the side where the tool rotation direction is opposite to the welding direction), as also indicated in Figure 2. In the following, the AS is displayed on the left in microscopic images and profiles (unless indicated otherwise).

A friction stir welded joint consists of various zones involving different microstructures and mechanical properties, as shown in Figure 3 [15]. The heat affected zone is the most distant from the joint line and is not deformed, but the dissolution and coarsening of precipitates (precipitation hardenable alloys) or dislocation density reduction (cold worked alloys) due to the thermal cycles influence the mechanical properties of this zone. The thermo-mechanically affected zone (TMAZ) is not only heated but also plastically deformed, while the nugget is highly deformed. Contrarily to the TMAZ, the nugget has undergone dynamic recrystallisation.

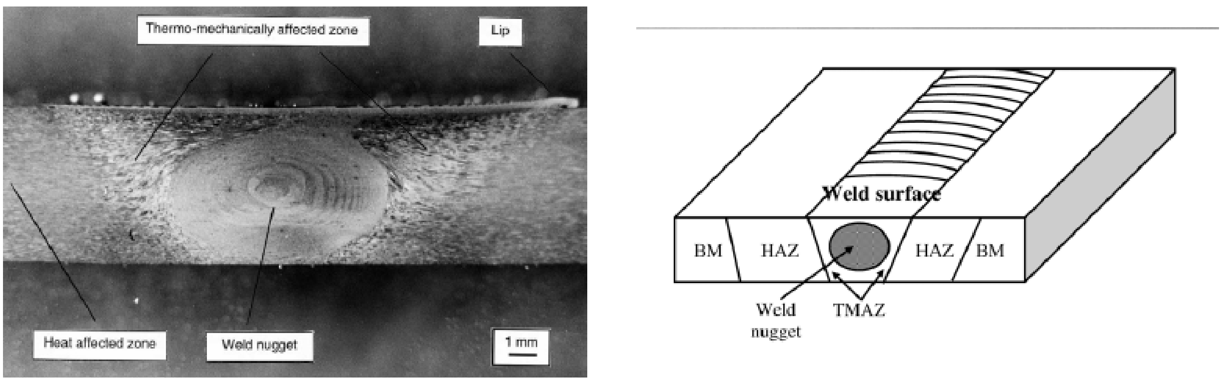

Figure 3: Microstructural zones of a friction stir weld – BM = base material; HAZ = heat affected zone; TMAZ = thermomechanically affected zone [15].

The dislocation density in the nugget zone is very low compared with the TMAZ. The nugget grains are equiaxed and have much a smaller size (in the order of a few μm) than the base material grains. Apparently, this small grain size has a second order effect on the hardness of the nugget in age-hardenable aluminium alloys, as this is much more affected by the presence, nature and distribution of precipitates. Under specific welding conditions, so-called onion rings can be observed in the nugget (see macrograph in Figure 3).

The FSW technique has proven to be particularly successful in production on low melting point alloys, with the most important ones from an industrial viewpoint being the aluminium alloys. For most of these alloys, common tool steel can be used for the FSW tool, and high production rates can be achieved with the technique in combination with outstanding joint properties and good visual aspect.

The main advantages of FSW applied to aluminium alloys are the following [16]:

- Fully automatic welding in all positions at high productivity and constant quality;
- Single pass welding of thicknesses down to 0,5 mm up to 65 mm;
- Successful joining of alloys or alloy combinations that cannot be fusion welded;
- Low thermal distortion, limited softening;
- Limited weld seam preparation (no need to remove the oxide layer);
- No consumables, filler materials or shielding gases;
- No UV radiation, spatter, weld fume, high electric current, electromagnetic fields;
- High energetic efficiency;
- Limited maintenance and wear parts;
- Relatively flat weld surface.

The most commonly cited limitations for a conventional tool FSW machine (as always used in project CASSTIR) are:

- Large process forces (high stiffness of the machine, rigid clamping equipment);
- Exit hole remains after tool withdrawal;
- Relatively high demands in terms of joint fit-up;
- Relatively high investment cost + licence cost;
- Other weld flaws are possible if the process is not properly optimised.

A listing of current and potential new industrial applications of the friction stir welding technique is included in [17] and [18].

The main welding parameters for the friction stir welding process are:

- Welding speed (expressed in mm/min);
- Tool rotation speed (in rev/min or rpm);
- Tool geometry (including tool cooling) and tilt angle;
- Plunge tool depth (in the case of displacement control) or plunge force (in the case of force control).

Additional influence factors (which are often much more difficult to control) are weld gap, workpiece thickness variation and mismatch, clamping equipment and stiffness of the FSW machine. Note that also the welding ratio is often used (expressed in rev/mm), which is defined as the tool rotation speed divided by the welding speed.

The higher this value, the more heat is introduced into the workpiece (hence the higher the resulting heat input should be).

1.4. Project CASSTIR

The project "Innovative joining of critical aluminium structures with the friction stir welding technique", briefly addressed to as "CASSTIR" (designated P2/00/02) was filed as a "clean technologies" project within the "Programme to stimulate knowledge transfer in areas of strategic importance" (TAP2) project call of mid-2006. Indeed, from §1.3, it becomes clear that, besides the economical and engineering advantages (high productivity, high reproducibility, high quality), there are very significant environmental advantages which should surely be taken into account when considering this welding process. When compared to conventional welding techniques, friction stir welding can be categorised under “ecotechnology” with good reason. Its high reproducibility is praised, resulting in fewer scrap and minimum repair welding. The ability to join high strength aluminium alloys (which are often not weldable with conventional processes) with limited strength loss allows the design of lighter structures. Finally, the technique results in much less inconvenience for the operator: no weld fumes, spattering, high intensity radiation, electrical currents or significant electromagnetic fields. In order to introduce this green technology in Belgium, of course the economic feasibility of the process should be demonstrated properly.

The project was approved for a period of 3 years, starting in December 2006. Its objectives are described in §(3)B. Within CASSTIR, BWI was responsible for the project coordination, as well as for metallography and destructive testing. Friction stir welding was performed by UCL and CEWAC. Besides this, UCL took care of residual stress measurements, and CEWAC for the non-destructive characterisation of the welded joints. UGent carried out the characterisation of the welded joints in terms of corrosion resistance. Finally, modelling of the FSW process was subcontracted by UCL and CEWAC to the research institute CENAERO.

1.5. Follow-up Committee

After project CASSTIR was launched, a Follow-up Committee was formed, which consisted of companies and institutions interested in the progress and the results of the research. During project CASSTIR, in total seven Follow-up Committee meetings were organised (at least two each year). There was a good understanding between the different partners at these meetings, and active feed-back was provided towards the research partners. During five of these meetings, a demonstration of the FSW process was given by UCL or CEWAC.

The members of the CASSTIR Follow-up Committee, coming from four different countries (Belgium, the Netherlands, Germany and Sweden), can be subdivided in the following groups:

- Representatives of federal and regional public institutions (Belgian Science Policy, IWT-Vaanderen);
- Companies (Aleris Aluminium Duffel, Aleris Aluminium Koblenz, Corus RD&T, MGG Antwerpen, ESAB Belgium, ESAB Sweden, Sapa RC Profiles, Sonaca, Vinçotte Laboratoria);
- Associations (Agoria, Aluminium Center Belgium);
- Research institutes (CENAERO, CLUSTA, Sirris, Vito).

Besides providing feed-back during the Follow-up Committee meetings, the industrial partners contributed to the project in kind by selecting industrially relevant applications for the project, supplying the base materials for the research and providing additional data concerning the required characteristics of the joints. Furthermore, contributions were made through e.g. optimisation of etching procedures, carrying out controlled heat treatments and the application of an organic coating. Other members contributed through dissemination actions.

2. EXPERIMENTAL WORK: methodology

2.1. Selection of the applications

The three applications selected for study within project CASSTIR, with agreement of the Follow-up Committee, were the following:

- Application 1: friction stir butt welding of hollow 6082-T6 extrusion profiles;
- Application 2: friction stir overlap welding of high-thickness 2124 rolled plate;
- Application 3: friction stir butt welding of low-thickness 5754-H111 rolled sheet.

Based on the elaborate description given in §3.1, §4.1 and §5.1, it will become clear that every application fulfils the following requirements:

- Making use of the FSW technique potentially leads to an improvement in terms of environmental friendliness and process economy compared to conventional techniques;
- The application should be relevant to at least one Belgian company, part of the Follow-up Committee, and be supported by the entire Follow-up Committee;
- The application (in aluminium alloy) can be subjected to the friction stir welding process by at least one of the two partners (UCL, CEWAC), taking into account the capabilities of their FSW equipment;
- The application should pose a technical/intellectual challenge to the research partners, and the experimental work should provide a significant scientific contribution in terms of development of the FSW technique.

2.2. Selection of the experimental methods

Where needed, input in terms of the experimental methods to be used (as a function of the requirements to be fulfilled by the friction stir welded joints) within the project for a given application was provided by the involved Follow-up Committee members.

2.2.1. Friction stir welding

Both UCL and CEWAC have FSW equipment and the necessary FSW licence (as indicated in §8.6.2). Moreover, their equipment is highly complementary.

Within CASSTIR, **UCL** conducted their experiments on a CNC milling machine equipped for FSW, shown in Figure 4 on the left. This equipment, which is only capable of friction stir welding in displacement control mode, is especially suited for lower thickness aluminium alloys:

- On the one hand, a high rotational speed is possible (up to 4000 rpm), which is necessary in order to produce good quality joints in low-thickness material;

- On the other hand, the stiffness of the machine is insufficient to welds alloys within a thickness higher than 8 mm.

Friction stir welding experiments at **CEWAC** were performed on two ESAB SuperStir™ FSW 53 STL machines. The larger of the two machines (displayed in Figure 4 on the right) is capable of welding up to 4 m weld length. Contrary to the UCL equipment, tool holder cooling can be applied with the CEWAC machines. This equipment is capable of carrying out FSW in either displacement control or in force control. Conventional (e.g. 6xxx series) aluminium alloys in thickness from 2 mm up to 30 mm can be welded:

- The rotational speed is limited to 2000 rpm, which is insufficient for welding low thickness (< 2 mm) material;
- The machine stiffness is much higher than that of the UCL equipment, making it possible to friction stir weld thick plate.

Figure 4: ***FSW equipment available within CASSTIR.***
Left: 12 kW HERMLE 3-axis CNC milling machine (UWF 1001 H) at UCL;
Right: one of the two ESAB SuperStir™ FSW 53 STL machines at CEWAC.

Due to the different range of application of the equipment available at UCL and CEWAC, friction stir welding of the different applications was carried out as follows:

- Application 1: UCL took care of displacement control FSW (maximum weld length: 600 mm), whereas CEWAC performed both displacement and force control FSW with a weld length up to 4 m;
- Application 2: CEWAC carried out force control FSW, with a maximum weld length of 400 mm;
- Application 3: UCL conducted displacement control welds with a maximum weld length of 600 mm.

Both at UCL and CEWAC, friction stir welding tools were selected based on prior experience and/or literature. In the case of application 1 and 3, the tool material consisted of H13 tool steel (X40CrMoV5-1), heat treated to 50 HRC. In the case of application 2, the tool material consisted of QRO 90 Supreme Cr-Mo-V alloyed hot-work tool steel [19].

2.2.2. Alternative welding processes

For application 1 and 3, alternative welding processes to friction stir welding were selected, based on input from industrial members of the Follow-up Committee and the experimental equipment available at CEWAC. This is discussed in §3.3 and §5.3, and the environmental and economic comparison is included in §6.

In application 2, no alternative welding process was included in the research programme, as the potentially interesting alternatives consisted of quite complex solid-state processes (since material is non-fusion weldable) with only a very limited amount of potential suppliers – see §4.3.

2.2.3. Weld characterisation methods

2.2.3.1. Non-destructive testing

Where possible (i.e., if allowed by the joint geometry), non-destructive characterisation of the welded joints was performed by CEWAC, using dye penetrant testing and/or radiography, according to the applicable European standards.

2.2.3.2. Conventional destructive testing

"Conventional" destructive testing (i.e., metallography, microhardness testing, bend testing, tensile testing) was carried out by BWI in accordance with the applicable European testing standards. For the microhardness measurements, a Struers Duramin A300-D automatic hardness indenter was used with a 27 s indentation time and appropriate spacing between individual indentations.

When reporting tensile test results of welds, the term "joint efficiency" is often used. In this report, the joint efficiency of a weld is equal to the tensile strength of the weld, divided by the tensile strength of the base material – this ratio is then expressed in percent.

The following etchants were used for metallographic examination:

- Application 1: different etching techniques, of which only electrochemical etching with Barker's (aqueous solution of 4% HBF_4) allowed for grain boundary etching;

- Application 2: Keller's modified – 1 ml 38-40% HF, 1,5 ml 37% HCl, 10 ml 70% HNO_3 and 100 ml water;
- Application 3: Poulton's – 40 ml 70% HNO_3, 35 ml 37% HCl, 2,5 ml 38-40% HF, 40 ml chromic acid (12 g anhydric CrO_3 in 40 ml water) and 2,5 ml water.

2.2.3.3. Fatigue testing

On application 1, transverse tensile-mode fatigue testing was performed on friction stir welds with an R-factor of 0,1 – meaning that the maximum stress equals 10 times the minimum stress, with both stresses being tensile. This was carried out on "flat" and "notched" specimens (depending on whether or not the vertical wall was fully machined). However, due to large variability of the results caused by specimen preparation and/or base material properties, no results are included in this report.

Furthermore, at BWI single-side and double-side friction stir welded profiles were subjected to static and dynamic four-point bend testing, in order to simulate an evenly distributed load (e.g. bulk goods) on the load floor of a trailer. The experimental set-up to which specimens with a width of 80 mm parallel with the welding direction were subjected is shown in Figure 5.

Attempts were also undertaken by CEWAC to apply the Infrared (IR) thermography [20] method to this application. This method, based on distribution of temperature on the surface of the studied object, has proven in previous research on steels to be able to locate the fatigue initiation point without visual examination, and to determine the endurance limit. However, due to experimental difficulties experienced during the measurements and the fact that aluminium alloys do not have the same fatigue behaviour of steels, this method could not be applied successfully within CASSTIR.

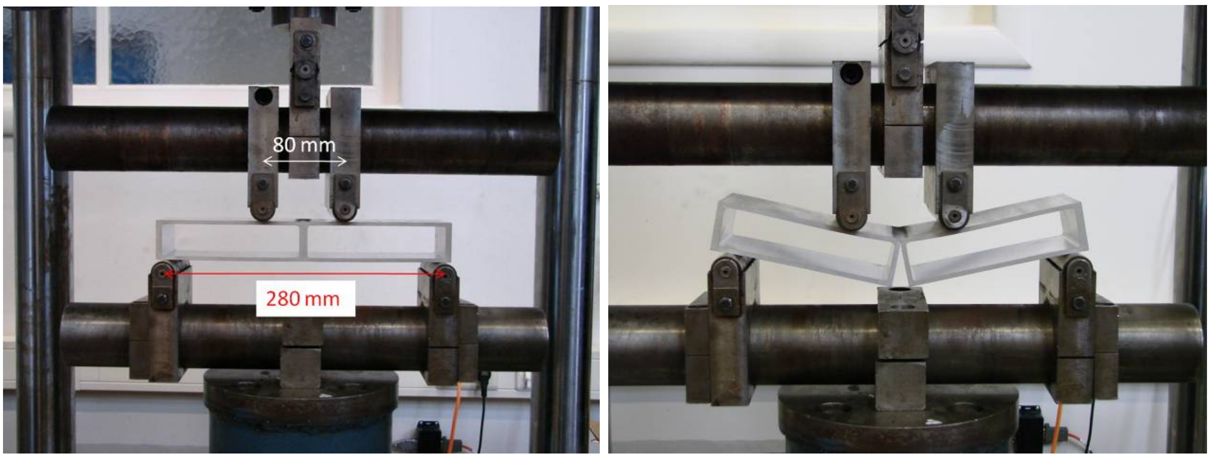

Figure 5: ***Left: experimental set-up at BWI for four-point bend tests. The distance between the axes of the upper rollers is 80 mm – it is 280 mm for the lower rollers. Right: single-side welded specimen during static testing.***

Finally, it should be noted that fatigue testing was also required as a preparatory step – namely the realisation of the fatigue "pre-crack" – for fracture mechanical testing applied to base material and selected welds in application 2 (see §2.2.3.7).

2.2.3.4. Residual stress measurements

The slitting method, also referred to as crack compliance method, is a destructive method which allows for the indirect measurement of average residual stresses in the thickness of a plate, developed by [21]. [22] used the method extensively and wrote a state of the art on this topic.

In this method, the strains resulting from the relaxation of the residual stresses originally present in the workpiece are used to deduce the residual stresses. The relaxation is caused by a cut (using wire electric discharge machining – WEDM) introduced along the plane normal to the residual stress to be measured. The induced strains were measured using strain gages (EA-13-062AQ-350/LE). The method consists in computing the original residual stress distribution which matches best the strains that are actually measured. It was therefore needed to develop inverse methods, easily implementable to convert the measured strains into residual stresses for a given specimen geometry. Within project CASSTIR, UCL managed to master this method, and the competence built up within the project will be used in future projects. All the measurements performed within CASSTIR were carried out using compact tension (CT) specimens – see also Figure 8 and §2.2.3.7 – extracted by milling from the welded plates.

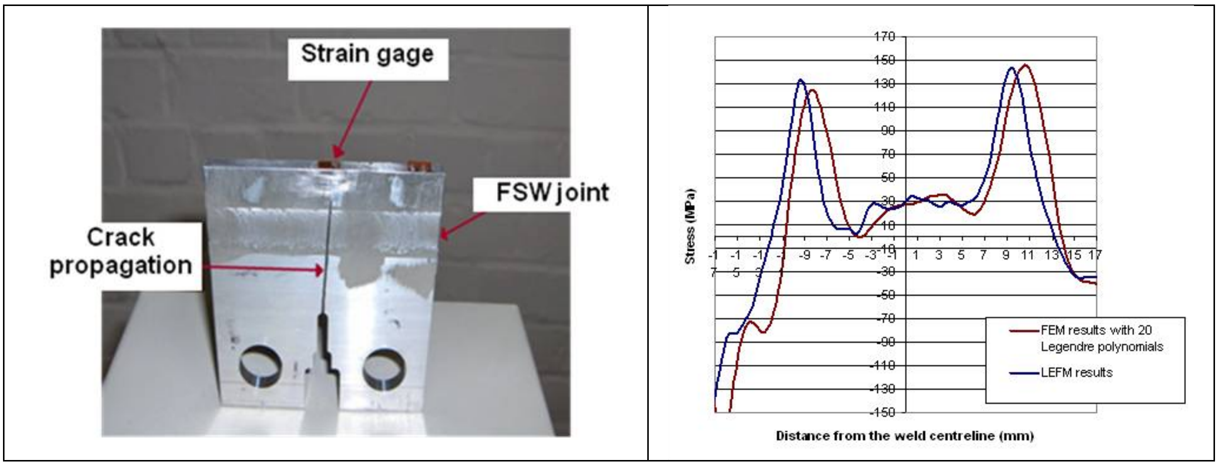

Figure 6: Left: specimen and crack location for residual stress determination; Right: typical result of residual stress profile in a friction stir weld generated at UCL.

2.2.3.5. Corrosion testing

Corrosion testing was carried out by UGent, based on the applicable ASTM standards. The extent of corrosion testing for the different applications was based on meetings with the companies in question.

It should be noted that in the case of application 1, a dedicated test set-up was developed in order to simulate the exposure of the non-welded side of single-side welded hollow profiles (e.g. the lower side of a trailer load floor) to de-icing salt. The non-welded side was immersed at room temperature during 1 hour in a saturated $CaCl_2$ solution (based on the ASTM F482 aircraft maintenance standard), after which the sample was pulled out of the solution and was allowed to dry during 23 hours through a fan and an infrared light bulb – see Figure 7. This sequence was repeated for the same test sample during 6 months.

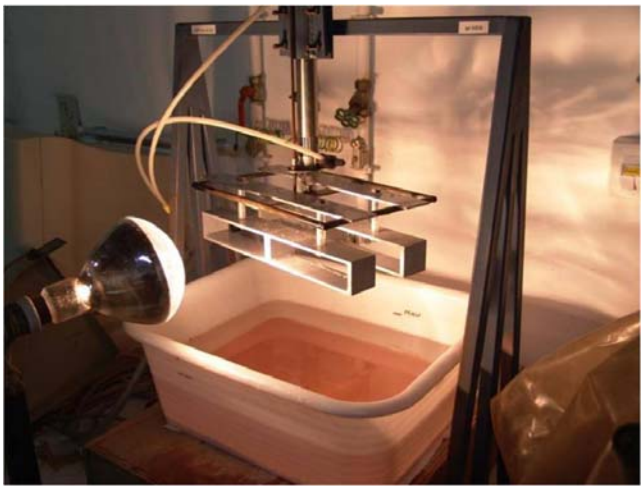

Figure 7: Test set-up for alternate immersion de-icing salt corrosion test (in the condition where samples are allowed to dry).

Electrochemical measurements were carried out on all three applications by means of potentiodynamic polarisation (calibrated by ASTM G 5), using a standard cell at room temperature. The electrolyte consisted of 3,5% NaCl, corresponding to 0,6 M Cl^-. The scanning rate was 0,17 mV/s, and the scanning range was equal to [OCP – 250 mV; OCP + 1600 mV], with OCP the open circuit potential. The scanning zone is a disk with a surface of 1 cm² - hence this allowed to sample distinct zones in the weld, and to compare their corrosion behaviour.

2.2.3.6. Heat treating

It should be stressed here that for welds from application 1 and 2 (which consist both of precipitation hardenable alloys), destructive testing was always carried out at least one month after welding. This allows for a certain degree of natural ageing, reducing variability in mechanical properties measured between different welds.

In the case of application 2, part of the 2124-T851 base material was subjected to a pre-weld heat treatment: it was put into T4 temper by Corus RD&T through solution heat treating and water quenching (performed in accordance with the specifications in AMS 2772C), followed by natural ageing during at least 1 month.

Post-weld heat treatments were carried out by BWI in the case of application 1, and by Corus RD&T in the case of application 2. The post-weld heat treatment consisted in the case of application 1 of maintaining the as-welded part during 32 hours at 150°C, followed by air cooling. Two different post-weld heat treatments were carried out by Corus RD&T on friction stir welding of application 2, namely:

- artificial ageing: 12 hours at 190°C + air cooling;
- solution heat treating + artificial ageing: heat treatment at 493°C + water quench + artificial ageing.

2.2.3.7. Fracture mechanical testing

Fracture mechanical testing was performed on application 2. Fracture mechanics consists of the application of the physics of stress and strain to microscopic crystallographic defects found in real materials, in order to predict macroscopic mechanical failure of bodies. In this project, use was made of linear elastic fracture mechanics (leading to K_{Ic} plain-strain fracture toughness) according to ASTM E 399 - 09, and elastic-plastic fracture mechanics (leading to the CTOD or crack tip opening displacement) according to ASTM E 1290 - 08. For this investigation, the compact tension (CT) geometry was used, shown schematically together with the sample extraction location in Figure 8.

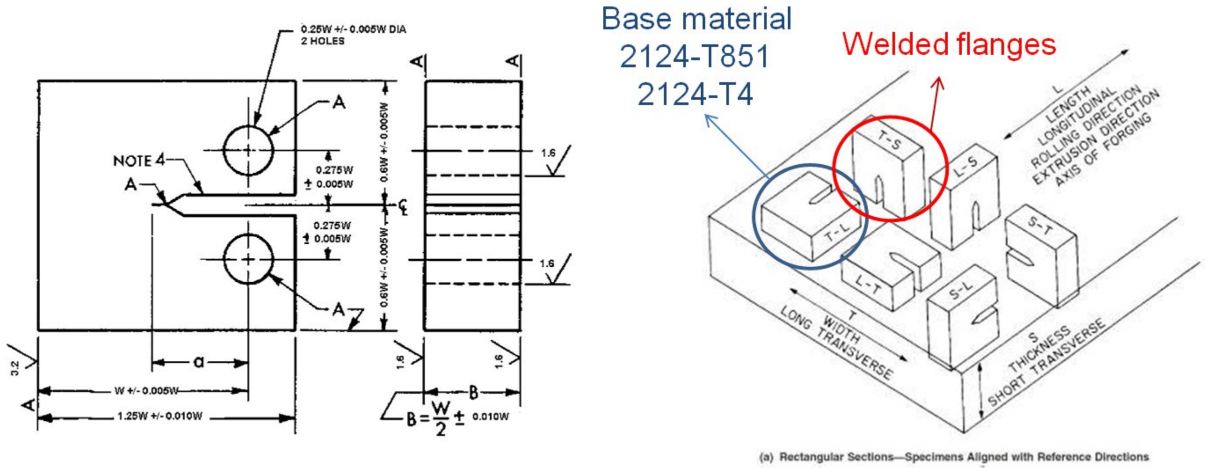

Figure 8: Left: compact tension geometry used for fracture toughness testing of application 2; Right: sample location relative to the plate dimensions.

2.2.4. Modelling of the FSW process

Numerical modelling within CASSTIR was subcontracted by UCL and CEWAC to CENAERO. Friction stir welding models were made with the manufacturing software MORFEO (Manufacturing Oriented Finite Element tOol), developed by CENAERO [23]. The result of numerical modelling was validated against experimental data, such as thermal measurements during FSW, torque measurements, hardness profiles and residual stress data.

3. APPLICATION 1: friction stir butt welding hollow 6082-T6 extrusion profiles

3.1. General information

This application is directed towards the production of mass-transportation goods (e.g. trains). However, the joining of hollow extrusion profiles by means of friction stir welding is not restricted to this domain. Other possible applications include for instance shipbuilding (fabrication of decks) and trailers (e.g. refrigeration boxes, dump bodies).

The main advantages of the FSW technique on this type of applications are:

- The ability to produce large panels starting from relatively simple extrusion panels, without the introduction of distinct filler material;
- Reduction of deformations due to the lower heat input (extremely important in large structures!);
- Reduction of strength loss due to the lower heat input compared to fusion welding techniques;
- Productivity and consistent quality;
- No need for oxide removal;
- Green process compared to fusion welding processes (e.g. MIG, hybrid laser welding), e.g. lower energy consumption, less scrap, no weld fumes...

In order to carry out the welding tests, a relatively uncomplicated rectangular hollow extrusion profile was selected (Figure 9). Modifications to this profile can be carried out by milling the available profiles. In terms of weight limitation and material use optimisation, reduction of the vertical wall thickness is important. This can easily be realised by the partners by milling the vertical wall. In that case, dedicated milling tools are used to reproduce the original outer radii of the profile.

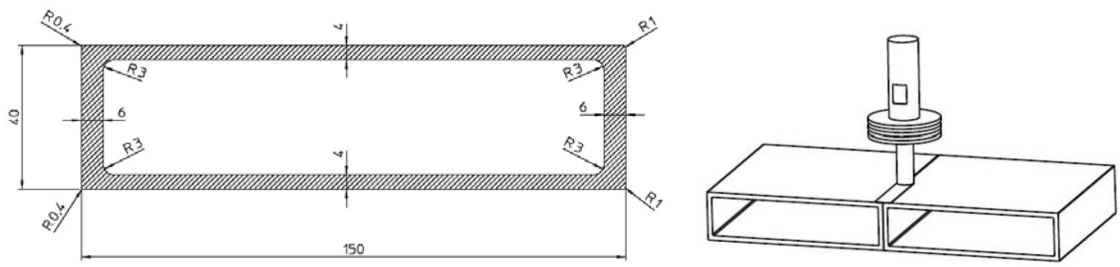

Figure 9: Left: design of hollow profile for application 1; Right: joint configuration.

The base material, 6082-T6 in the geometry shown in Figure 9 on the left, is delivered by Sapa RC Profiles. More information about the base material is given in §1.1.1.

The main technical challenge within this investigation is the determination of the final profile design, which should provide an optimum in:

- "weight of the structure" versus "weld quality" (related to the thickness of the vertical walls of the profile);
- "productivity in the extrusion process" versus "productivity and quality in the welding process" (related with the outer radii of the profile).

Friction stir welding work for this application is executed by both UCL and CEWAC. Where possible, the properties of friction stir welds produced by the two machines with equal welding parameters were compared.

3.2. Experimental work: friction stir welding

3.2.1. Preliminary investigation: FSW of 4 mm thick flat 6082-T6 profiles

In the first stage of the examination, the friction stir welding process was optimised on flat 6082-T6 extrusion profile with a thickness of 4 mm. The same welding tool geometry was selected by UCL and CEWAC, based on common experience, in order to maximise joint properties and visual aspect – as is shown in Figure 10.

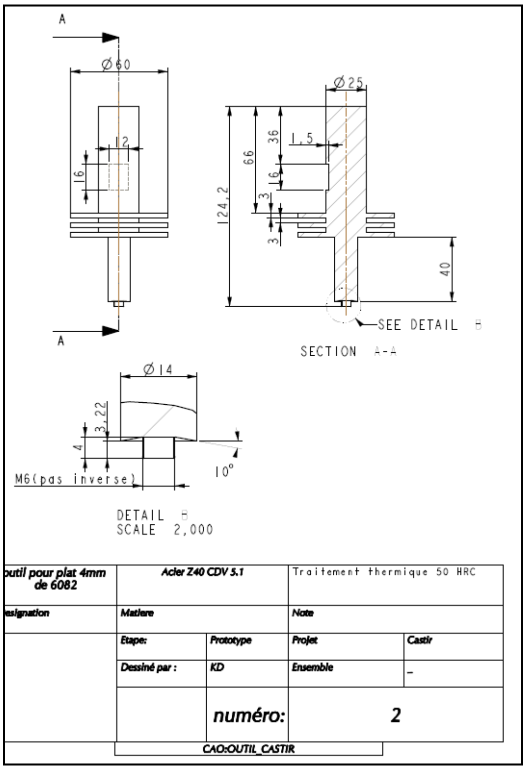

Figure 10: Friction stir welding tool used for application 1.

For the preliminary study, both UCL and CEWAC conducted FSW in displacement control mode. Establishing the welding parameter sets at UCL was carried out by the determination of the limiting (highest and lowest) values of the tool rotational speed and the welding speed as well as the appropriate value of the plunge depth for obtaining sound welds (U1, U2, U3, U4 in Figure 11). Those values were determined based on the result of visual inspection and a root bend test. At CEWAC on the other hand, the tool rotation speed was kept constant at 1000 rpm and the advancing speed was varied (C1 to C6 in Figure 11). Note that, for this initial investigation, one parameter position was in common for CEWAC and UCL (*U3* and *C2*). Both for the CEWAC as the UCL welds, the plunge depth was kept constant.

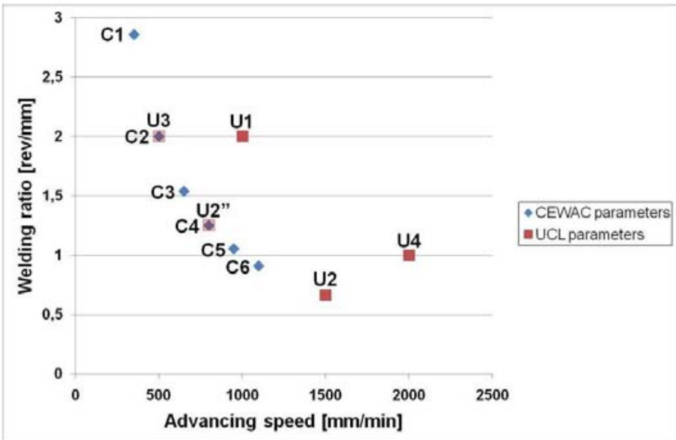

***Figure 11:** Graphical representation of (displacement control) FSW parameters for 4 mm thick 6082-T6 flat profile. Constant plunge depth for the different welding parameter sets by UCL resp. CEWAC.*

After welding, non-destructive testing (visual, dye penetrant, radiography) was carried out at CEWAC, on both the UCL and CEWAC welds. After non-destructive testing, BIL carried out the destructive characterisation.

Due to the fact that tunnel defects were detected at parameter position *U2*, in the following research the welding condition *U2"* was used in order to obtain a parameter domain for UCL, defined by 4 stable conditions. That way, also an additional overlapping parameter set was made with CEWAC (*C4* and *U2"* in Figure 11) for future work. These welds were again subjected to non-destructive testing at CEWAC and destructive characterisation at BIL. The following trend between welding ratio and mechanical properties could be noted for the UCL welds:

- Joint efficiency (see §2.2.3.2) increased from 80% for *U3* (highest weld ratio) up to 83% for *U4* (lowest weld ratio);
- Elongation at fracture decreased from 7,5% for *U3* to 6% for *U4.*

In all cases, fracture took place in the heat affected zone on the RS.

UGent carried out intergranular attack (IGA) testing according to ASTM G110 on the UCL welds with parameter conditions *U1*, *U3* and *U4*. After 700 hours, the following could be observed:

- The base material is prone to IGA;
- The weld face of higher heat input conditions (*U3* and *U1*) is prone to IGA;
- The weld root is resistant to IGA.

Furthermore, CEWAC delivered additional *C6* welds (which were approved by non-destructive testing) to UGent. After organic coating at Sapa RC Profiles, filiform corrosion testing by UGent was carried out in accordance with DIN 65472 (Lockheed Test – 1000 hours) as well as the APA test (144 hours).

The APA test showed that the structure is prone to filiform corrosion; however, a same degree of attack was noted on the base material, the weld face and the weld root. On the other hand, the base material and the weld zone are resistant to filiform corrosion according to the Lockheed test.

UCL also performed residual stress measurements – these results, together with results obtained from hollow profiles, are described in §3.2.2.

3.2.2. FSW of 6082-T6 hollow profiles: parameter optimisation

In this investigation, the optimisation procedure at UCL and CEWAC on the actual 6082-T6 hollow profiles was carried out with the same tool geometry as shown in Figure 10.

For the weld tests using <u>displacement control</u>, CEWAC applied the same welding parameter sets as for the flat profiles (*C1* to *C6*) – see Figure 11. In each case, the firmly clamped profiles were welded on one side along the 1 mm outer radius side (right hand side of the technical drawing in Figure 9), with a vertical wall thickness of 2 x 6 mm (original), 2 x 5 mm and 2 x 4 mm. On the profiles with reduced wall thickness, the 1 mm outer radius was reproduced by milling. All 18 welds were subjected at BIL to metallography and tensile testing. Prior to transverse tensile testing, the remaining vertical wall was machined down to the weld root.

It was noted that (at a rotation speed of 1000 rpm) the welding speed at which no tunnel defects were created decreased from 650 mm/min to 500 mm/min when the vertical wall thickness was reduced. Furthermore, the joint efficiency in defect-free welds decreased significantly when the vertical wall thickness was lowered from 6 mm to 5 mm or 4 mm (e.g. for *C2* condition: 82,4% compared to 76,3%). The elongation at fracture also decreased when the wall thickness was lowered. If no tunnel defects were present, fracture occurred in the HAZ (either on the RS or on the AS). As an example of the joint appearance, macrographs of CEWAC welds with *C2* parameters are shown in Figure 12.

2 x 6 mm wall thickness	2 x 5 mm wall thickness	2 x 4 mm wall thickness

Figure 12: Keller's mod. etched macrographs of friction stir welds realised by CEWAC with* C2 *welding parameters.

UCL on the other hand started its investigation by welding the profiles on one side along the 0,4 mm radius side (left hand side of technical drawing in Figure 9) with the original wall thickness, using the parameter conditions *U1*, *U2"*, *U3* and *U4*. Metallography of the welds was carried out by BIL. None of the welds contained tunnel defects.

Tensile testing by BIL on these UCL hollow profile friction stir welds showed that fracture always occurred on the advancing side. This was most probably related to asymmetry of the joint: the centre of the weld face was off-set towards the advancing side of the joint, causing more heat concentration (hence softening) on that particular side. The highest joint efficiency (82,4%) was encountered for the condition with the lowest welding ratio *U4*. Microhardness measurements showed that the HAZ in the hollow profiles especially becomes <u>wider</u> compared to that of flat profiles; a pronounced effect on the hardness minimum values was however not noticed. This led to a mild increase of the elongation at fracture (up to around 8%) compared to the friction stir welded flat extrusions. Attempts by UCL to realise defect-free friction stir welds with a vertical wall thickness lower than 4 mm, with an adapted FSW tool, were not successful due to shortage of base material remaining for the optimisation.

UGent carried out an elaborate corrosion research on the UCL hollow profile welds.
<u>Potentiodynamic polarisation tests</u> on the weld face of *U3* and *U4* (highest resp. lowest weld ratio) pointed out that the different zones (i.e. base material, HAZ and weld surface) possess a similar electrochemical behaviour.

Pitting and crevice corrosion tests in accordance with ASTM B117 were carried out in a salt spray cabinet on all four UCL welds (*U1*, *U2"*, *U3* and *U4*) during 1000 hours.
In <u>pitting corrosion testing</u>, only the weld face was studied. Significant pitting and intergranular attack was especially found in the HAZ on the advancing side of weld *U4* – see Figure 13. This is partly influenced by the presence of weld flash.

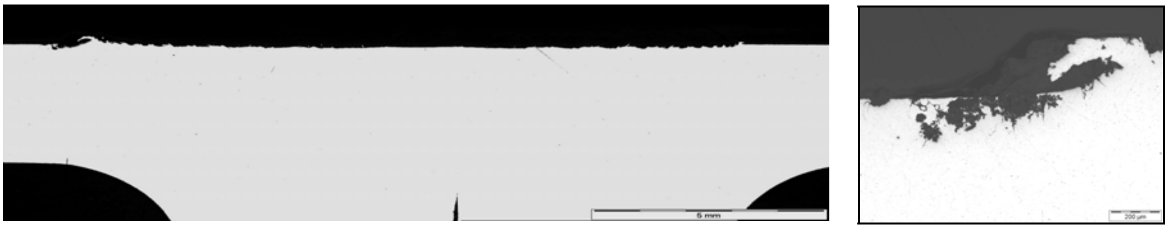

***Figure 13:** Left: unetched tranverse section of a crevice corrosion test sample (weld U4); Right: detail of the HAZ on the advancing side.*

Concerning <u>crevice corrosion testing</u>, the “natural” crevice was used that exists on the root side between two single-side welded hollow profiles. It was found that the intergranular attack along the crevice was especially a function of the crevice geometry. The more "white rust" found on the root side of the profiles, the more intergranular attack had taken place along the crevice.

Finally, UGent carried out <u>alternate immersion tests</u> on single-side friction stir welded hollow profiles with original wall thickness (realised by UCL with the parameter sets *U3* and *U4*), in order to check for proneness to de-icing salt corrosion on the root side of the profiles – see also §2.2.3.5 and Figure 7. The result is given in Figure 14. Despite the harsh conditions, only very limited attack occurred, meaning that this configuration does not pose large risks in terms of corrosion.

Figure 14:** Results of de-icing salt corrosion testing. Left: sample from* **U3; Right: sample from* **U4***. Top: side view; Bottom: view on the face exposed to the solution.*

UCL performed residual stress measurements (see §2.2.3.4) on flat and hollow profiles using widely varying welding parameters. In order to compare the influence of the welding machine, the machines of both UCL and CEWAC were used.

The shape of the residual stress profile obtained in every measurement was similar to the one presented schematically in Figure 15. The longitudinal residual stresses were always compressive further away from the weld centreline, and tensile in the high temperature region (the HAZ) with a reduction of their magnitude in the weld centre (nugget). This so called “M-shape” is in agreement with the experiments reported in literature (see e.g. [22]). In Figure 15, it is indicated how two characteristic values were extracted from each curve. These are *M*, the maximum residual stress, and *W*, the distance between the peak stress measurements. Figure 16 (left) presents *W* on flat plates and hollow profiles divided by the tool shoulder diameter (equal to 14 mm) as a function of the advancing speed. Figure 16 (right) presents *M* divided by the minimum specified base material yield strength (equal to 240 MPa) as a function of the advancing speed. The results for welds performed with the two different machines are also presented in Figure 16.

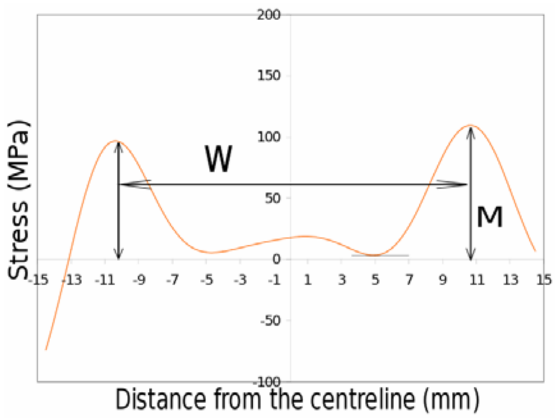

Figure 15: Schematic representation of a typical residual stress distribution across the welds observed for the experiments on 6082-T6 alloys.

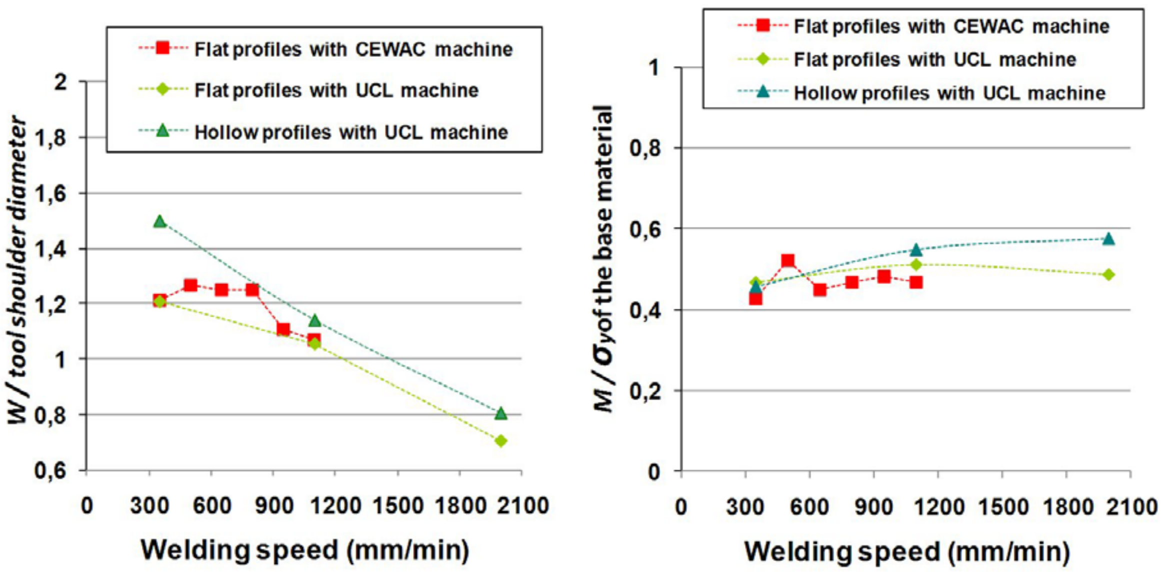

Figure 16: ***Influence of the welding speed on (left) distance between peak tensile longitudinal residual stresses and (right) maximum longitudinal residual stress in friction stir welds performed on 6082-T6 alloy with a rotational speed of 1000 rpm with two welding machines and for flat or hollow profiles.***

The maximum longitudinal residual stress ranges from 40 to 60% of the base material yield strength. It is interesting to note that in the present case, there is no effect of the welding machine on the residual stress profile (even though in the case of the CEWAC machine, tool cooling was applied). The distance *W* between peak tensile residual stresses increases if the welding speed decreases. This is due to the "hotter" characteristics of the welds performed at low welding speeds leading to a wider HAZ. The maximum normalised residual stress increases by increasing the advancing speed. This may be attributed to the steeper temperature gradients in the case of welding with a lower heat input.

The hollow profiles present a larger *W* and a higher maximum normalised residual stress than the flat profiles at a given advancing speed. Larger *W* may be related to the thermal cycle. Using the same welding parameters, welds performed on hollow profiles are" colder" than welds performed on flat profiles, which was confirmed throughout the project by means of hardness measurements. The slightly larger value of the maximum residual stress for hollow profiles compared to flat profile (Figure 16 on the right) may be attributed to the different temperature distribution in the hollow profiles.

CENAERO performed thermo-mechanical simulations on hollow profile, based on thermal measurements (by both UCL and CEWAC), torque measurements and microhardness profiles, in order to predict time-temperature profiles, as well as longitudinal residual stresses to be compared to the measurements presented above.

For the time-temperature profiles, a good correlation was found between the experimental data and the predictions. The thermomechanical simulation of the friction stir welds on the hollow extruded profiles was generated and chained to a cool-down, release of the part, machining of the test specimen and a final release simulation. Furthermore, a yield stress reduction caused by welding was taken into account (see Figure 17). The simulation was made in the assumption that backing plate, tool and clamping system play no significant role in the thermal behaviour of the weld.

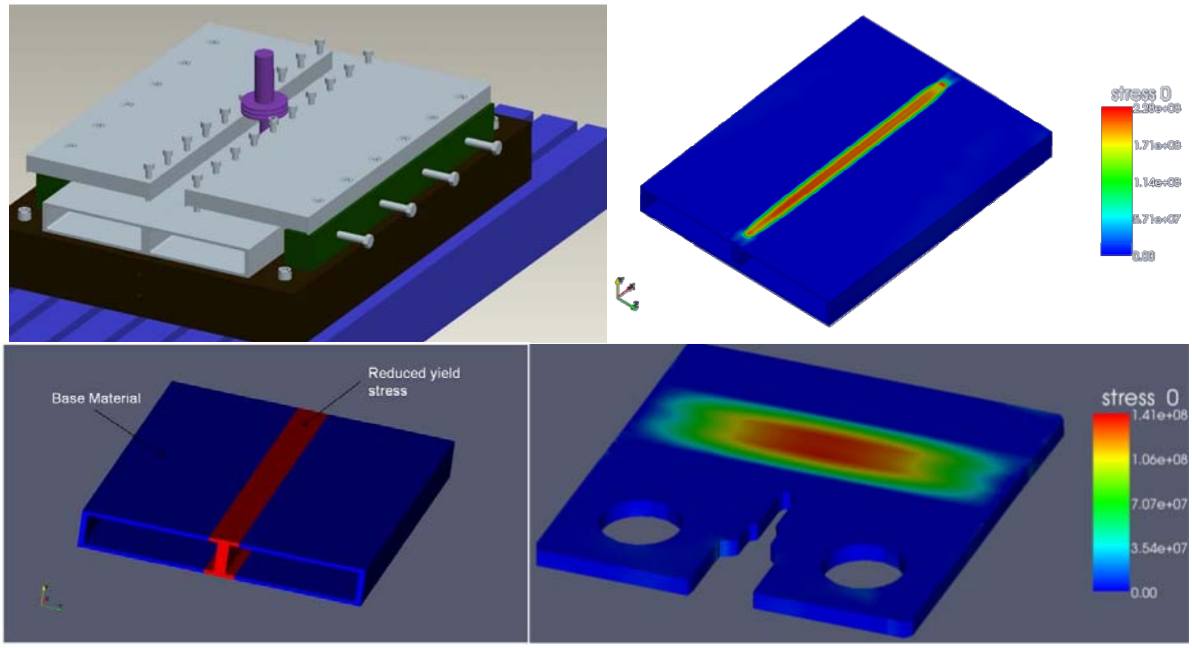

Figure 17: ***Top left: modelled clamping system for profiles during FSW;***
Top right: residual stress distribution during welding;
Bottom left: illustration of the reduced yield stress model;
Bottom right: stress distribution after machining and release.

Figure 18 proves that the modelling approach followed by CENAERO, taking into account both a yield stress reduction in the weld region and the machining of the test specimen, produces a good correlation with the experimental results. The magnitude of the stresses in the pre-machined structure is predicted accurately. However, further work is required in coupling the simulation to a metallurgy model to simulate in detail the softening effects in the material due to welding – this work fell outside the scope of project CASSTIR.

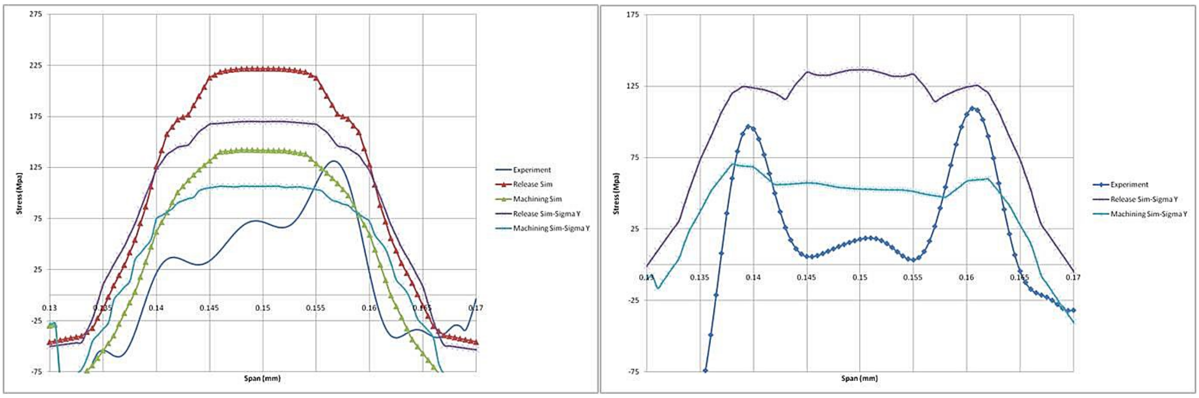

Figure 18: ***Comparison between experimental and simulated residual stress profiles in hollow profiles friction stir welded by UCL (left: welded at 350 mm/min at 1000 rpm; right: welded at 1100 mm/min at 1000 rpm).***

3.2.3. FSW of 6082-T6 hollow profiles: pre-industrial welds

CEWAC optimised the FSW process on hollow profiles with a length of 4 meter in the joint geometry shown in Figure 9 on the right, using the same tool as given in Figure 10. Welding was performed at a welding speed of 2000 mm/min, a tool rotation speed of 1400 rpm and a 1,5° tilt angle, aiming at a 4 mm weld penetration.

Welding was performed on both sides of the joint line. After welding the first side of the weld and unclamping ("first weld"), the welded profile was deformed in the longitudinal direction with a maximum deflection, occurring at half the weld length, of 6 mm above the horizontal axis. The welded profiles were turned over, and welded along the other side after firmly clamping ("second weld"). After this procedure, the deflection in the longitudinal direction was close to 0 mm.

The same welding parameters were used for displacement control welding (with a programmed plunge depth of 4,4 mm below the profile surface) and force control welding (with a vertical plunge force of 18 kN). Both welds were subjected to metallography (etching with Barker's reagent), HV0,2 microhardness testing and tensile testing. Moreover, in this investigation also part of the "force control weld" was subjected to a post-weld heat treatment (PWHT), consisting of artificial ageing at 150°C during 32 hours, followed by air cooling.

Figure 19 shows macrographs of the displacement control and force control welds in etched condition. The location of the microhardness indentations is also visible. In the force control weld, no defects were found, whereas in the displacement control weld, some small tunnel defects are present in the lower side of the nugget on the advancing side. This indicates that, for the realisation of long weld lengths, working in force control mode is desirable as the process becomes less sensitive to thickness or height variations of the profiles to be welded.

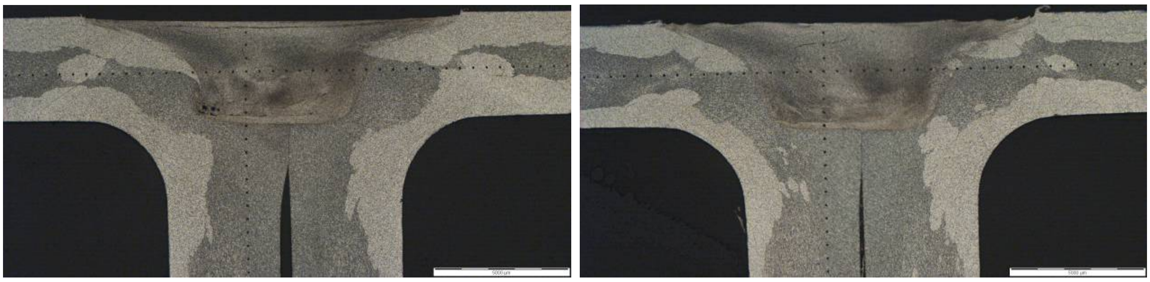

Figure 19: ***Barker's etched macrographs of the weld area in the displacement control weld (left) and the force control weld (right).***

Figure 20 on the left shows the nugget microstructure in the force control weld that was not subjected to PWHT. Clearly, the microstructure is very fine.

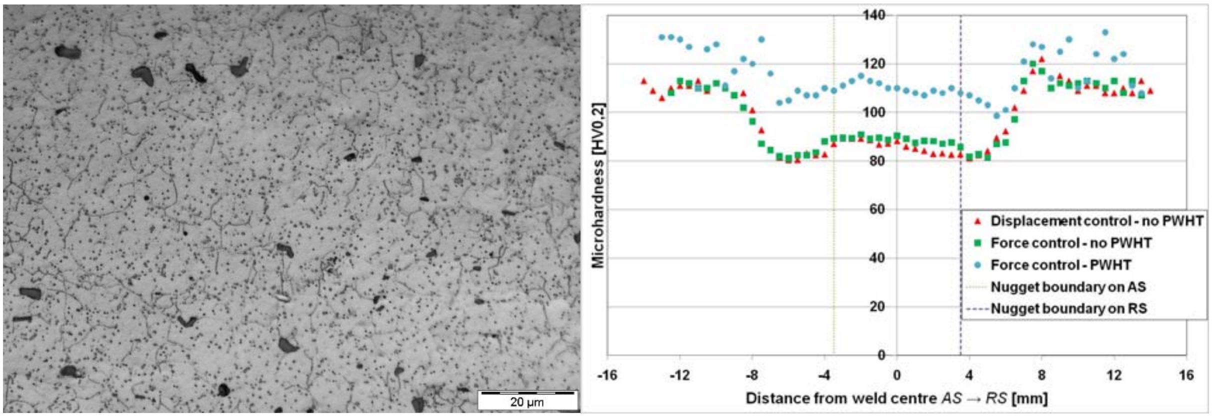

Figure 20: ***Left: Barker's etched micrograph in the nugget area of the force control weld (no PWHT).***
Right: HV0,2 microhardness results.

Figure 20 on the right shows microhardness profiles performed on the various welds in the horizontal direction at mid-thickness. The following can be derived:

- The non-PWHT base material microhardness is in the order of 110 HV0,2;
- The microhardness profiles of the non-PWHT welds are very comparable (which is also expected, given the fact that the main welding parameters governing the heat input were the same):
  - The minimum hardness (around 80 HV0,2) is noted in the heat affected zone, at around 6 mm from the weld centreline. No significant differences can be noticed in the AS or the RS.
  - The microhardness in the nugget area (85-90 HV0,2) is somewhat higher than that in the HAZ, which is consistent with literature [24].

- In general, the microhardness profile of the PWHT force control weld is some 20 HV0,2 higher than the non-PWHT counterpart – the same is also valid for the base material microhardness, which indicates that the base material too still possesses a significant age hardening potential;
- Both in the non-PWHT and in the PWHT condition, the base material microhardness is reached at 10 mm away from the weld centreline.

The various welds were subjected to transverse tensile testing. Two tensile tests were carried out for each condition. Samples were machined down to the 4 mm horizontal profile thickness, without weld flash removal. The results are summarised in Table 7. The joint efficiency relates to the actual base material tensile strength.

Table 7: Results of transverse tensile testing

<table>
<tr><th></th><th>Yield strength $R_{p0,2}$ [MPa]</th><th>Tensile strength R_m [MPa]</th><th>Elongation $A_{50\ mm}$ [%]</th><th>Joint efficiency [%]</th><th>Fracture location</th></tr>
<tr><td rowspan="3">Displacement control First weld (no PWHT)</td><td rowspan="3">183 ± 1</td><td rowspan="3">237 ± 6</td><td rowspan="3">4,3 ± 0,1</td><td rowspan="3">76</td><td>HAZ AS</td></tr>
<tr><td>HAZ AS</td></tr>
<tr><td>HAZ AS</td></tr>
<tr><td rowspan="3">Displacement control Second weld (no PWHT)</td><td rowspan="3">181 ± 3</td><td rowspan="3">241 ± 4</td><td rowspan="3">3,4 ± 1,1</td><td rowspan="3">77</td><td>HAZ AS</td></tr>
<tr><td>HAZ AS</td></tr>
<tr><td>HAZ AS</td></tr>
<tr><td rowspan="3">Force control First weld (no PWHT)</td><td rowspan="3">175 ± 5</td><td rowspan="3">248 ± 7</td><td rowspan="3">5,1 ± 0,9</td><td rowspan="3">79</td><td>HAZ RS</td></tr>
<tr><td>HAZ RS</td></tr>
<tr><td>HAZ RS</td></tr>
<tr><td rowspan="3">Force control Second weld (no PWHT)</td><td rowspan="3">176 ± 7</td><td rowspan="3">252 ± 10</td><td rowspan="3">5,2 ± 0,5</td><td rowspan="3">81</td><td>HAZ RS</td></tr>
<tr><td>HAZ RS</td></tr>
<tr><td>HAZ RS</td></tr>
<tr><td rowspan="3">Force control First weld (PWHT)</td><td rowspan="3">263 ± 7</td><td rowspan="3">298 ± 4</td><td rowspan="3">2,6 ± 0,1</td><td rowspan="3">96</td><td>HAZ RS</td></tr>
<tr><td>HAZ RS</td></tr>
<tr><td>HAZ RS</td></tr>
</table>

No significant differences in terms of tensile properties can be noted between the first and second pass of the non-PWHT welds. Even though the microhardness profiles of the non-PWHT welds are very alike, some differences are noted in the tensile test results. First of all, in the displacement control welds fracture occurs in the HAZ on the AS, whereas in the force control welds fracture takes place in the HAZ on the RS. Moreover, a higher joint efficiency with respect to the 6082-T6 base material and a somewhat higher elongation at fracture is obtained for the force control welds.

The post-weld heat treatment strongly influenced the tensile properties. The yield strength and tensile strength increased significantly, whereas the elongation at fracture was reduced. Especially the very high joint efficiency of 96% (calculated based on the 6082-T6 base material tensile strength from Table 2) should be noted, and compared to the joint efficiency of around 80%, which was found for the non-PWHT force control welds.

Non-PWHT force control welds were subjected to four-point bend tests, in order to simulate an evenly distributed load (e.g. bulk goods) on the load floor of a trailer. This investigation was applied to both double-side as single-side welded specimens. The experimental set-up is described in §2.2.3.3, and shown in Figure 5.

Both static (i.e., with continuous increase of the load until a maximum load is reached) and dynamic tests were carried out. For the dynamic tests, an R-factor of 0,5 was specified, which means that the maximum load is twice as high as the minimum load. Due to the very high deformations, only a frequency of 2 Hz could be used. Dynamic testing was stopped after a certain level of the upper former displacement (namely, the displacement at maximum load + 5 mm) was reached. Run-out was set at 1 million cycles. The results are shown in Figure 21. The "loads" are expressed in kN/m, and should be interpreted as the load per meter weld length. Clearly, the double-side welded specimens possess, due to their much higher stiffness, a far higher static and dynamic resistance to four-point bend loading compared to the single-side welded configuration (where a notch is present right below the nugget – see Figure 19). During dynamic testing, failure of single-side welded specimens occurred by plastic failure in the nugget, whereas in the double-side welded specimens, cracking occurred in the HAZ on the RS of the lower weld.

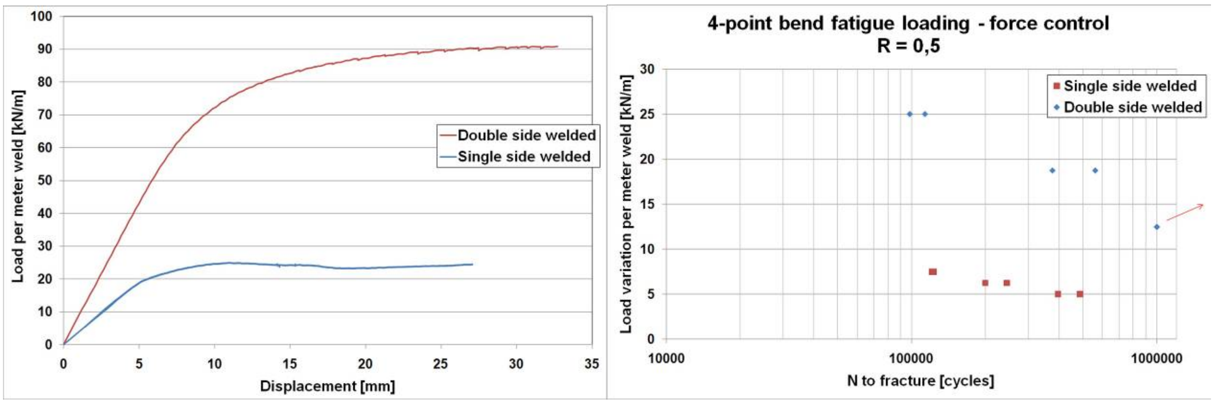

Figure 21: Results of static (left) and dynamic (right) four-point bend tests carried out on single-side and double-side force control welds (in non-PWHT condition).

3.3. Experimental work: alternative process

For this application, hybrid laser welding (HLW) was selected as an alternative process. Both HLW and FSW operate fully automatic and with a high productivity – i.e. with welding speeds above 1 m/min. The low heat input of both FSW and HLW techniques results in less degradation of the mechanical properties and lower deformation of the welded parts. Moreover, these fully automated processes enable a higher productivity than the traditional arc welding processes applied to aluminium alloys (MIG, TIG). The HLW technique, developed in the late 1970's [25], concerns a combination of laser welding and arc welding processes, acting simultaneously in the same process zone. For the current application, the main advantages are that on the one hand HLW is, just like FSW, an automated welding process which allows for a high welding speed, and that filler wire can be introduced in a controlled manner to the weld area (which is very difficult with conventional laser welding) in order to avoid hot cracking. More information about HLW can be found in [26]. It should be noted here that the results mentioned here would not have been possible without the collective research projects ALUWELD [27] and ARCLASER [28].

Hybrid laser welding was performed by Laser Center Flanders of VITO, using a 4,4 kW diode pumped Nd:YAG laser of Rofin Sinar (DY044) and a Fronius Transpuls Synergic 5000 MIG welding source. Direct current with electrode positive was used for all experimental runs. The laser welding and the arc welding process (with the laser leading the arc, with 2 mm distance between laser and arc) are combined in a Fronius hybrid laser welding head. The welding head is mounted on an ABB robot. For hybrid laser welding, Argon 4.8 (99,998% pure Ar) was used as shielding gas with a flow rate of 11 m/min.

Initially, the optimisation of the HLW process on 4 mm thick 6082-T6 flat extrusion profiles was carried out, at a welding speed of 1,8 m/min. The maximum available laser power of 4,4 kW was used – the arc settings were 103 A at 17,7 V. ER 5183 (Al Mg4,5Mn0,7) filler material, supplied by the company Soudokay, with a diameter of 1,2 mm was applied to the weld zone with a wire feed rate of 6 m/min. The result is shown in Figure 22. An acceptable amount of uniformly distributed weld metal porosity was present, and a joint efficiency of 80% was achieved, which is comparable to that obtained in friction stir welding.

Figure 22: Macrograph of a hybrid laser weld in 6082-T6 flat extrusion profile.

After these trials, hybrid laser welding was applied to the hollow profiles in the same joint geometry as shown in Figure 9 on the right. It was however not possible to produce relatively pore-free welds with a 4 mm penetration depth. The reason for that is two-fold. First of all, in beam welding processes full penetration welding is always desirable – this is not possible in the current geometry, unless the vertical wall is affected (which has an influence on the profile stability). Secondly, the flat extrusion profiles were not firmly clamped to a backing table, given the fact that HLW is a non-contact welding method. In the case of flat profiles, less heat dissipation occurred compared to the hollow profile (where heat can escape from the weld zone through the vertical walls of the profile). This effect was so pronounced, that it even became impossible to achieve full penetration through 4 mm material thickness with the available hybrid laser welding equipment, without significantly reducing the welding speed. For that reason, a better-suited extrusion profile shape is preferable – examples of which are shown in Figure 23.

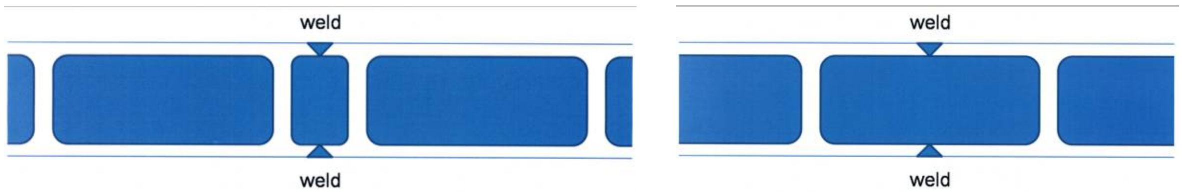

Figure 23: Sketches of alternative extrusion profile geometries considered more suitable for beam welding processes.

For realistic comparison in terms of environmental friendliness and process economy (§6.1.1 and §6.2.1, respectively), it is assumed that indeed one of these profile geometries are available for welding with hybrid laser welding, in order to make a comparison with friction stir welding possible.

3.4. Conclusions

After initial parameter optimisation on flat profile, friction stir welding was applied to the hollow profile with increasingly smaller vertical wall thickness (which acts as a support for the high downforce during FSW), striving to find an optimum between friction stir weldability, extrudability of the base material and weight limitation. This finally resulted in the realisation of 4 m long friction stir welded extrusion profiles with significantly reduced vertical wall thickness, produced at a welding speed of 2 m/min. Friction stir welding can be applied in either displacement control or force control mode. For the realisation of long weld lengths, where thickness or height variation along the weld joint becomes possible, only FSW in force control mode yielded defect-free welds, hence this is the preferred approach for this type of application. Optimised friction stir welds of application 1 were subjected to testing procedures developed by BWI and UGent, including dynamic four-point bend tests and de-icing salt corrosion tests.

A study of residual stresses was conducted by UCL, and modelled by CENAERO. “M-shape” residual stress profiles were always found on 6082-T6. The influence of the geometry, the welding machine and the welding conditions was investigated. The distance between the peak residual stresses increases with decreasing advancing speed, while the maximum residual stress increases with increasing advancing speed. No significant machine influence was noticed.

4. APPLICATION 2: friction stir overlap welding of high-thickness 2124 rolled plates

4.1. General information

This application concerns the production of complex aerospace wing elements (slats) in 2124 aluminium alloy, which are currently produced at Sonaca S.A. as heavily machined parts (Figure 24 on the left). Use of 2124 material is mainly restricted to aerospace applications; the material is considered not fusion weldable due to its very high hot cracking tendency. The flanges indicated in Figure 24 on the right are 30 mm high. For the present application, it was suggested to build up the flanges by means of friction stir overlap welding.

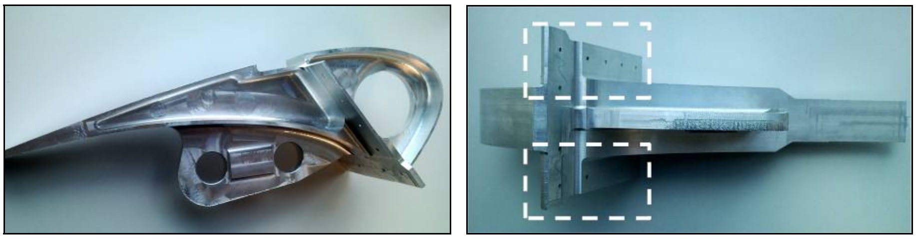

Figure 24: ***Photographs of the deeply machined aerospace part. Left: side view; Right: top view (note the vertical flanges, indicated by the white rectangles) – Courtesy of Sonaca S.A.***

Overlap welding 30 mm 2124 material (which is much more difficult to weld than 6xxx series of alloys) in one single pass is not possible with the FSW equipment available at CEWAC. Therefore, the flanges are built up by friction stir overlap welding two lower-thickness 2124 material plates onto a 44 mm thick base plate (in order to make abstraction of the rest of the piece). In the production route sketched in Figure 25 and below, the thick plate is addressed to as "base plate", whereas the thinner plates which serve to build up the flange are referred to as "flange plates". The black zone represents the clamping equipment (see also Figure 26).

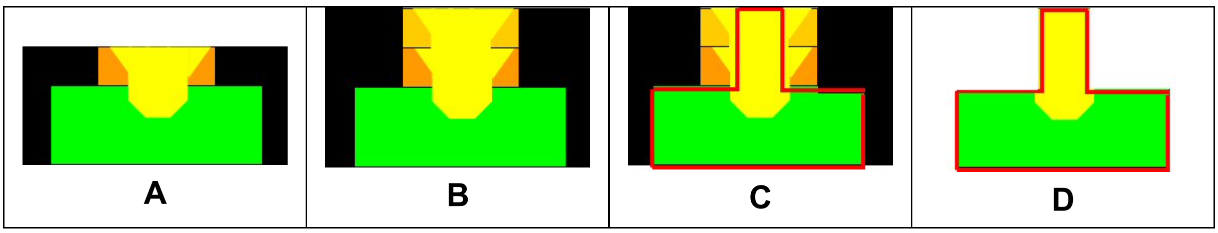

Figure 25: ***Schematic processing route for the production of flanges in 2124 material - Courtesy of Sonaca S.A.***

- The first 17 mm thick “flange plate” is overlap welded onto the base plate (Figure 25-A);
- After welding, the top 2 mm of the weld is removed by milling;

- One week after realisation of the first weld pass, a second 17 mm thick flange plate is overlap welded onto the previous weld pass (Figure 25-B).

In actual production, machining would be carried out in order to obtain the final desired dimensions of the part (Figure 25-C and D). This way, the flange will consist, after milling, of fully recrystallised material.

This production route can in fact be considered as Pro-Stir™ [29], which is a near-net shape processing technique using consecutive friction stir overlap weldments to produce the final part (after a final milling step). At this point, hardly any use of Pro-Stir™ is reported [29]-[30], so the experience obtained with this application will be valuable to assess whether for other applications Pro-Stir™ might be an appropriate technique. This technique allows:

- Building up of structures which would otherwise necessitate, using other techniques (fusion welding, machining, forging), a great degree of material loss in order to produce the desired structure;
- Manufacturing of complex structures which are difficult/impossible to produce with conventional techniques.

The main potential advantages of the new processing route that can be recognised for this case are:

- Very significant material savings compared to the current production route (estimated to 40-50%);
- Time savings (hence economical benefits);
- Economic alternative for casting, forging or linear friction welding;
- No available alternative in fusion welding processes such as MIG, TIG, (hybrid) laser welding or electron beam welding given the aforementioned high proneness to hot cracking of 2124 alloy;
- Flange built up of ultrafine-grained material.

A number of technical challenges are readily recognised in this application:

- Tool geometry optimisation in order to prevent weld defects in the overlap zone;
- Parameter optimisation in order to prevent undesired effects in the material undergoing two thermal cycles;
- Selection of the most appropriate temper and the sequence of heat treatment with respect to the welding process in order to obtain optimum properties:
    - Welding in T851 condition, no post-weld heat treatment (PWHT);
    - Welding in T4 condition, no PWHT;
    - Welding in T4 condition, followed by a PWHT consisting of artificial ageing;

   - Welding in T4 condition, followed by a PWHT consisting of solution annealing and artificial ageing;
- Adequate determination of the joint properties.

More information about the base material is given in §1.1.2. Friction stir welding work for this application is executed solely by CEWAC: such high material thicknesses are considered not suitable for welding with the UCL FSW equipment, as described in §2.2.1

The high-thickness plates were sawn to appropriate dimensions, followed by milling down to the correct thickness. The final dimensions for welding are:

- base plate: 400 mm long, 155 mm wide and 44 mm thick;
- flange plates: 400 mm long, 65 mm wide and 17 mm thick.

4.2. Experimental work: friction stir welding

Linear friction stir welding experiments were carried out CEWAC on the "smaller" ESAB SuperStir™ FSW 53 STL machine (§2.2.1). All welding experiments were carried out in force control mode. The optimised clamping system which was used for the processing route described in §4.1 is shown in Figure 26: the base plate (1) is bolted directly to the machine table with the clamping system (A), which assures a good clamping between the flange plate (2) and the base plate (1). After realisation of the first weld pass and machining off the top 2 mm from the first flange plate, clamping system (A) is replaced by clamping system (B) for welding the second flange plate. In order to avoid generation of excessive heat in the parts, a water cooled clamping system was used. Furthermore, the tool holder was cooled with a mixture of 65% water and 35% glycol, with a maximum flow rate of 5,5 l/min.

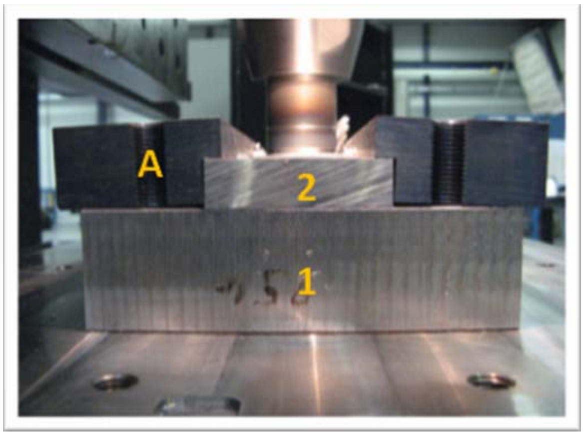

Figure 26: Experimental setup at CEWAC of the backing plate and clamping equipment for application 2.

4.2.1. Initial parameter optimisation

The welding parameters (in force control) used for this investigation are summarised in Table 8. Note that the first two digits of the designations indicate the temper of the parent material (T8: 2124-T851, T4: 2124-T4), the second digit mentions the number of weld passes, and finally the third digit gives the "tool number". Further data about the tool geometry are included in Table 9.

Table 8: Welding parameters of the current investigation; (*) see Table 9

Designation	Temper	# passes	Tool geometry (*)	Welding speed [mm/min]	Rotation speed [rev/min]	Plunge force [kN]	Tilt angle [°]
T8-1-0	T851	1	St. 1 (tool 0)	5	200	30-31	1,5
T8-2-0	T851	2	St. 1 (tool 0)	5	200	26	1,5
T4-2-08	T4	2	St. 1 (tool 0)	5	200	32,5-30	1,5
T4-1-0	T4	1	St. 1 (tool 0)	60	300	62,5	1,5
T4-2-0	T4	2	St. 1 (tool 0)	60	300	55-62,5	1,5
T4-2-1	T4	2	St. 2 (tool 1)	55	300	55-65 40-65	1,5
T4-2-2	T4	2	Triflat™ (tool 2)	55	300	55-65 40-55	0
T4-2-3	T4	2	Triflute™ (tool 3)	55	300	52,5-65 55-52,5	0

Table 9: FSW tool geometry data

	"Standard" tools		Triflat™ tool	Triflute™ tool
	Tool 0	*Tool 1*	*Tool 2*	*Tool 3*
Drawing	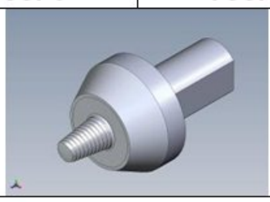		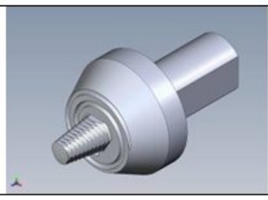	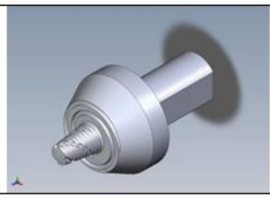
Ø shoulder [mm]	35			
Tool shoulder angle [°]	*St. 1:* 1,5 *(concave)*	*St. 2:* 1,5 *(concave)*	0	0
Shoulder features	/		spiral machined with Ø 2,5 mm ball-shaped tool	spiral machined with Ø 2,5 mm ball-shaped tool
Ø pin [mm]	15 *(shoulder)* 10 *(extremity)*			
Pitch of thread [mm]	1,5	2	2	2
Pin features	/		3 flats @ 120° 0,75 mm below pin surface	3 threads with 35 mm pitch
Pin length [mm]	20			

In 2124-T851 material, it was very hard to achieve welds without tool fracture (occurring at the base of the pin, near the shoulder). For that reason, the welding speed could not be increased above 5 mm/min. Moreover, it was not possible to include more tool features than an unprofiled concave tool shoulder and a conical threaded pin: other features such as shoulder spirals or pin flutes made the tool weaker, and fracture became more likely to occur. As a result, the 2124-T851 base material was put into the T4 temper by heat treating (see §2.2.3.6).

Intentionally, one weld in 2124-T4 material (designated *T4-2-08*, with the “8” at the end indicating that the same welding parameters as for 2124-T851 were used) was performed with comparable parameters as those used for 2124-T851.

In 2124-T4 parent material, the welding speed could be increased significantly without tool fracture (by a factor of more than 10: e.g. compare *T4-2-0* with *T8-2-0*). This led to believe that it would become possible to use more advanced shoulder and pin geometries in order to avoid the generation of weld defects.

It should be noted that for the welds *T4-2-1*, *T4-2-2* and *T4-2-3* the welding speed and rotation speed were intentionally kept the same, in order to allow for a comparison between these three different tool geometries.

Welds *T8-1-0* and *T4-1-0* were performed for comparison with *T8-2-0* and *T4-2-0*, respectively – this was done in order to check whether the realisation of a second weld pass had an influence on the base plate characteristics (more precisely: on the microhardness).

The result of optical microscopy on 26 mm thick 2124 parent materials, as well as microhardness values, are shown in Figure 27 (the same tendency was noted for the 44 mm parent materials). The displayed microhardness values are based on at least 20 individual microhardness measurements performed throughout the thickness of each parent material sample. The standard deviation is also mentioned.

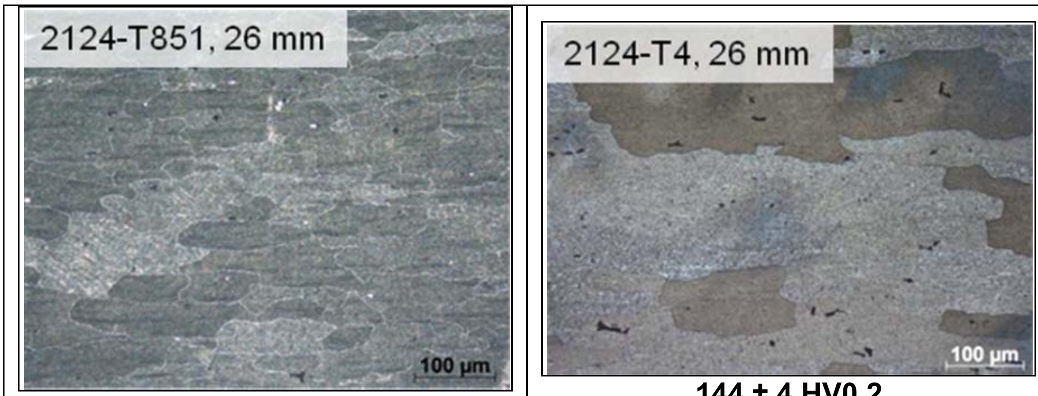

153 ± 4 HV0,2	144 ± 4 HV0,2

Figure 27: 26 mm thick 2124 parent materials microstructure and HV0,2 microhardness.

It can be derived that the T4 base material heat treatment has only a minor effect on the microhardness when compared to the original T851 temper, which indicates that the microhardness follows the same tendency as the tensile strength of the parent materials (Table 4). Furthermore, the base plate material and the flange plate material of the same temper have the same microhardness.

Macrographs of the various welds included in this investigation (see Table 8) are shown in Figure 29. No voids (tunnel defects or other) were found in the two welds in 2124-T851. In weld *T4-2-08* on the other hand, relatively small voids were visible on the advancing side near the face of the second pass which is the region where defects, assuming that they are present, tend to appear. An example of these voids – sometimes surface-breaking near the start of the weld – is shown in Figure 28.

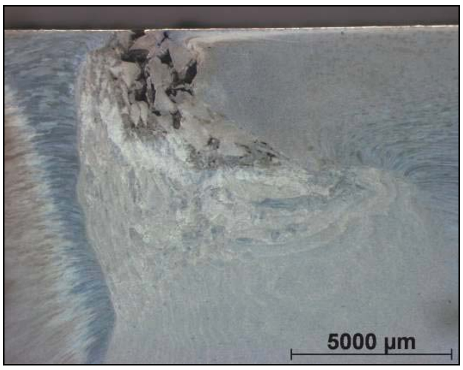

Figure 28: Macrograph of voids on AS of second pass in weld T4-2-0 (as an example).

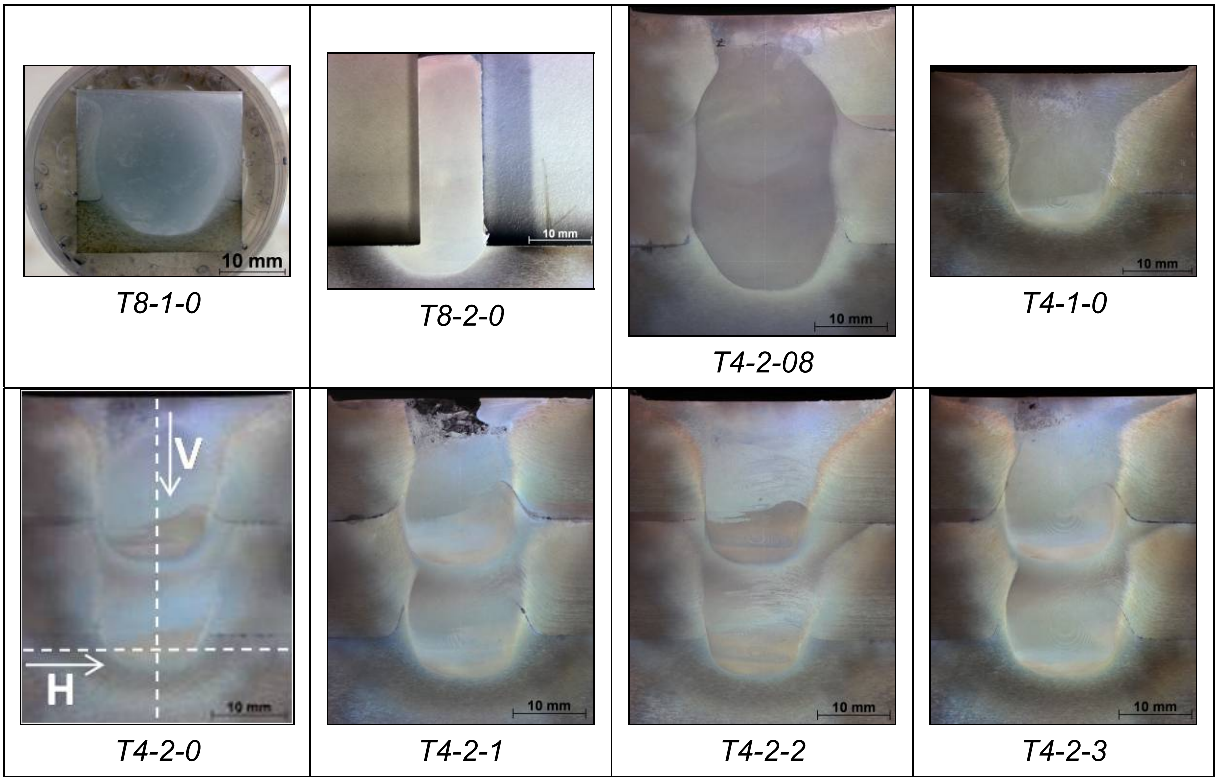

Figure 29: Etched macrographs of the joints included in this part of the investigation.

The only weld in 2124-T4 where these voids were not observed in either of the two metallographic samples extracted from each weld was *T4-2-2* (in other words: the weld realised with the Triflat™ tool). Furthermore, the nugget shape of that weld is somewhat different: it has some sort of “chalice”-like shape with relatively straight edges, whereas the nugget shape of the other welds is more rounded.

Furthermore, the metallographic samples were subjected to microstructural investigation. Some details are shown in Figure 30.

Despite large differences in welding speed, hence heat input (*T8-2-0* and *T4-2-08* compared to e.g. *T4-2-2*), the nugget grain size is very fine compared to the parent material grain size (see Figure 27) and of the same order of magnitude in all cases, namely around 2-5 µm (see Figure 30). Due to the heat treatment that the first weld pass has undergone during the realisation of the second weld pass, grain boundaries become hard to distinguish. However, no significant coarsening seems to have taken place in the nugget of the first weld pass.

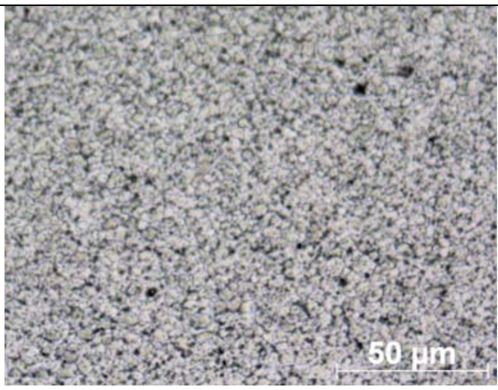

Stir zone – 2nd weld pass of *T8-2-0*

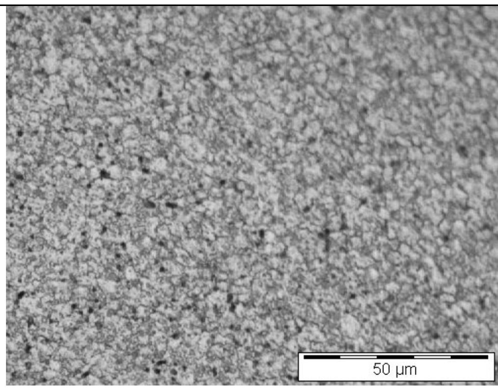

Stir zone – 2nd weld pass of *T4-2-08*

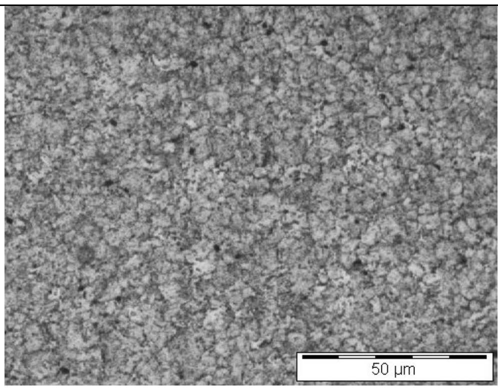

Stir zone – 2nd weld pass of *T4-2-2*

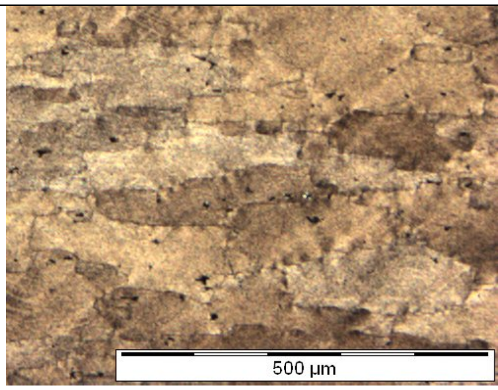

HAZ on AS of base plate in *T4-2-0*

Figure 30: Selected etched microscopic details.

Figure 31 gives the horizontal and vertical hardness traverses (refer to *H* and *V* in Figure 29, sample *T4-2-0*) for the 2 two-pass welds carried out with a very low welding speed. It is clear from Figure 31 that the microhardness profiles are more or less comparable for both states. Even though the base material temper was different, the nugget hardness of first weld pass is more or less comparable (around 70 to 80 HV0,2), meaning that due to the very high heat input, the nugget material is put into more or less the same metallurgical state in terms of precipitation; moreover it was already indicated in Figure 30 that the nugget grain size is more or less comparable.

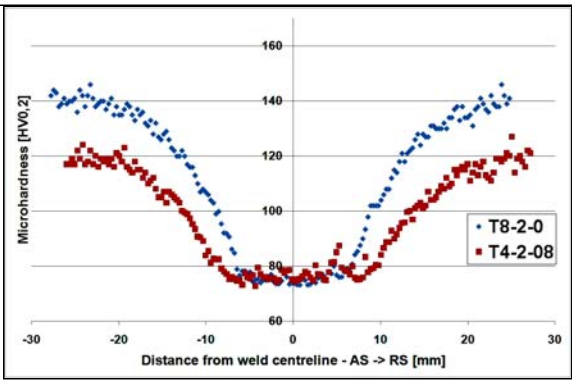

Horizontal profiles

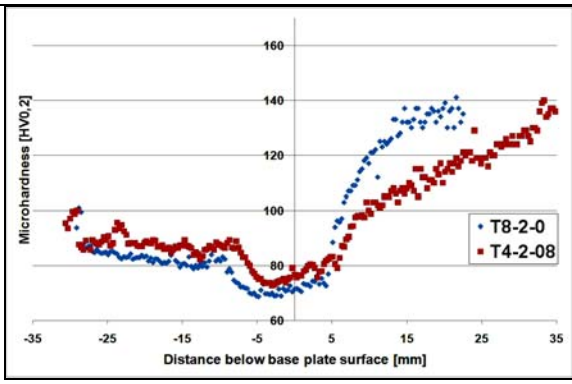

Vertical profiles

***Figure 31: HV0,2 microhardness profiles for welds* T8-2-0 *and* T4-2-08.**

In Figure 32, the hardness profiles are given of all four double-pass friction stir welds in 2124-T4, executed with more or less the same welding speed and rotation speed but with different tool design.

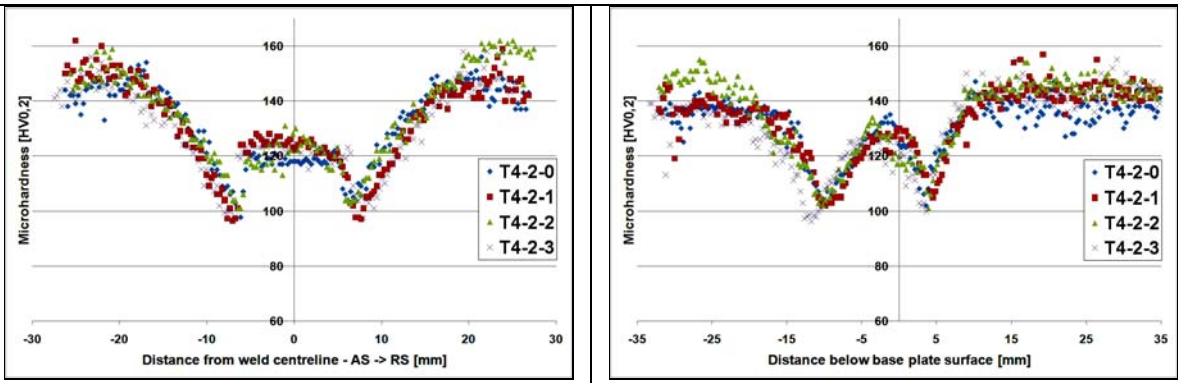

Horizontal profiles	Vertical profiles

Figure 32: HV0,2 microhardness profiles for the four different FSW tools on 2124-T4.

First of all, the attention should be drawn to the significantly different shape of the hardness profiles compared to those shown in Figure 31. In the current case, the nugget hardness (between 115 and 125 HV0,2) lies between the minimum hardness, noted in the HAZ close to the nugget (of which a micrograph is shown in Figure 30 on the lower right) with a value around 95-100 HV0,2 for the different profiles, and that of the parent material with values between 140 and 160 HV0,2. No significant differences are noted in hardness behaviour for the different tools.

Finally, Figure 33 shows the influence of the second weld pass on the first weld pass. As shown in Table 8, the welds were performed using a tool with the same geometry, but with significantly different welding parameters and a different parent material temper. No significant differences are noted in the base plate hardness development for welds realised in the same temper, which means that the influence of the second weld pass is limited to the underlying first weld pass.

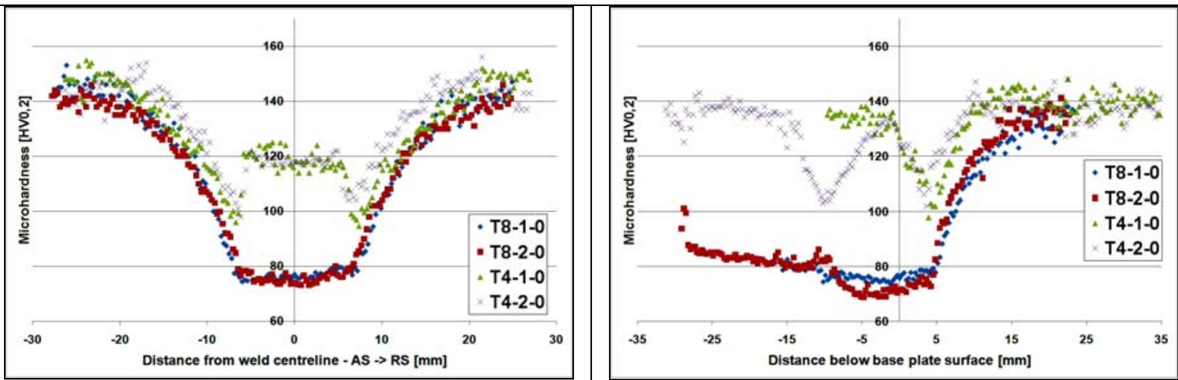

Horizontal profiles	Vertical profiles

Figure 33: HV0,2 microhardness profiles: influence of second weld pass.

Specifically for the friction stir welds in 2124-T4, the depth of penetration as well as the dimensional "interface properties" were measured, based on the macrographs – see Figure 34. The way these distances were measured is indicated in the top left figure of Figure 34. All data indicated in the graphs are based on measurements of two separate metallographic samples.

The following observations were made:

- *d* (maximum depth under the surface of the underlying plate where recrystallised material is found)
  - The penetration depth is clearly the highest for the weld realised with the lowest welding speed (*T4-2-08*), which is most likely due to the much higher heat generation, causing easier penetration.
  - Comparable penetration depths are found for the welds performed with the 4 different tool geometries and comparable welding parameters.
  - In all cases, the penetration depth of the first weld pass is lower than that of the second weld pass. Most probably, this is due to the fact that the heat can escape much more easily in the massive base plate during the realisation of the first pass, while during the second weld pass the heat will mainly escape through the lower thickness flange plates. Additionally, the base plate possesses a higher hardness during the realisation of the first weld pass than the first flange plate during the realisation of the second weld pass.
- *h* (distance that the hook extends in the flange material in vertical direction)
  - The highest *h*-values are found for *T4-2-08*, which must be related to the lower welding speed. This assumption is justified when comparing these with *T4-2-0*, executed with the same tool geometry but at a 12 times higher welding speed.
  - For the welds executed with different tool geometries but comparable welding parameters, the h-value is the lowest for tool 0 (standard tool 1) and tool 2 (Triflat™), and the highest for tool 1 (standard tool 2) and tool 3 (Triflute™).
  - No consistent tendencies could be found in terms of *h*-value for the first and second weld pass, nor for the advancing or retreating side.

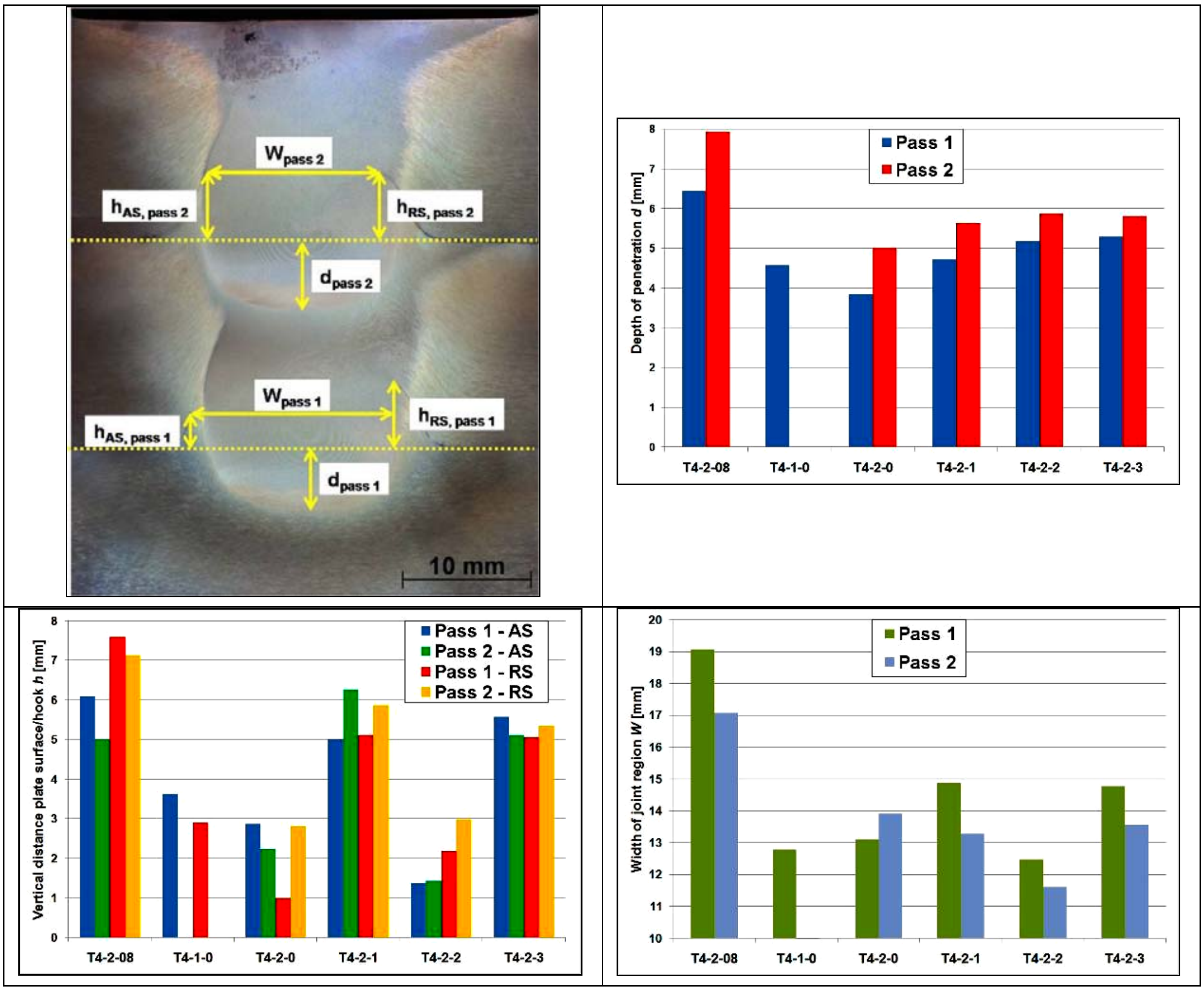

Figure 34: Depth of penetration and interface properties in 2124-T4 welds.

- *W* (width of the joint region)
  - The highest heat input condition resulted in the largest joint width.
  - With the exception of weld *T4-2-0*, the largest joint width is noticed in the first weld pass.
  - The narrowest joint width is found for weld *T4-2-2*; this is due to the fact that in this Triflat™ weld, hooking on the retreating side extends quite deeply in the horizontal direction.
  - In all conditions, the joint width is higher than 10 mm, which means that a flange of 10 mm can easily be machined out of the structure without exposing cracks to the surrounding.

4.2.2. Final study

From the results given in §4.2.1, it became clear that it is possible to realise flanges in high thickness EN AW-2124 aerospace aluminium alloy by means of consecutive friction stir overlap welds. Especially the importance of parent material temper was striking: the use of an appropriate "welding temper" allows a higher productivity on the one hand, and the use of more advanced tool geometries without risking tool pin fracture on the other hand. These more advanced tool geometries might lead to a further increase in productivity, but they have an influence especially in the generation (or avoidance) of joining defects. The optimum tool geometry at this point seemed to be the Triflat™ tool: this tool allows achieving sound welds in this material without the creation of voids. For the current application, the disadvantage of significant hooking on the retreating side in the horizontal direction encountered with this tool is of less significance, as a flange of 10 mm can still easily be machined out of the structure without exposure of this hooking to the surrounding.

In the final study, 2124-T4 base material was welded in force control mode with a TriFlat™ (see Table 9) tool. The first weld pass was carried out at 50 mm/min, with a rotation speed of 300 rpm and a plunge force of 63 kN. The second weld pass, performed one week after the first weld pass, was also realised at 50 m/min with a rotation speed of 300 rpm- however, the plunge force was reduced to 58 kN. Friction stir welds were examined in the following three "conditions":

- Naturally aged condition (duration: 1 month) – designated *NA;*
- Artificial ageing (12 hours at 190°C) – designated *AA;*
- Solution heat treatment at 493°C, followed by water quench and artificial ageing – designated *SHT+AA.*

These three conditions were subjected to metallography, microhardness testing, microtensile testing, fracture toughness testing and corrosion testing.

Etched macrographs of metallographic samples are shown in Figure 35. The *NA* and *AA* samples showed a comparable grain size in the nugget area, in the order of 2-5 µm. In the *SHT+AA* samples however, abnormal grain growth occurred (already clearly visible in the macrograph on the right in Figure 35). The occurrence of abnormal grain growth in solution heat treated friction stir welds in certain aluminium alloys has been reported in literature (e.g. [31],[32]). Abnormal grain growth occurs during the high temperature solution heat treatment; at that point, many of the fine particles present in the stir zone, used to pin the grain boundaries, are dissolved which means that grain growth can occur. As the original ultrafine-grained microstructure in the stir zone is unstable, grain growth starts in one grain which grows to a very large size, consuming all small grains in its surrounding. Furthermore, the hooking in horizontal direction, occurring to a limited extent in *NA* and *AA* samples, became more pronounced in the *SHT+AA* samples.

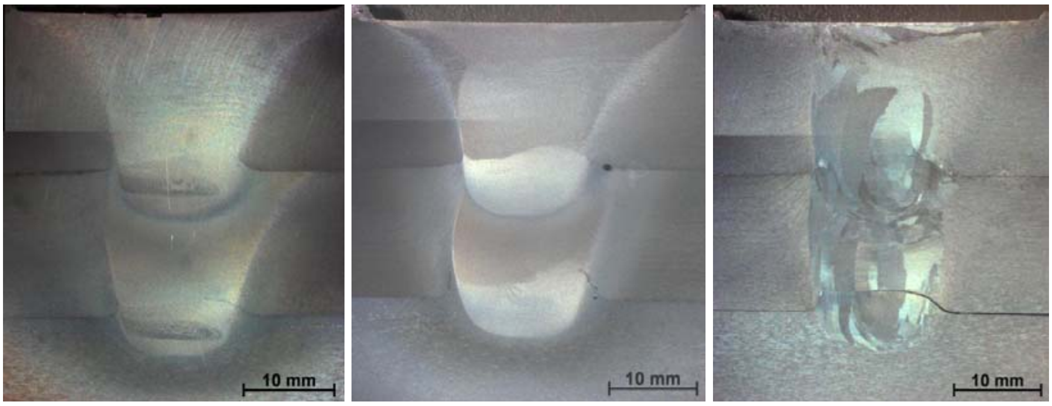

Figure 35: Macrographs of the friction stir welds in NA (left), AA (middle) and SHT+AA (right) condition.

Near the end of the weld, intergranular cracking was found in one of the *SHT+AA* samples (see Figure 36). SEM analysis of the crack surface proved that at least partial liquation had taken place along the grain boundaries. A possible approach in order to avoid this might be to apply stress relief annealing prior to the SHT.

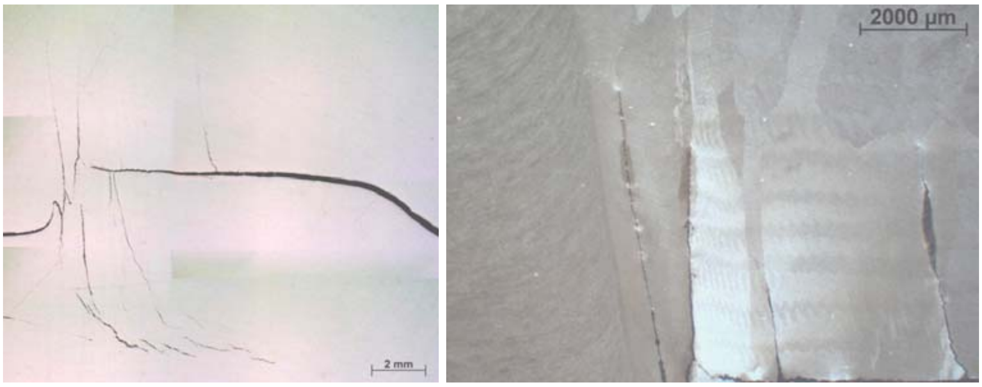

Figure 36: Cracking found in the SHT+AA sample extracted near the end of the weld.

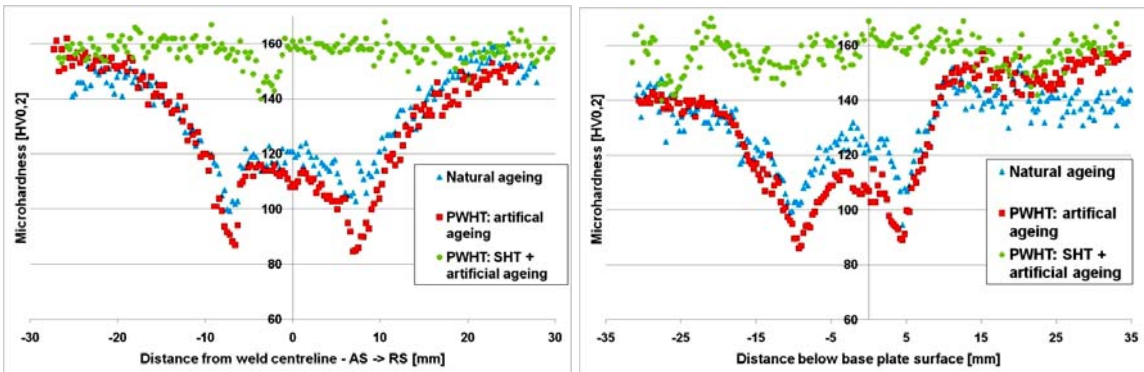

Figure 37: Microhardness results – left: horizontal hardness traverse; right: vertical hardness traverse.

The results of HV0,2 microhardness testing are shown in Figure 37. It is observed that the reduction in microhardness, found in the weld area of the *NA* and *AA* samples, is practically entirely restored by the *SHT+AA* heat treatment. Surprisingly, the *AA* sample shows lower microhardness in the weld zone compared to the *NA* sample. The microhardness results were largely confirmed by the microtensile test results performed by UCL – see Figure 38.

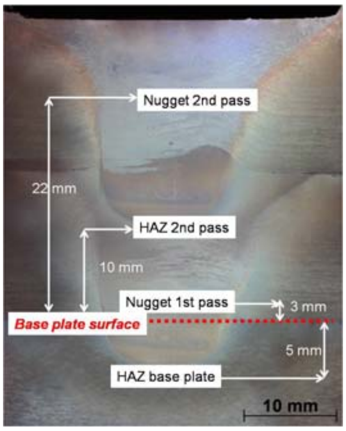

Weld condition	Location	Yield strength $R_{p0,2}$ [MPa]	Tensile strength R_m [MPa]	Elongation A_{50} [%]
NA	nugget 2nd pass	307 ± 8	455 ± 6	14,9 ± 0,3
	HAZ 2nd pass	219 ± 1	346 ± 2	11,6 ± 1,8
	nugget 1st pass	291 ± 4	418 ± 1	8,9 ± 0,5
	HAZ base plate	232 ± 9	366 ± 4	7,0 ± 0,1
	base material	306 ± 1	463 ± 5	19,6 ± 1,0
AA	nugget 2nd pass	316 ± 1	427 ± 1	8,0 ± 0,4
	HAZ 2nd pass	190 ± 2	285 ± 3	8,0 ± 1,4
	nugget 1st pass	268 ± 1	352 ± 2	6,4 ± 0,1
	HAZ base plate	227 ± 7	333 ± 8	5,4 ± 0,3
	base material	433 ± 7	484 ± 1	5,2 ± 0,3
SHT+AA	nugget 2nd pass	361 ± 5	402 ± 2	2,2 ± 0,3
	HAZ 2nd pass	367 ± 1	402 ± 7	1,6 ± 0,3
	nugget 1st pass	380	384	0,4
	HAZ base plate	383 ± 2	464 ± 1	0,7 ± 0,1
	base material	401 ± 7	478 ± 7	6,8 ± 0,5

Figure 38: Left: indication of the location where microtensile test specimens with a section of 6 mm² were extracted; Right: results of microtensile testing.

Concerning the fracture mechanics test results (see §2.2.3.7), summarised in Table 10, it was found that valid K_{Ic} values were only obtained for the 2124-T851 base material – all other samples were too thin and/or too ductile for a valid K_{Ic}. It is generally accepted that material with a crack tip opening displacement (CTOD) ≥ 0,1 mm has a good fracture resistance. The highest CTOD values were obtained for the *NA* flanges, and the lowest CTOD values for the 2124-T851 base material. It is noteworthy that, despite the very coarse microstructure, the CTOD values of the SHT+AA samples were comparable to that of 2124-T4 base material.

Table 10: Results of fracture mechanical testing

Material	Thickness [mm]	Orien-tation	K_Q (ASTM E 399) [MPa m$^{1/2}$]	ASTM E 399 - 09: valid test?	K (ASTM E 1290) [MPa m$^{1/2}$]	CTOD [mm]	ASTM E 1290 - 08: valid test?
2124-T4 base material	12,5	T-L	34,3	no (*)	48,4	0,077	no (***)
			35,7	no (*)	45,8	0,062	no (***)
			33,8	no (*)	48,7	0,096	yes
	25		53,8	no (*)	56,8	0,117	no (***)
			47,0	no (*)	56,4	0,112	no (***)
			53,4	no (*)	58,9	0,120	no (***)
2124-T851 base material	12,5		32,0	yes	32,3	0,025	yes
			31,9	no (**)	31,9	0,016	no (***)
			31,3	yes	31,8	0,020	yes
	25		31,1	yes	31,2	0,016	yes
			30,0	yes	30,3	0,015	yes
			32,8	yes	32,7	0,019	yes
welded flange natural ageing	12,5	T-S	33,7	no (*)	46,6	0,265	no (***)
			23,6	no (*)	44,8	0,266	no (***)
			27,5	no (*)	46,6	0,245	no (***)
welded flange PWHT: artificial ageing			/	no (specimen failure)	/	/	no (specimen failure)
			23,2	no (*)	44,5	0,201	yes
			29,6	no (*)	46,3	0,095	yes
welded flange PWHT: SHT + artificial ageing			35,2	no (*)	54,3	0,094	no (***)
			31,3	no (*)	52,2	0,085	no (***)
			34,2	no (*)	52,6	0,088	yes

(*) did not fulfill requirement { P_{max} / P_Q ≤ 1,10 } nor { W - a ≥ 2,5(K_Q/σ_{YS})² }
(**) did not fulfill requirement { W - a ≥ 2,5(K_Q/σ_{YS})² }
(***) valid test when applying less stringent fatigue crack front criteria according to BS 7448:Part 2

As for aerospace applications the corrosion resistance is of particular importance, base materials and selected welds were subjected to dedicated corrosion tests, namely:

- electrochemical measurements by means of potentiodynamic polarisation (calibrated by ASTM G 5);
- stress corrosion testing according to ASTM G47;
- exfoliation corrosion testing according to ASTM G34.

Stress corrosion was only found in the *SHT+AA* sample, again indicating that a very undesirable microstructure had developed during the solution heat treatment. In the *NA* and *AA* samples, exfoliation corrosion occurred in the HAZ within the base plate (caused by the first weld pass) and in the HAZ within the first weld pass (caused by the second weld pass). However, the amount of exfoliation corrosion was found to be fairly limited.

In order to get an idea of the temperatures during friction stir welding in this application, an additional weld was prepared by CEWAC with the same welding parameters as cited in the beginning of this paragraph. The temperature cycles during welding were recorded at 10 different locations. CENAERO then generated a model in MORFEO (see §2.2.4), in which also the thermal conduction into the backing plate and the clamping system was taken into account – see Figure 39. The peak temperature, reached just below the tool, was found to be approximately equal to the solidus temperature of the material (450°C). Good correlation was obtained between the simulated results and the thermocouple measurements by CEWAC.

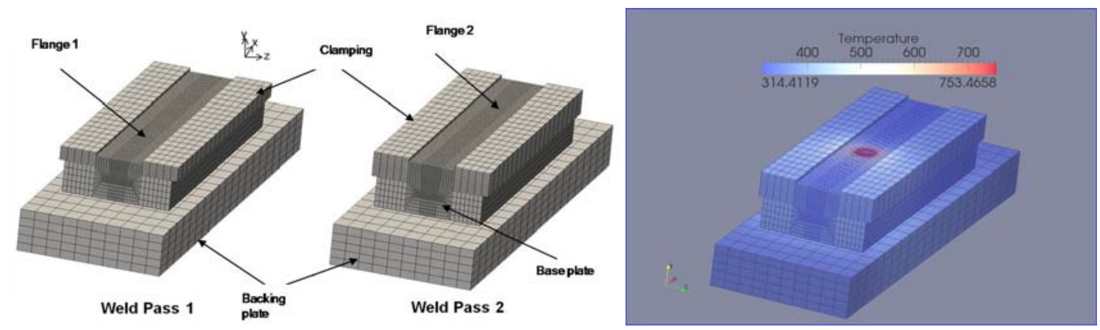

Figure 39: ***Modelling work by CENAERO. Left: setting up of the model; Right: temperature development (in Kelvin) during realisation of the second weld pass.***

4.3. Alternative production processes

As already indicated, alloy 2124 is considered non-fusion weldable due to its high hot cracking sensitivity. For that reason, only non-fusion production techniques can be considered here. The current production route consists of machining high thickness plate to the desired dimensions, which is a time-consuming process leading also to a high degree of material waste. The latter is exactly the reason why friction stir welding was considered in this project.

Production techniques besides FSW that could also lead to a significant reduction in base material waste would be casting and forging. However, it is clear that, due to the high die costs (any desired modification to the design of the part requires the production of a new die), both production techniques are only economically feasible in the case of high production series for each different design. Moreover, a high degree of specialisation is required for the casting or forging of such high added value aluminium parts, which would result in a relatively limited amount of potential suppliers – further resulting in cost increase. Other techniques that could be used for the production of the part are linear friction welding or diffusion welding. For both welding techniques, only a very limited amount of potential machine suppliers or subcontractors exist, hence these were not considered in this investigation.

4.4. Conclusions

This investigation proves that the friction stir welding technique can be applied as a sort of near-neat shaping technology in material that is practically impossible to weld by other techniques. It should be clear that, using the new production approach, the base material consumption can be significantly reduced compared to the current production route (consisting of milling).

The main challenge at this point for application 2 is to select the optimum processing route in terms of initial base material temper, welding conditions and post-weld heat treatment. This might lead to the prevention of the very undesirable ultra course-grained microstructure in friction stir welds that underwent a solution heat treatment (SHT), as well as the cracking that was observed.

In the current investigation, it became clear that welding 2124 alloy in the hardest temper (T851) in the current thickness is not feasible with the current equipment. The base material was therefore heat treated to the T4 temper, which allowed a factor of 10 increase in welding speed (50 mm/min instead of 5 mm/min), to use more advanced tool geometries, and to reduce the risk of tool fracture.

However, an even softer, but instable temper exists (namely "as fabricated" – F), e.g. in the case that the base material after the initial solution heat treatment did not receive sufficient time for natural ageing. Welding in F temper might result in further reduction of forces and increase in welding speed. This was not studied within CASSTIR, as this is very difficult from a "logistic" point of view (the material becomes harder as a function of time). It is at this point uncertain what the influence of a post-weld heat treatment would be on material friction stir welded in F-temper – it might even be possible that the undesirable microstructures and cracking noted in the solution heat treated friction stir welds no longer occur.

5. APPLICATION 3: friction stir butt welding of low-thickness 5754-H111 rolled sheet

5.1. General information

The aim of the third application was to investigate a domain which had received little scientific attention so far, namely the friction stir butt welding of sheet with a thickness lower than 1 mm (sometimes addressed to as "micro-FSW" or "µFSW"). The application foreseen with this specific case is the production of de-icing channels in aeroplane wing parts. Currently, these channels are produced in titanium, or aluminium extrusions which are drawn to the appropriate thickness and diameter.

Given the stringent tolerances imposed on these aforementioned extrusions (resulting in a limited number of potential subcontractors and high costs), an economical solution for the company could be to purchase sheet with the desired thickness (around 0,7 mm), and to produce tubes by longitudinally friction stir welding of the sheets after bending the sheet to the desired tube diameter. Very little work is published about the topic of FSW applied to low thickness sheet. Interest is however expected to increase, given the attention from e.g. the automotive sector as well. Therefore, it can be stated that the experience obtained in this application will be valuable for other applications as well, especially since 5754 material is considered somewhat <u>more</u> difficult to friction stir weld (hence more challenging) compared to e.g. 6xxx series aluminium alloys.

The foreseen advantages of the technique for this application are:

- Potentially a cost-effective alternative for titanium tubes, or aluminium tubes produced with the current production route (extrusion + drawing);
- Greater degree of freedom in terms of tube geometry (thickness, diameter);
- Possibility to produce the required tubes by the company itself (hence reducing delays);
- Environmentally friendly joining technique, which yields more or less identical properties in the weld zone as in the base material.

The main challenge in this application was the limited amount of – publicly accessible – knowledge, which means that welding problems previously not mentioned or neglected might turn up, such as thinning due to the shoulder imprint or higher sensitivity to micro-defects.

More information about the base material is given in §1.1.3. Friction stir welding work for this application was executed solely by UCL. In the limited amount of available literature on this ([33]-[35]), it is indicated that a high tool rotation speed is necessary in order to produce proper welds in material with a thickness lower than 1 mm. The UCL equipment allows for much higher tool rotation speeds than that of the current CEWAC equipment (4000 rpm at UCL compared to 2000 rpm at CEWAC) hence the former was considered more suitable.

Finally, it is important to note that micro-welding techniques are gaining importance in Belgium, as miniaturisation is one of the domains where metal-working companies can still make a difference with respect to competitors from low-wage countries. For that reason, different alternative welding techniques were tried out on this application: laser beam welding (LBW), MIG, TIG and Cold Metal Transfer (CMT) – see §5.3.

5.2. Experimental work: friction stir welding

With this experimental set-up available at UCL, two 0,8 mm thick 5754-H111 base material sheets with 600 mm length and 70 mm width were joined. The welding direction is parallel with the rolling direction. The sheet edges are milled prior to welding in order to limit the occurrence of unintentional weld gaps. Both sheets are rigidly clamped on both sides along the entire length by means of a line contact at 12 mm from the joint centreline (see Figure 40).

Figure 40: Clamping device for µFSW 0,8 mm thick 5754-H111 alloy.

In this research, two different tool geometries were used for the optimisation of the µFSW process applied to 0,8 mm thick 5754-H111 alloy. The first tool geometry was based on that described in [35], with a convex shoulder – this tool is designated "tool1" (Figure 41, left). The second tool geometry on the other hand has a concave tool shoulder – this tool is further described as "tool2" (Figure 41, right). In both cases, a conical unthreaded pin is used. In fact, the only difference between both tool geometries is the angle between the shoulder surface and the vertical axis: this is 95° in the case of "tool1", while it is 80° in the case of "tool2".

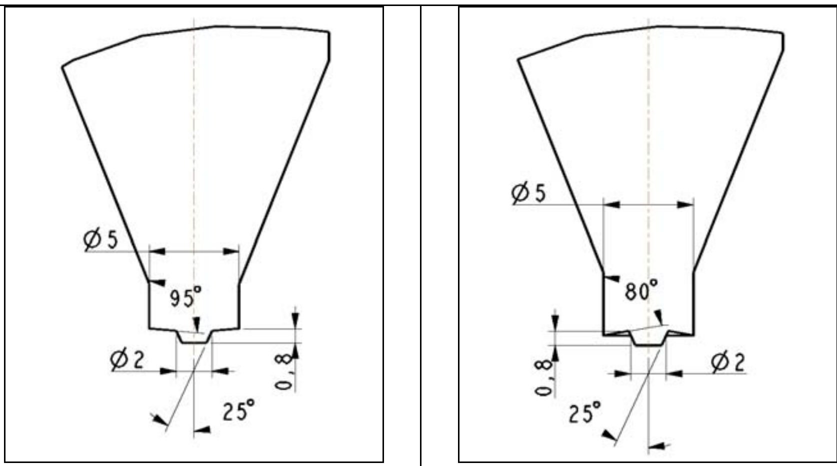

Tool1 – convex shoulder | **Tool2 – concave shoulder**

Figure 41: Tool geometries used for the FSW investigation.

All investigated welding parameters are shown in Table 11. The tool rotation speed is kept constant at 4000 rpm for all welding conditions; this corresponds to the maximum available rotation speed with the current FSW equipment. It was envisaged to study the influence of tool geometry (first digit of the experiment designation indicates whether FSW was executed with "tool1" or "tool2") and the tilt angle (second digit). Three different welding speeds were applied for each condition, namely 100 mm/min, 500 mm/min and 1000 m/min. This leads to different heat inputs: the last letter *H*, *I* or *L* corresponds respectively to “high”, “intermediate” and “low” heat input.

Table 11: µFSW parameters

Designation	Welding speed [mm/min]	Tool shoulder geometry	Tilt angle [°]	Rotation speed [rev/min]
10H	100			
10I	500	convex ("tool1")	0	4000
10L	1000			
11H	100			
11I	500	convex ("tool1")	1	4000
11L	1000			
12H	100			
12I	500	convex ("tool1")	2	4000
12L	1000			
21H	100			
21I	500	concave ("tool2")	1	4000
21L	1000			
22H	100			
22I	500	concave ("tool2")	2	4000
22L	1000			

Figure 42 shows transverse sections of the friction stir welds realised with "tool1":

- At 0° tilt angle, the weld quality was very poor: tunnel defects were present on the advancing side, and lack of penetration is evident (Figure 44). In *10I*, even surface-breaking defects are visible. There is however little weld flash or underfill.
- At 1° tilt angle, good penetration was found. A large amount of flash is generated on the RS, and an abrupt transition in thickness on the AS.
- Concerning the 2° tilt angle condition, a large flash was generated only in *12H*. The amount of underfill was considerably less compared to the 1° tilt angle condition. The welds *12H* and *12I* showed good penetration; in *12L* however, a joint line remnant was found (Figure 44).

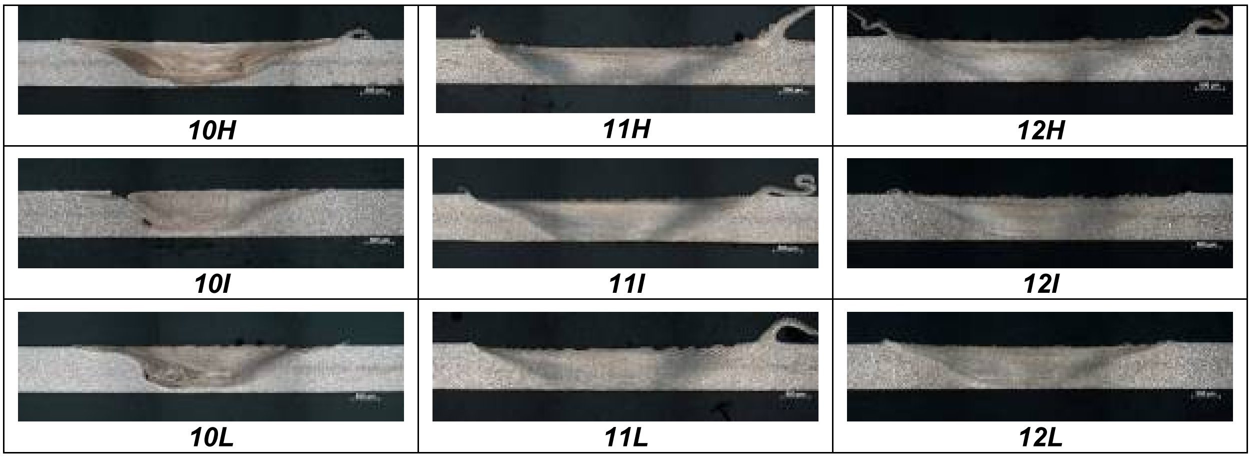

Figure 42: Etched transverse sections of the friction stir welds realised with "tool1".

Transverse sections of friction stir welds made with "tool2" are shown in Figure 43:

- In the 1° tilt angle condition, large flash was generated on both sides of the weld. Abrupt underfill occurred on the RS. In *21I* and *21L*, joint line remnants were noticed.
- In the 2° tilt angle however, the amount of weld flash was reduced, as well as the amount of underfill on the RS. In *22I* and *22L*, lack of penetration was found.

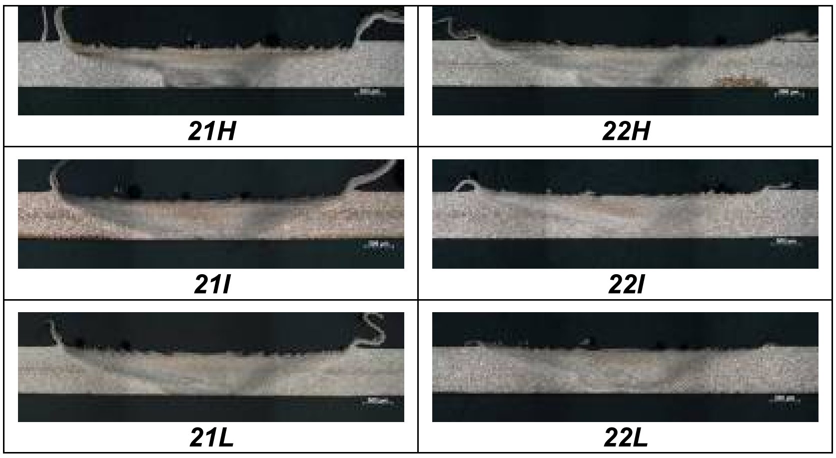

Figure 43: Etched transverse sections of the friction stir welds realised with "tool2".

***10L* – tunnel defect**

***10L* – lack of penetration**

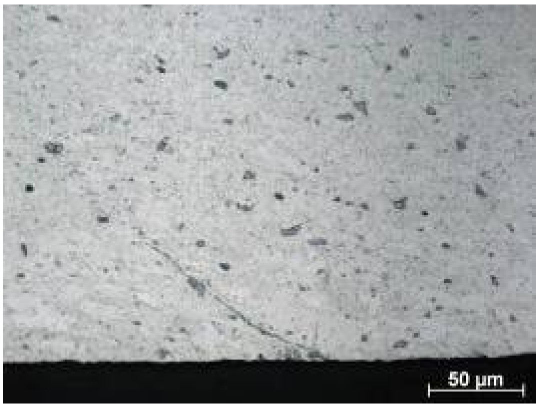

***12L* – joint line remnant**

Figure 44: Microstructural defects observed in welds realised with "tool1".

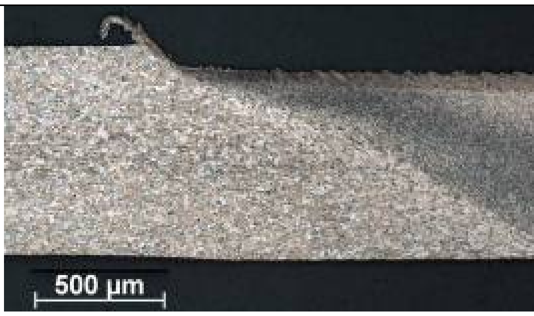

***11I* – advancing side**

***21I* – retreating side**

Figure 45: Main underfill locations in welds realised with "tool1" (*11I*) and "tool2" (*21I*).

Transverse tensile test results are shown in Table 12. High scatter between individual samples was only noted in *10H*. The best welds (highlighted in Table 12) are those of which both tensile test specimens fractured outside the weld region. These were all realised with "tool1". In the other welds, fracture in the weld zone took place due to:

- Underfill, which has a large influence with "tool2". It is remarkable that with "tool1", underfill fracture took place on the AS, whereas with "tool2", underfill fracture often occurred on the RS; these fracture locations can be associated with the abrupt thickness transition detected with metallography (see Figure 45).

- Tunnel defects, which occurred only with "tool1" in the 0° tilt angle condition; these had a large influence on the elongation after fracture and the tensile strength.
- Lack of penetration, which occurs especially in low heat input conditions.

Table 12: Tensile test results (weld flash not removed)

	Yield strength $R_{p0,2}$ [MPa]	Tensile strength R_m [MPa]	Elongation A_{50} [%]	Joint efficiency [%]	Fracture location
10H	117 ± 1	186 ± 44	8,1 ± 4,9	82	AS (underfill) nugget (tunnel defect)
10I	118 ± 1	177 ± 5	3,8 ± 0,9	78	nugget (tunnel defect)
10L	119 ± 2	181 ± 4	2,5 ± 0,2	79	nugget (tunnel defect)
11H	112 ± 5	229 ± 1	20,1 ± 0,3	100	base material
11I	116 ± 1	230 ± 1	18,0 ± 2,1	101	base material AS side (underfill)
11L	126 ± 3	227 ± 2	15,0 ± 1,6	100	AS side (underfill)
12H	113 ± 2	232 ± 1	20,5 ± 0,1	102	base material
12I	116 ± 1	232 ± 1	20,7 ± 0,9	102	base material
12L	129 ± 7	229 ± 1	15,9 ± 0,7	100	nugget (incomplete penetration)
21H	125 ± 10	211 ± 1	8,0 ± 0,3	93	RS (underfill)
21I	114 ± 3	220 ± 1	10,9 ± 0,2	96	nugget centre (underfill)
21L	125 ± 4	227 ± 4	15,9 ± 3,1	100	RS (underfill) base material
22H	115 ± 1	229 ± 1	17,7 ± 2,1	100	base material RS (underfill)
22I	118 ± 1	223 ± 7	12,5 ± 4,0	98	nugget (incomplete penetration)
22L	105 ± 16	211 ± 1	12,8 ± 6,2	93	nugget (incomplete penetration)

Face and root bend testing of the welds was performed over a bending angle of 180°, using a former diameter of 3 mm. Weld flash was not removed prior to bend testing. The following conclusions could be drawn:

- Tool1, 0°: failure during both face and root bend testing, due to – respectively – tunnel defects and lack of penetration;
- Tool1, 1°: all welds passed bend testing;
- Tool1, 2°: root bend failure only in low heat input condition;
- Tool2, 1°: root bend failure only in low heat input condition;
- Tool2, 2°: only high heat input condition passed all bend tests.

HV0,2 microhardness results are shown in Figure 46. The base material hardness ranges between 60 and 65 HV0,2. The nugget hardness is 75 - 80 HV0,2 for *12H* and *12L*, and 72 – 75 HV0,2 for *22H* and *22L*. No HAZ softening was found – which was expected given the fact that H111-temper is almost equivalent to O-temper. Figure 47 compares the base material and nugget microstructure at the same magnification. The base material microstructure is clearly refined to a typical nugget grain size of 4 to 5 µm – this was true for the nugget area of all friction stir welds.

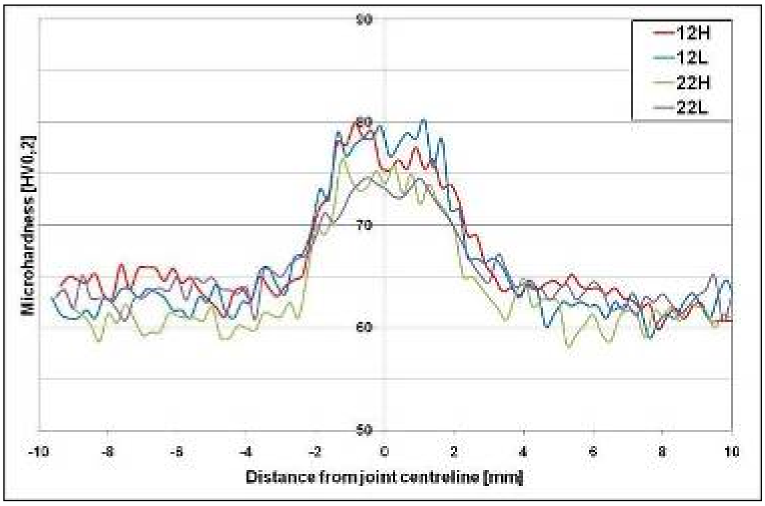

Figure 46: HV0,2 microhardness profiles, performed at mid-thickness.

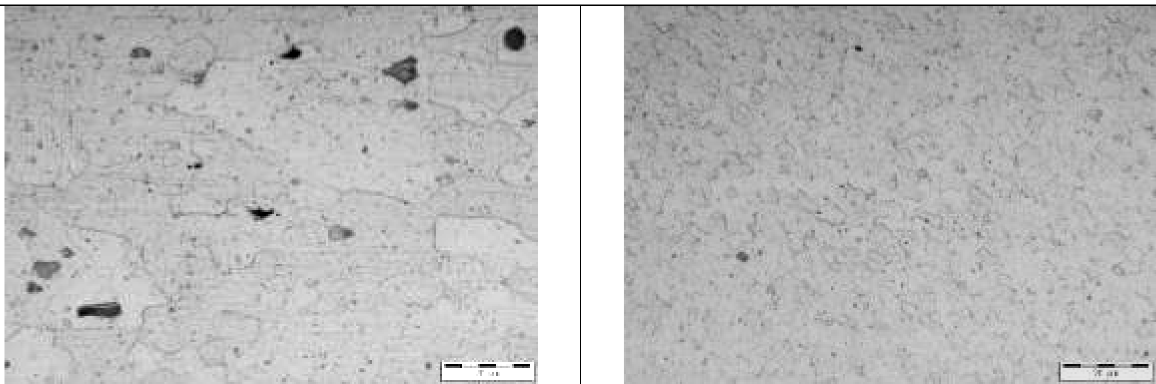

5754-H111 (0,8 mm) base material	Nugget

Figure 47: Microstructures observed in weld* 12l*.

For comparison with "conventional thickness FSW", previously unpublished results obtained in earlier work by the authors are mentioned here, carried out within project ALUWELD [27]. Friction stir butt welding was executed with the same FSW equipment on 4 mm thick 5754-O alloy, with a welding speed of 317 mm/min and a rotation speed of 1350 rev/min – an etched transverse section of the weld in question is shown in Figure 48. During tensile testing, fracture occurred in the base material. The result of HV0,5 microhardness testing is shown in Figure 49. As in Figure 46, no softening in the HAZ was found. However, attention should especially be given to the fact that the amount of hardening in the recrystallised area of the joint in Figure 49 is very limited compared to that found in Figure 46. When micrographs of the nugget microstructure are compared with the base material microstructure for the 4 mm 5754-O (Figure 50) and 0,8 mm 5754-H111 (Figure 47), the difference in grain size is evident – note that the microstructures in Figure 47 were obtained at twice the magnification of Figure 50.

Figure 48: Macrograph of the friction stir weld in 5754-O (4 mm).

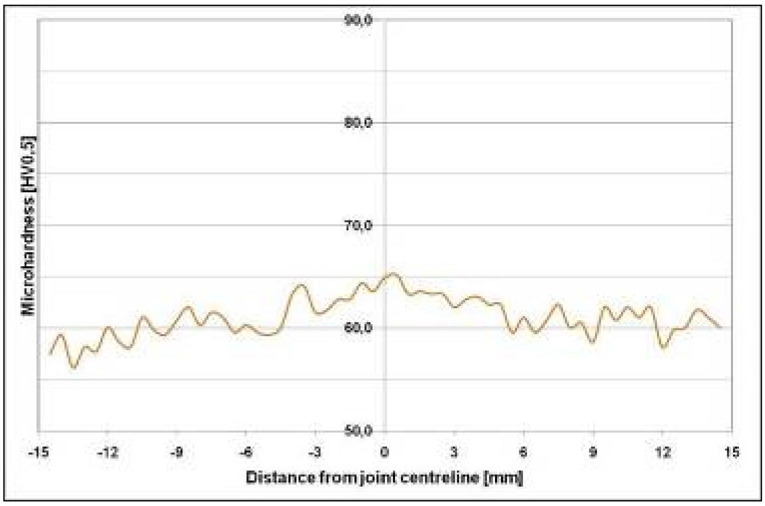

Figure 49: HV0,5 microhardness profile of the friction stir weld shown in Figure 48, measured at mid-thickness.

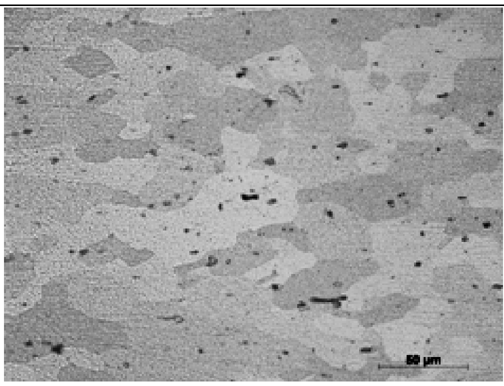

5754-O (4 mm) base material

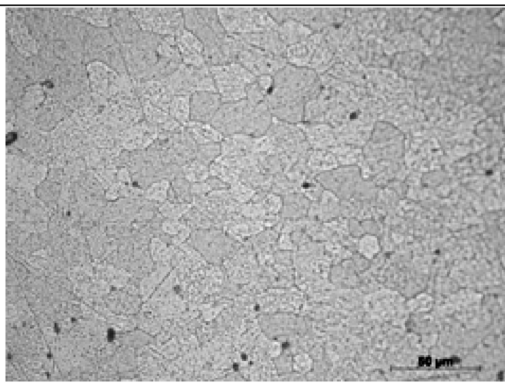

Nugget

Figure 50: Microstructures observed in the friction stir weld shown in Figure 48.

Given the foreseen application, good corrosion behaviour of the welded joints is a necessity. The amount of literature data on friction stir welds in 5754 alloy (or alloys which have a comparable chemical composition) is relatively limited ([36]- [38]).

In CASSTIR, two welds were selected for an elaborate corrosion investigation, namely *12H* and *12L*. Both welds were executed with a convex tool shoulder and 2° tilt angle. This investigation was found particularly interesting on these two welding parameter conditions, due to the larger difference in heat input (*12L* was executed at a 10 times higher welding speed than *12H*, with all other welding parameters kept constant), as well as the fact that *12L* revealed a root defect on the joint line during root bend testing; this defect was shown in Figure 44. Excessive weld flash was removed by milling in order to prevent the occurrence of unintended crevices which might distort the outcome of the corrosion tests.

Electrochemical measurements were carried out by means of potentiodynamic polarisation (calibrated by ASTM G 5). From the potentiodynamic curves of all zones tested in *12H* and *12L*, it was clear that the anodic branch of the curve was very comparable for all zones and both welds, indicating very similar corrosion behaviour. Some differences were noted in the cathodic branch; however, there seems to be no consistent trend, and this branch is also far less important in terms of corrosion behaviour of the 5754 material itself. The open circuit potentials of both welds were very comparable.

Pitting corrosion testing was carried out in a salt spray cabinet according to ASTM B 117, using a 5% NaCl solution, with pH buffered between 6,5 and 7,2. The fog flow rate (on 80 cm²) ranged between 24-48 ml/24 hours, and the testing temperature was 35°C. A long exposure time (1000 hours) was used, in order to be able to observe tendencies between the two welds. After 1000 hours, no pitting could be determined visually. However, more corrosion products were found on the root of *12H* than on that of *12L*.

Crevice corrosion testing was carried out using a Multiple Crevice Assembly, according to ASTM G 78. This test ran for 21 days at 30°C in a 3,5% NaCl solution. On both sides of the sheet, PTFE nuts were mounted with a torque of 1,6 Nm. This way, both on the root and on the face side, 20 square-type crevices are formed. After the test, the number of attacked squares was counted. The results are shown in Figure 51 – note that the "mean number of attack" is an average of 3 tests per condition.

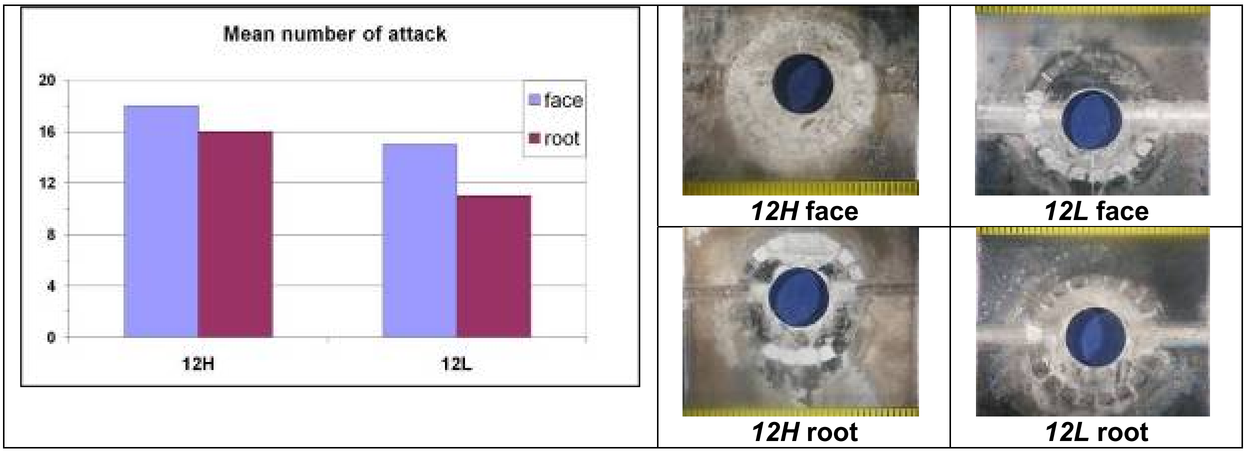

Figure 51: Results of crevice corrosion testing in accordance with ASTM G 78.

Due to the small size of the joint, only a limited amount of squares are sampling the friction stir welded area. However, it was found that the crevice corrosion resistance of the friction stir welded zone was comparable to that of the base material. The root side of the welded sheet yielded somewhat better results than the face side; furthermore, the *12H* welded sheet was attacked more than *12L*.

The resistance against <u>intergranular attack</u> was tested in accordance with ASTM G 67 (NAMLT test). This test consists of the immersion of samples during 24 hours in concentrated HNO_3 at 30°C. Specimens are weighed prior and after testing. If the weight loss is less than 15 mg/cm², the material is considered resistant to intergranular attack. Neither *12H* nor *12L* were found prone to intergranular corrosion, as the weight loss was in the order of only 1 mg/cm².

Finally, <u>exfoliation corrosion testing</u> was carried out according to ASTM G 66 (ASSET test). Macrographs of representative samples are shown in Figure 52. Exfoliation was not observed in any of the samples. Pitting corrosion took place especially on the root side of the specimens, both in the base material and along the original joint centreline. Figure 52 points out that pitting corrosion along the joint centreline is more pronounced in the case of *12L*. Most probably, this is due to the occurrence of a joint line remnant (Figure 44), which also caused failure during root bend testing.

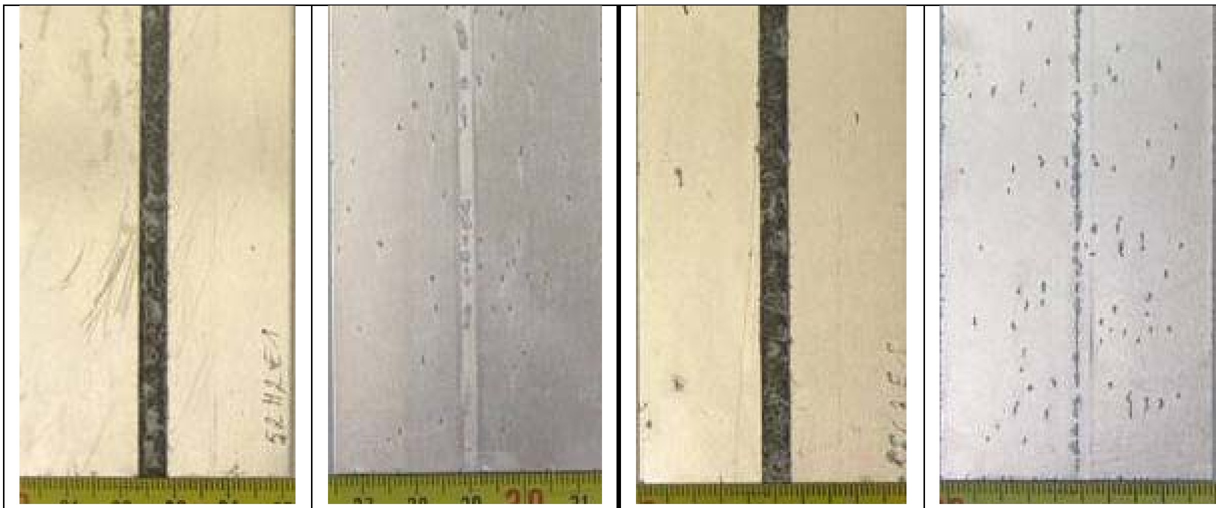

12H face	*12H* root	*12L* face	*12L* root

Figure 52: Macrographs of representative corrosion samples subjected to exfoliation corrosion testing in accordance with ASTM G 66 (ASSET).

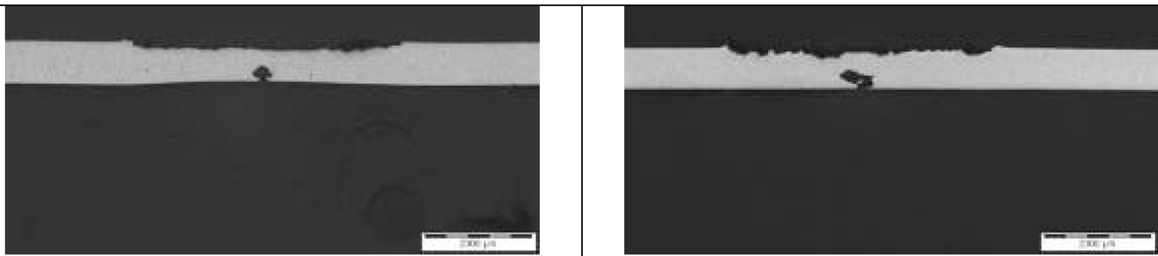

12H	*12L*

Figure 53: Transverse sections of the samples shown in Figure 52.

Figure 53 shows macrographs of transverse sections, extracted from regions in which the root was attacked. The pitting corrosion on the joint centreline runs up to half the base material thickness. On the other hand, the weld face of *12H* is attacked quite uniformly, while local depressions are noted in on the weld face of *12L*.

<u>Residual stress measurements</u> (see §2.2.3.4) were performed on friction stir welds performed with a rotation speed of 4000 rpm and three different welding speeds (namely 100, 250 and 1000 mm/min). The results are shown in Figure 54. The distributions of the residual stresses of the three friction stir welds present a similar shape. A primary maximum is situated exactly in the weld centre and two secondary ones, far away from the border of the tool, at more or less 6 mm from the weld centreline. It is more pronounced on the advancing side (negative x) where it is systematically present, which is not the case on the retreating side. The maximum tensile residual stress is between 90 and 120 MPa. This latter value is equal to the yield strength of the base material (see Table 6). The distribution of residual stress and the magnitude of their maximum is different compared to what is reported in the literature for aluminium alloys [22] and in the case of application 1 (§3.2.2).

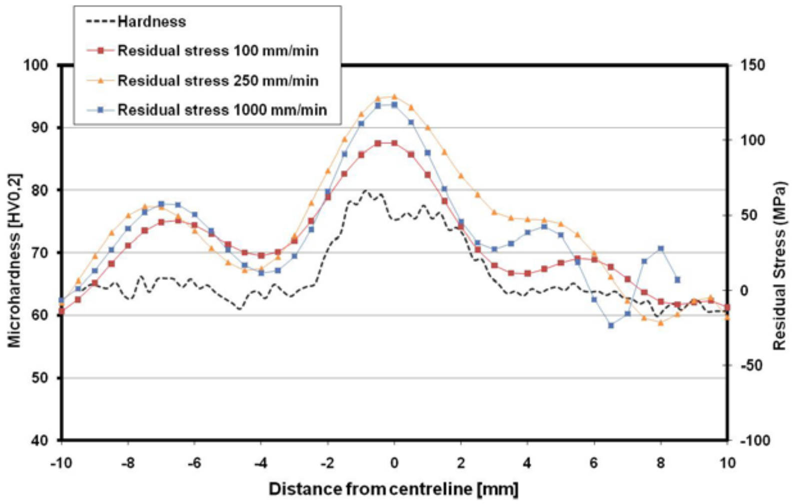

Figure 54: ***Residual stress measurements. On the same graph, in dotted line, the hardness profiles corresponding to the 100 mm/min welding speed weld is given.***

The residual stress profile may however be in relation with the hardness measurements performed previously and represented by the dotted line in Figure 54 for the case of the hotter weld. Indeed, the hardness in the weld nugget is increasing substantially in all welds (all hardness profiles are identical to the one shown) and hence the yield strength follows this increase. Nevertheless, as the tool used is “non-conventional” and has a convex shoulder and a conical pin, this as well as other phenomena may also have a significant influence on the final residual stress distribution.

5.3. Experimental work: alternative processes

As 5754-H111 alloy possesses good weldability, various welding processes could be applied to compare with FSW, namely MIG, TIG, CMT (an innovative process variant of MIG [39]) and LBW. MIG, TIG and LBW were carried out by CEWAC, and CMT by the company Interlas. The comparison with FSW in terms of energy concerns and process economy is given in §6.1.2 and 6.2.2, respectively. The main welding parameters of the various processes (including the optimised friction stir weld), together with macrographs, are given in Figure 55.

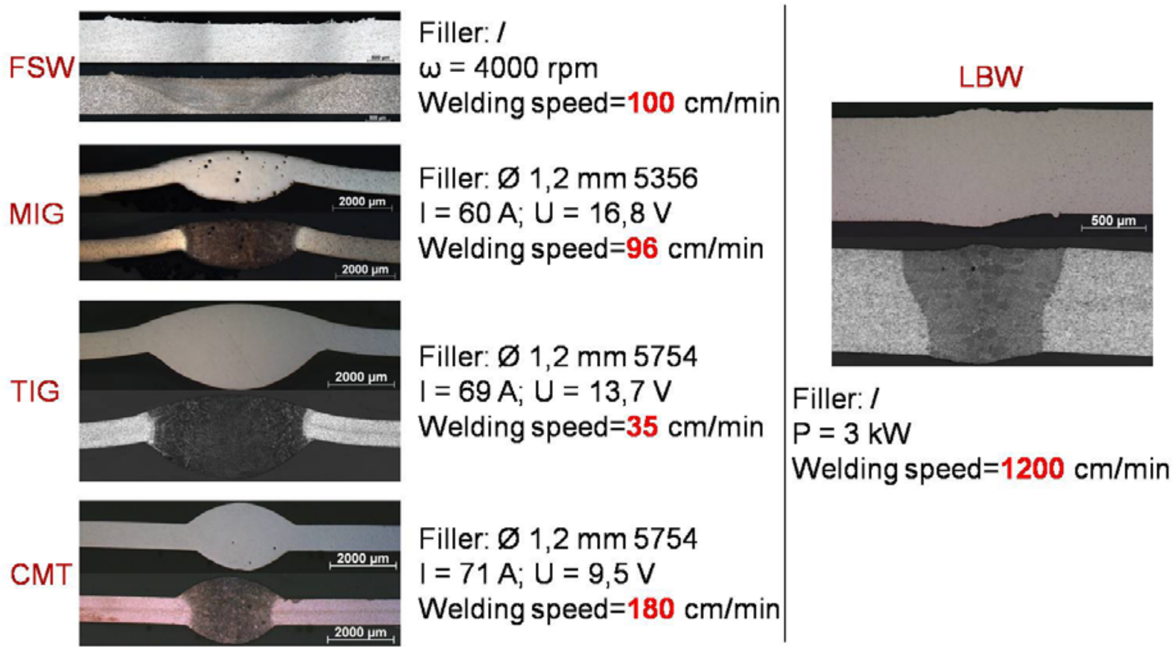

Figure 55: Unetched and etched macrographs of the welds for application 3 performed with the different processes, mentioning the main welding parameters.

Tensile test results are given in Table 13. Bend testing was also carried out on the welds realised with alternative processes. All these welds could withstand bending over 180° without cracking, using a former diameter of 3 mm.

Table 13: Tensile test results for the various processes applied to application 3

	$R_{p0,2}$ [MPa]	R_m [MPa]	A_{50} [%]	Joint efficiency [%]
FSW	126 ± 3	227 ± 2	15,0 ± 1,6	100
TIG	89 ± 7	241 ± 2	12,0 ± 2,0	106
MIG	110 ± 2	236 ± 4	15,5 ± 1,5	104
LBW	115 ± 1	239 ± 1	16,6 ± 1,0	105
CMT	110 ± 3	243 ± 1	17,4 ± 1,2	106

For the microhardness profiles (see Figure 56) and the residual stress investigation it should be mentioned that the MIG weld was not included, as MIG welding was considered intermediate in terms of heat input between TIG and CMT.

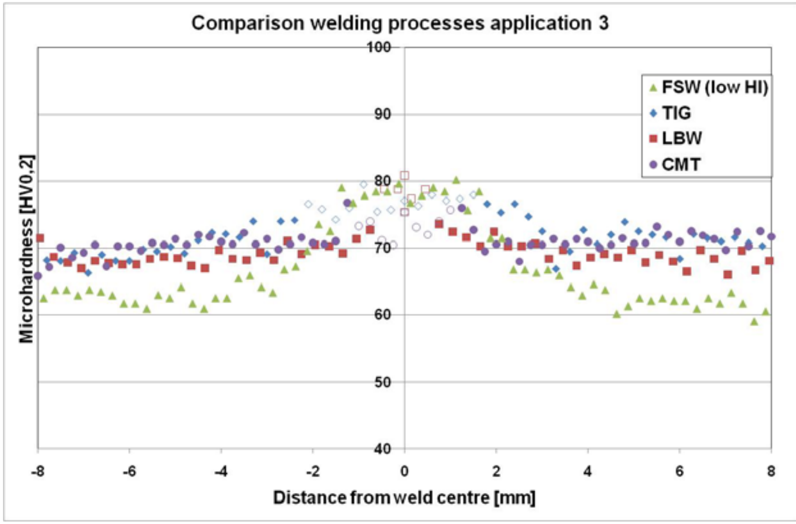

Figure 56: Microhardness profiles for the various processes applied to application 3.

Figure 57 shows the average residual stress profile of three alternative techniques together with the residual stress profile of the friction stir weld with a welding speed of 250 mm/min.

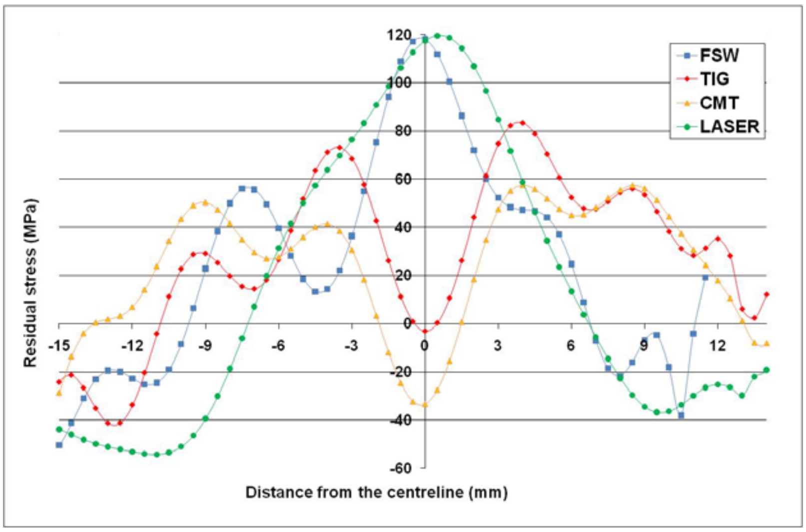

Figure 57: Residual stress measurements on 5754-H111 0,8 mm thick sheet welded with different processes.

Considering the four residual stress profiles, the two main trends are:

- The welding processes using filler material, TIG and CMT, have a tensile residual stress distribution decreasing significantly in the centre;
- Contrarily, friction stir welds and laser welds have a maximum in the weld centre, close to the base material yield strength.

Comparing the two profiles of TIG and CMT, the TIG profile is more tensile and it seems that it follows the M-shape found generally in the literature concerning aluminium friction stir welding, whereas the CMT profile has a more pronounced tensile decrease, reaching a compressive maximum residual stress of 33 MPa.

Comparing the two profiles of the FSW and LBW, the laser weld has the same maximum tensile residual stress as the friction stir weld (120 MPa), which corresponds to the yield strength of the base material (Table 6).

5.4. Conclusions

This investigation points out that FSW with a convex tool shoulder might be a good approach to successfully friction stir weld thin (< 1 mm thick) sheet. Within CASSTIR, good quality joints were produced with FSW at an acceptable welding speed (up to 1 m/min) by using a "non-conventional" tool geometry, namely with a convex tool shoulder. For such low thickness friction stir welds, the selection of a correct tilt angle is very important in terms of defect formation (tunnel defects, lack of penetration) and joint appearance (weld flash, underfill). It was found that phenomena which are not as important in high thickness alloys, such as thinning due to the tool imprint, may have a significant effect on the mechanical properties in lower thickness material. Two selected friction stir welds have been subjected to corrosion testing, which were performed with a different heat input. Both welds have proven to be resistant to intergranular attack and exfoliation corrosion, and possessed a similar behaviour during potentiodynamic polarisation. Marked differences in terms of pitting corrosion are most likely related with differences in terms of penetration and Fe pick-up during FSW.

Residual stress profiles on FSW show a maximum in the centre and two secondary maxima outside the weld seam, which is a different situation compared to application 1 (see §3.2.2).

Besides FSW, also conventional (TIG, MIG) and more advanced (LBW, CMT) fusion welding processes were applied. Given the good fusion weldability of 5754 alloy, good quality joints could also be realised with these alternative welding techniques. In terms of residual stresses, it should be noted that TIG and CMT welding (the two processes using a filler material) show a tensile drop in the centre, which is most pronounced in the CMT welds. Laser welds and friction stir welds on the other hand show a tensile maximum residual stress in the centre, with a magnitude equal to the yield strength of the base material.

6. ENVIRONMENTAL AND ECONOMIC COMPARISON

6.1. Environmental comparison

6.1.1. Application 1

Based on electrical-mechanical power measurements of both the FSW and the HLW process for application 1, Table 14 could be drawn up for the optimised welding parameter sets. Clearly, the total energy required for the realisation of 1 cm weld is much lower for FSW (2,9 kJ/cm) compared to HLW (16,3 kJ/cm). This is of course due to the high energy efficiency of the friction stir welding process. The heat input, calculated taking into account power losses due to machine movement, laser wall plug efficiency and thermal efficiency of the respective welding processes, was found to be 0,66 kJ/cm for friction stir welding, and 1,66 kJ/cm for hybrid laser welding.

Table 14: Comparison of FSW and HLW: energy aspects (application 1)

	FSW	HLW
Welding speed [mm/min]	2000	1800
Total required power [kW]	9,5	48,8
Total energy per cm weld [kJ/cm]	2,9	16,3
Power loss due to machine movement [%]	75,7	6,1
Laser wall plug efficiency [%]	/	10
Thermal efficiency [%]	95	80
Heat input [kJ/cm]	0,66	1,66

Finally, it should be mentioned that currently, laser sources with much higher wall plug efficiency than a diode-pumped Nd:YAG laser are on the market, such as the disc laser and the fibre laser [45].

6.1.2. Application 3

Using the same methodology as in §6.1.1, Table 15 was drawn up for the different welding processes applied to application 3.

Table 15: Comparison of different processes applied to application 3: energy aspects

	FSW (high HI)	FSW (low HI)	MIG	TIG	LBW	CMT
Welding speed [mm/min]	100	1000	960	350	12000	1800
Total required power [kW]	4,0	4,4	1,0	0,9	93,0	0,7
Total energy per cm weld [kJ/cm]	24,1	2,6	0,6	1,6	4,7	0,2
Power loss due to machine movement [%]	84,6	81,8	n/a	n/a	1,1	n/a
Laser wall plug efficiency [%]	/	/	/	/	3,3	/
Thermal efficiency [%]	71	75	80	60	80	80
Heat input [kJ/cm]	2,64	0,36	0,5	0,97	0,12	0,19

It should be noted that in this table, the "high heat input" (HI) weld was performed at 100 mm/min, and the "low HI" weld at 1000 mm/min, using the same rotational speed (i.e., 4000 rpm) and the same tool. From Table 15, it can be derived that the "high HI" friction stir weld requires the highest total energy per cm weld, whereas the "low HI" friction stir weld has lower energy requirements than LBW.

6.1.3. Discussion

The environmental comparison in terms of energy consumption was only carried out for applications 1 and 3, as no conventional welding process was available for application 2 (see §4.3). It is clear that FSW is in general a very environmental-friendly and safe process (symbolised in Figure 58):

Figure 58: ***A number of hazards / risks with respect to the environment which are reduced or avoided when applying FSW instead of conventional welding techniques.***

- In order to obtain acceptable joint properties in aluminium and its alloys using conventional welding processes (MIG, TIG, LBW, resistance welding), either grinding operations or corrosive and hazardous chemical cleaning agents are needed to remove the oxide layer;
- No shielding gases or filler metals are used. Emission of the inert gases used for welding aluminium alloys (Ar, He) does not lead to environmental problems – however, the production of these gases has an environmental impact;
- No fumes or ozone are generated during the process – this implies that a costly weld fume extraction system is not required and that there is no air pollution;
- No weld spatter, hence no risk of burn wounds and no fire hazard;
- No large electromagnetic fields compared to conventional arc welding processes;
- FSW is a relatively quiet process, hence the noise pollution is limited;

- In practice, the same rules in terms of safety apply as for operating a milling machine, which means that e.g. appropriate eye protection (safety goggles) remains necessary;
- Conventional welding processes normally result in excess weld metal, which can either remain in the structure (leading to additional weight), or needs to be removed (resulting in additional scrap and costs). FSW creates joints without excess weld metal, while the strength reduction due to welding is lower than encountered in conventional welding processes. Moreover, FSW allows the realisation of butt joints in aluminium alloys which could previously only joined by mechanical means (e.g., riveting). In the latter case, overlap is always required, resulting in a weight penalty.

It is well established that the FSW technique offers a high energy efficiency; this can be further optimised when applying a well-dimensioned FSW machine for the application in question – in other words, using a large FSW machine for the realisation of low-thickness joints will lead to a very significant reduction of the energy efficiency, as noted in application 3 (§6.1.2).

By all means, as FSW is a process which does not introduce additional material into the joint area, the dimensional tolerances on the workpieces to be joined are important. In the case of butt joints, a perfect I-joint is preferable, whereas for overlap joints, the contact between the workpieces should be as perfect as possible. This might require in some cases an additional milling operation. In that respect, it should be noted that for conventional arc processes applied to higher thickness aluminium alloys, a specific weld seam preparation is necessary (e.g. V-joint, X-joint…), which is often more costly and definitely leads to more scrap.

In each case, the design of the product should be adapted to the specific welding process which will be used, and this is also true for friction stir welding. In friction stir welding, basically only two welding geometries are preferable [13]: butt joints with an I-joint preparation, or overlap joints – fillet joints (which are very common with conventional welding processes) are <u>not</u> possible. For that reason, it may sometimes be hard to compare two different welding techniques.

A striking example of this is noted with application 1: the joint configuration for FSW of the hollow profiles (Figure 9 on the right) was well-suited for FSW. More heat was available in the joint area compared to FSW of flat extrusions, because the latter are always firmly clamped to a backing table (through which heat is dissipated easily). For HLW on the other hand, this joint geometry was not well-suited. In HLW (and the same is also true for classic LBW), it is always preferable to achieve a full-penetration weld, which was not possible in the present case. Moreover, while HLW of flat sheet resulted in good welds with a reasonable productivity, the hollow profile configuration in fact represented a "colder" welding condition. Indeed, in the case of HLW, the workpieces need not be firmly clamped to a backing table as it is a non-contact welding method. In the case of flat sheet, less heat dissipation occurred compared to the hollow profile, where heat could escape from the weld zone through the vertical walls of the profile. This effect was so pronounced, that it even became impossible to achieve full penetration through 4 mm material thickness with the available HLW equipment without significantly reducing the welding speed.

6.2. Economic comparison

6.2.1. Application 1

For the economic comparison between HLW and FSW, the welding cost for products was calculated, using the optimised welding parameters for the processes (Figure 59 on the left). The "product" consisted of 4 meter long double-side welded extrusion panels in 6082-T6 alloy with a 4 mm wall thickness – this means that in total, the product contains 8 meter of weld length. The calculation was made in the assumption of welding the same product during the amortisation period (set at 5 years) in 1, 2 or 3 shifts of 1750 hours per shift. Wages + overhead were assumed 40 €/h for 1 shift, 44 €/h for 2 shifts and 52 €/h for 3 shifts. By all means, increasing the amount of shifts also increases the total amount of products produced (Figure 59 on the left).

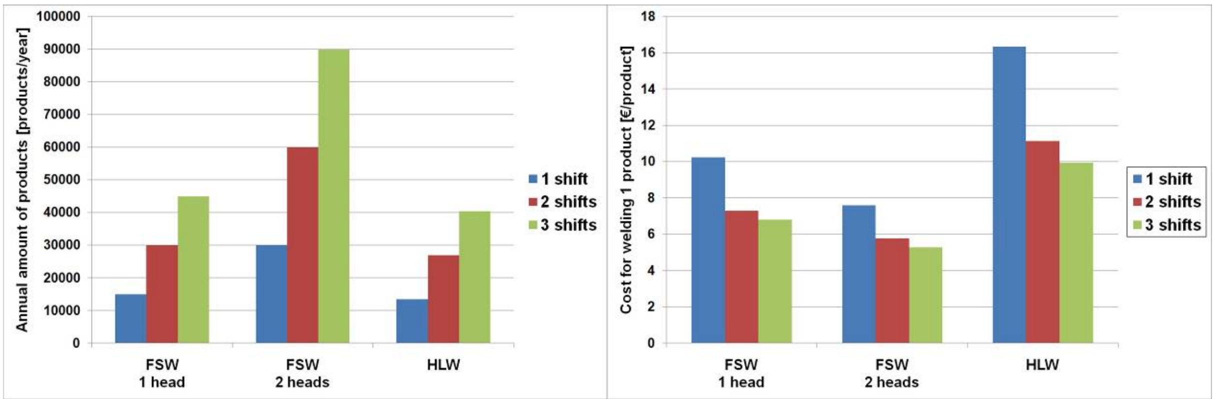

Figure 59: ***Economic comparison for application 1. Left: total annual amount of product as a function of process and amount of shifts. Right: cost for welding 1 product as a function of process and amount of shifts.***

Costs of shielding gas, filler wire, water and electricity were based on commercial data from February 2010. For the FSW tool, it was assumed that 1 tool of 270 € would last for an average of 2 km total weld length. Both for HLW and FSW, the duty cycle was set at 60%, while the up time corresponded to 95%.

The total investment cost for the HLW equipment (625 k€) was based on the cost of the equipment which was used for the hybrid laser welding experiments. For the total investments in FSW equipment, two different commercial machines, both capable of friction stir welding 4 m long panels, were taken into account. The first machine possesses 1 friction stir welding head and costs 298 k€, whereas the second machine has 2 friction stir welding heads (cost: 414 k€). As for the second machine, both sides of the product can be welded simultaneously, the production speed is doubled. Only for the FSW process a license cost has to be taken into account – the "TWI member" license cost for FSW was set for this application at 26,2 k€/year. For all equipment, a residual value of 10% of the initial investment cost was assumed. Annual maintenance and insurance costs were set at respectively 0,5% and 0,2% of the total investment cost. Interest was set at 5%, and the annual cost increase was set at 2%.

Assuming that annually 25.000 products should be produced, it can be derived from Figure 59 on the left that this is possible with HLW or FSW (1 head) in 2 shifts, and also by FSW (2 heads) in 1 shift. This corresponds to, based on Figure 59 on the right, roughly 7 €/product for FSW, and 11 €/product for hybrid laser welding.

Please note that in this calculation, the pre- and post-processing costs are not taken into account. Furthermore, recently more cost-effective laser sources such as the disc laser and fibre laser are available on the market [45]. With these lasers, showing far better laser beam quality compared to the current laser source, increased welding speed and penetration will be possible. However, for these laser sources no data were available on this application in a hybrid laser welding configuration.

6.2.2. Application 3

Using the same methodology as in §6.1.2, Figure 60 was prepared for the different welding processes with the study on application 3. In this case, the cost per meter weld length is given. Note that the calculation was only carried out for the low HI friction stir weld (i.e. welded at 1 m/min).

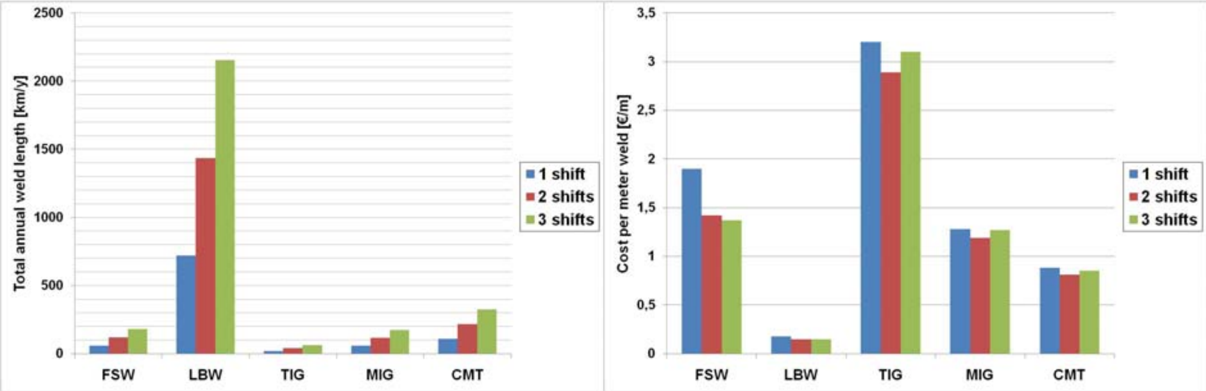

Figure 60: Economic comparison for application 1. Left: total annual weld length as a function of process and amount of shifts. Right: cost for the realisation of 1 meter weld length as a function of process and amount of shifts.

For application 3, all the same input values were used as mentioned in §6.2.1, except for the investment costs. These were the following:

- FSW: 166 k€ (the price for an adapted milling machine);
- LBW: 212 k€ (based on communication with a laser equipment supplier);
- TIG: 90 k€ (based on COSTCOMP™ programme for mechanised TIG);
- MIG: 80 k€ (based on COSTCOMP™ programme for mechanised MIG);
- CMT: 100 k€ (gross estimate).

From Figure 60, it should be derived that FSW can be performed on a conventional adapted milling machine, competitive with conventional arc welding processes.

6.2.3. Conclusion

The economic comparison of FSW with other welding processes, carried out for applications 1 and 3, proved that FSW can be highly cost-effective, even though an important license cost is associated to the process. However, it is clear that FSW is especially interesting when joints with high quality and good visual aspect are demanded, for products which have large production series and/or large weld length in common. Every welding process has its own domain of application, and the friction stir welding technique forms no exception to that rule. For instance, FSW applied to application 3 yielded good results in terms of weld properties (see 5.2) – however, as alloy 5754 has good fusion weldability, other welding processes can be considered more cost-effective for the given application. On the other hand, this investigation has also proven that a conventional milling machine adapted for FSW can successfully friction stir weld aluminium alloys (which may not be fusion weldable) with thicknesses below 5 mm. The results described in §6.2.1 and §6.2.2 were obtained using an Excel sheet, developed by the project coordinator. This Excel sheet can be delivered upon request, free of charge [46].

7. EVALUATION OF PROJECT CASSTIR BY THE AUTHORS – PERSPECTIVES

Based on the results described in this report, it should be concluded that the objectives of project CASSTIR have been largely fulfilled, albeit with minor modifications – the most pertinent being that, based on the demands of the Follow-up Committee, the amount of applications to be studied within CASSTIR was increased from 2 to 3 in order to cover a broader range than that put forward in the original project proposal.

Significant interest in the CASSTIR results has always been present, given the relatively high degree of attendance of the Follow-up Committee during the meetings on the one hand, and the large amount of accepted contributions to magazines, workshops, congresses and journals (see §8.1-8.3).

Unfortunately, nowadays many companies have to face the large challenge of surviving in the current economic climate – to give an explicit example: one of the industrial Follow-up Committee members closed down mid-2009. The economic crisis might be expected to have a decelerating effect on the industrial implementation of FSW in Belgian aluminium-processing companies compared to the timing that the research partners had anticipated when introducing the project proposal in the summer of 2006. As in the meantime one of the hurdles has been overcome, namely standardisation of the process (see §8.6.1), this delay is mainly attributed to the necessary investments in FSW equipment and FSW licence, which are relatively high. However, it is clear that innovation is the key word for companies in the metalworking sector in order to maintain, let alone expand their activities in Belgium. The benefits offered by friction stir welding will most certainly convince multiple innovation-minded companies within the next five years to invest in friction stir welding. A large growth is especially expected as from 2014, when the second TWI patent expires (in the assumption that this patent will not be prolonged, or that no other patent will become applicable). In the course of implementing the technique in production, these companies can count on the expertise gathered within project CASSTIR by the research partners: even though a limited number of applications was studied within CASSTIR, the results of this project can be extrapolated (or, given the very broad thickness range covered, "interpolated" might be more correct) to other products, and most of the good practice guidelines that can be derived implicitly from the research remain valid for other applications. In the meantime, the research partners strive to continue to develop their competence in the field of friction stir welding (e.g., micro-friction stir welding, friction stir spot welding, friction stir welding of steels) through both projects for industry and publicly funded research projects.

8. DISSEMINATION AND VALORISATION

8.1. Peer review articles

- Details: "Friction stir overlap welding of 2124 aluminium plate" – W. Van Haver, A. Geurten, B. de Meester, J. Defrancq
  Journal: Sustainable Construction & Design volume 1, 2010, pp. 73-84 (ISBN 978-9-49072-600-3 – ISSN 2032-7471)
- Details: "Residual stresses measurements on friction stir welding of aluminium alloys" – K. Deplus, A. Simar, W. Van Haver, B. de Meester
  Journal: Science and Technology of Welding and Joining – FSW special issue (submitted)
- Details: "Chaining of Friction Stir Welding and Machining simulations" – V. Madhavan, L. D'Alvise, K. Deplus, B. de Meester
  Journal: Science and Technology of Welding and Joining – FSW special issue (submitted)

8.2. Other publications

- Details "Friction stir butt welding of thin 5754-H111 sheet for aerospace applications" - W. Van Haver, K. Deplus, B. de Meester, A. Simar, W. Van Daele, J. Defrancq, A. Dhooge
  Journal: Conference proceedings of the 7th International FSW Symposium, 20-22 May 2008, Awaji, Japan (ISBN 13-978-1-903761-06-9)
- Details: "Friction stir welding van aluminium" / "Friction Stir Welding d'aluminium" - Wim Van Haver
  Journal: Metallerie / Métallerie 117 (September 2008), pp. 74-76
- Details: "Applications technologiques – Friction stir welding" – Alban Geurten
  Journal: AIHE Revue, n° 162, avril-mai 2009, pp. 48-50
- Details: "Applications technologiques – Friction stir welding (suite)" - Alban Geurten
  Journal: AIHE Revue, n° 163, juin-juillet 2009, pp. 32-33
- Details: "Innovaties Friction Stir Welding" / "Friction Stir Welding: Innovations" - Wim Van Haver
  Journal: Metallerie / Métallerie 129 (September 2009), pp. 65-69
- Details: "Nieuwe lastechnologie bij BIL en CEWAC" - Luc De Smet (reporter of Vraag&Aanbod – based on interview with Wim Van Haver on 25/06/2009)
  Journal: Vraag&Aanbod nr. 36, jaargang 56 (di 08-09-09), pp. 14-15

- Details: "Friction stir overlap welding of thick 2124 aluminium plate" - W. Van Haver, A. Geurten, B. de Meester, J. Defrancq
  Journal: Proceedings (abstracts: ISBN 978-80-88734-61-1 – paper: on CD-ROM) of the First IIW International Congress in Central and East European Region on "Progressive structural materials and their joining technologies", 14-16 October 2009, Stará Lesná, High Tatras, Slovakia
- Details: "Vergelijking van Friction Stir Welding met andere verwerkings-procédés" - Wim Van Haver
  Journal: Proceedings of BIL / NIL Lassymposium 2009, 24-25 November 2009, Het Pad, Gent, Belgium
- Details: "Characterisation of consecutive friction stir overlap welds in thick 2124 aluminium plate for build-up of flanges for aerospace applications" - W. Van Haver, A. Geurten, J. Defrancq, B. de Meester, A. Simar
  Journal: **abstract approved** for oral presentation during 8th International FSW Symposium, Timmendorfer Strand, 18-20 May 2010, Germany
- Details: "Friction stir and hybrid laser welding of hollow extrusion profiles for transportation purposes" - W. Van Haver, B. de Meester, A. Geurten, J. Verwimp, J. Defrancq
  Journal: **abstract approved** for oral presentation during 11th INALCO 2010 "New frontiers in light metals", – 23-25 June 2010, Eindhoven, NL

8.3. Other actions

- Webpages dedicated to CASSTIR by various partners (among which three members of the Follow-up Committee):

BWI:

EN: http://www.bil-ibs.be/nl/Onderzoek/pdf/CASSTIR_proposal.pdf
NL: http://www.bil-ibs.be/nl/Metallerie/pdf/casstir-NL.pdf
FR: http://www.bil-ibs.be/fr/Metallerie/pdf/Casstir-FR.pdf
NL: http://www.bil-ibs.be/nl/Metallerie/pdf/Metallerie%20129%20-%20CASSTIR%202009%20-%20NL.pdf
FR: http://www.bil-ibs.be/fr/Metallerie/pdf/Metallerie%20129%20-%20CASSTIR%202009%20-%20FR.pdf

UCL:

EN: http://rch.adre.ucl.ac.be/search_project.php?cid=2&eid=2&unit=PRM &project=10019915
FR: http://rch.adre.ucl.ac.be/search_project.php?cid=3&unit=PRM &project=10019915&newlang=fr&

CEWAC:

FR: http://www.cewac.be/index.php?page=news&idnews=newspage18.html
FR: http://www.cewac.be/Actualites/docwebcasstirrev2.pdf

CENAERO:

EN: http://fsw.cenaero.be/index.php?option=com_content&task=view&id=61&Itemid=105

Sapa RC Profiles:

EN: http://www.sapagroup.com/en/Company-sites/Sapa-RC-Profiles/Other/Research/
DE: http://www.sapagroup.com/de/Company-sites/Sapa-RC-Profiles/Sonstiges/Forschung/
FR: http://www.sapagroup.com/fr/Company-sites/Sapa-RC-Profiles/Autre/Recherche/
NL: http://www.sapagroup.com/nl/Company-sites/Sapa-RC-Profiles/Overige/Onderzoek/

Belgian Science Policy

EN: http://www.belspo.be/belspo/Fedra/proj.asp?l=en&COD=P2/02
NL: http://www.belspo.be/belspo/home/publ/pub_ostc/PAT/PAT_nl.pdf
FR: http://www.belspo.be/belspo/home/publ/pub_ostc/PAT/PAT_fr.pdf
EN: http://www.belspo.be/belspo/home/publ/pub_ostc/PAT/PAT_en.pdf

- Website http://fsw.cenaero.be allowing the Follow-up Committee members to download all relevant CASSTIR documents through a password.
- Distribution of CASSTIR project information
  Event: Official opening of the Friction Stir Welding Center – Ghlin (19/01/2007)
- Poster presentation about project CASSTIR
  Event: "Graduate School in Mechanics" – Louvain-La-Neuve (11/05/2007)
- Poster presentation about project CASSTIR
  Event: "MecaTech" – Louvain-La-Neuve (14/06/2007)
- Poster and continuously running presentation mentioning project CASSTIR
  Event: Welding Week – Antwerp (16-19/10/2007)
- Presentation "Friction stir Welding"
  Event: Journée Technique "Assemblage et ingénierie de surface" – Nivelles (31/01/2008)
- Paper presentation "Friction stir butt welding of thin 5754-H111 for aerospace applications"
  Event: 7th International FSW Symposium – Awaji (JP) (21/05/2008)
- Presentation about FSW within "2.23 – Aluminium and aluminium alloys"
  Event: Course "International Welding Engineer" – Brussels (04/11/2008)
- Presentation "Warm verbinden van metalen"
  Event: CLUSTA workshop "Verbindingen in metaal" – Nazareth (12/11/2008)
- Presentation "Onderzoek naar de Friction Stir Welding techniek in België"
  Event: "NIL-BIL Lassymposium 2008" – Eindhoven (NL) (26/11/2008)
- Paper presentation "Friction stir overlap welding of thick 2124 aluminium plate"
  Event: First IIW International Congress in Central and East European Region on "Progressive structural materials and their joining technologies" – High Tatras (SK) (16/10/2009)
- Presentation "Vergelijking van Friction Stir Welding met andere verwerkings-procédés"
  Event: "BIL / NIL Lassymposium 2009" – Ghent (24/11/2009)

- Paper presentation "Residual stresses measurements on friction stir welding of aluminium alloys"
  Event: "FSWP 2010" – Lille (FR) (28/01/2010)
- Paper presentation "Chaining of Friction Stir Welding and Machining simulations"
  Event: "FSWP 2010" – Lille (FR) (28/01/2010)
- Paper presentation "Friction stir overlap welding of 2124 aluminium plate"
  Event: "Day of Research 2010" – Ghent (10/02/2010)
- Poster presentation about (among other BWI projects) project CASSTIR
  Event: "Day of Research 2010" – Ghent (10/02/2010)
- Poster presentation about (among other BWI projects) project CASSTIR
  Event: "METAPRO 2010" – Brussels (9-12/02/2010)
- Distribution of CASSTIR project information
  Event: "METAPRO 2010" – Brussels (9-12/02/2010)

8.4. Foreseen action: FSW seminar

On June 8th, 2010, a half-day workshop will be organised by the CASSTIR research partners, entitled "Friction stir welding of aluminium alloys". The programme of this workshop consists of 5 technical presentations (at Hôtel Mercury Mons, Nimy), followed by a FSW demonstration at the nearby company Sapa RC Profiles (Ghlin), that belongs to the CASSTIR Follow-up Committee. This workshop is open to all interested companies and institutions. The following presentations are foreseen:

- "TAP2 project CASSTIR – main results" – by W. Van Haver (BWI)
- "Sapa and FSW" – by M. Ryckeboer (Sapa RC Profiles)
- "Qualification of FSW equipment – application to an FSW robot" – by S. Zimmer (Institut de Soudure, France)
- "Friction stir welding of aluminium aerospace alloys" – by A. Norman (Corus Reseach and Development, the Netherlands)
- "ESAB – A world leading FSW machine supplier" – by J. Norström (ESAB AB, Sweden)

8.5. Technological advisory service

Technological advisory services are present at both BWI (in Flanders funded by IWT, in Wallonia by DG06) and CEWAC (funded in Wallonia by DG06). These advisors are in very close contact with the respective promoters of project CASSTIR, and are well aware of the results obtained within the project. Publicly accessible information will always be handed out upon request to interested companies. In case of doubt, the promoter will ask approval of the Programme Administrator.

8.6. Standardisation work – license issues

Within project CASSTIR, attention also went out to standardisation of FSW applied to aluminium alloys, as well as towards the license(s) connected to the application and development of the FSW technique. The Follow-up Committee members were informed about these issues during the Follow-up Committee meetings.

8.6.1. Standardisation work

Given the increasing number of contracts and subcontracts for FSW activities, international agreements needed to be made with respect to weld quality requirements, as well as harmonisation and standardisation of welding procedure specification and welding procedure qualification record in the field of friction stir welding – see Figure 61 [47]. This should further accelerate the commercial use of FSW. For that matter, in 2003 a new working group for standardisation of FSW applied to aluminium and its alloys was started up within the framework of the International Institute of Welding (IIW), This standardisation work has in the meantime resulted in the final draft international standard EN ISO 25239 ("Friction stir welding – Aluminium"), subdivided in 5 parts:

- Part 1: Vocabulary;
- Part 2: Design of weld joints;
- Part 3: Qualification of welding operators;
- Part 4: Specification and qualification of welding procedures;
- Part 5: Quality and inspection requirements.

The CASSTIR partners supported in the preparation of this standard, by sending comments to the Belgian standard body (NBN) on ISO/DIS 25239 in January 2008, and ISO/FDIS 25239 in September 2009.

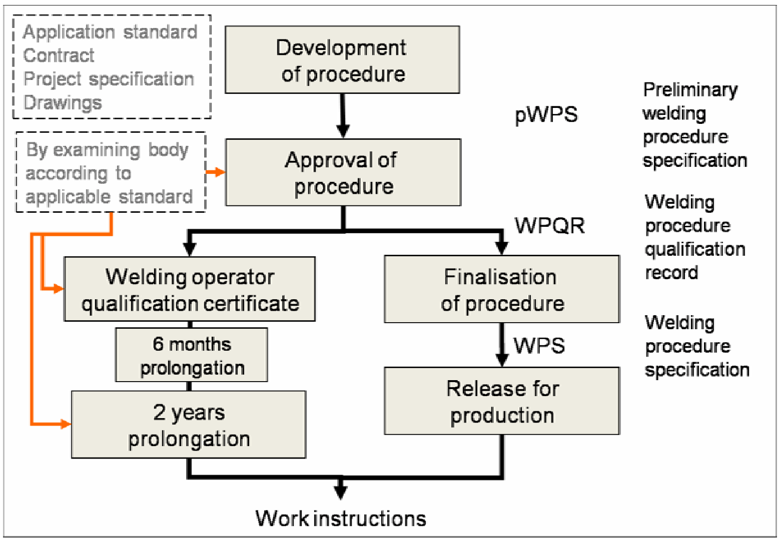

Figure 61: Stages in FSW approval.

8.6.2. Licence issues

As already indicated in §1.3, the FSW technique was invented and patented by TWI in 1991 [1]. However, in 1995 a second patent was granted – first to Hydro [48], which was assigned shortly afterwards to TWI [49]. The latter patent expires in 2014. The first commercial use of FSW was by Hydro, in 1995 (refrigeration panels). In 2008, 178 organisations were holding an FSW licence, distributed as follows [50]:

- UK + EU: 57 (industry: ±55%)
- Japan: 40 (industry: ±66%)
- USA + Canada: 42 (industry: ±45%)
- China + South-East Asia: 39 (industry: ±25%)

The annual licence fee is stated to be £ 23.000 for TWI members, and £ 33.100 for non-TWI members. However, in some cases the fee is based on the amount of relevant income, and there are also arrangements between TWI and a limited amount of FSW equipment manufacturers, so these figures cannot be generalised. It should be mentioned here that also individual arrangements with TWI are required for universities and non-commercial research centres. In Belgium, UCL has a permanent FSW licence since 2002, while the FSW licence of CEWAC was incorporated in the purchase of the FSW equipment in 2005.

Companies or research institutions interested in carrying out friction stir welding are strongly advised to step into direct negotiations with TWI – see [51].

In 1996, the first third party FSW related patents were filed. In 2008, more than 1900 patents filings were recorded (an actual list is available in [52]), with an average 30% success rate. The patent topics are distributed as follows:

- Products and applications: 52%
- Apparatus / equipment: 18%
- Tool shape and configuration: 8%
- Process variation: 18%
- Friction spot and friction stir spot welding: 4%

9. ACKNOWLEDGEMENTS

The research partners wish to thank the Belgian Science Policy, which funded the research of the CASSTIR project within the "Programme to stimulate knowledge transfer in areas of strategic importance". Furthermore, they are grateful to the members of the CASSTIR Follow-up Committee for their active support, the companies outside the Follow-up Committee which provided input to the project, the subcontractor CENAERO, and finally all colleagues from the BWI, CEWAC, UCL and UGent which have contributed in the experimental work and valorisation.

10. REFERENCES

[1] W.M. Thomas et al.: "Friction Stir Butt Welding", International Patent Application PCT/GB92/02203, GB Patent Application 9125978.8, 6 Dec. 1991
[2] http://www.eaa.net/eaa/education/TALAT/lectures/110001.pdf
[3] http://www.eaa.net/eaa/education/TALAT/lectures/1102.pdf
[4] http://www.world-aluminium.org/production/processing/properties.html
[5] http://www.azom.com/details.asp?ArticleID=1446
[6] J. Moran: "Effects of Metallurgical Variables on the Corrosion of Aluminium Alloys", ASM Handbook, volume 13A, ASM International (2003), 275-278
[7] "Aluminum and Aluminum Alloys", ASM Specialty Handbook, ed. J. R. Davis (1993), 784 pages
[8] "Aluminum: Properties and Physical Metallurgy", ASM International, ed. J. E. Hatch (1984), 424 pages
[9] http://www.aluminium.matter.org.uk/content/html/eng/default.asp?catid=49
[10] Emiel Wettinck: "Lasmetallurgie van non-ferro legeringen", UGent syllabus
[11] G. Mathers: "The welding of aluminium and its alloys", Woodhead Publishing ISBN 1 85573 567 9, September 2002, 248 pages
[12] http://www.twi.co.uk/content/jk21.html
[13] R. S. Mishra, Z. Y. Ma: "Friction stir welding and processing", Materials Science and Engineering: R: Reports, Volume 50, Issues 1-2, 31 August 2005, pp. 1-78
[14] W. M. Thomas et al.: "Developments in Friction Stir Welding", ASM Materials Solutions 2003 Conference & Exposition, 13-15 October 2003, Pittsburgh, Pennsylvania, USA
[15] A. Simar: "A multiscale multiphysics investigation of aluminium friction stir welds from thermal modelling to mechanical properties through precipitation evolution and hardening" (2006)
[16] G. Stöcklin: "Innovative welding of aluminium alloys Hybrid Laser Welding and Friction Stir Welding Literature: review, Friction Stir Welding - State of the Art" (project ALUWELD – IWT 30909)
[17] http://www.twi.co.uk/content/fswapp.html
[18] S. Zimmer et al.: "Le soudage par Friction Malaxage – Friction Stir Welding – Manuel Pédagogique", ISBN 978-2-900781-67-8, 47 pages
[19] http://www.uddeholm.be/french/files/Uddeholm_QRO_90_Supreme_E2.pdf
[20] T. Ummenhofer, J. Medgenberg: "On the use of infrared thermography for the analysis of fatigue damage processes in welded joints", International Journal of Fatigue, Volume 31, Issue 1, January 2009, pp. 130-137
[21] I. Finnie and W. Cheng: “Residual Stress Measurement and the Slitting Method”, Mechanical Engineering Series, 2007.
[22] M. B. Prime: “Residual stress measurement by successive extension of a slot: The crack compliance method”, Applied Mechanics Reviews, 1999, Vol.52 No.2, pp.75-96.
[23] http://www.cenaero.be/Page_Generale.asp?DocID=21686&la=1&langue=EN
[24] T. Khaled: "An Outsider looks at Friction Stir Welding", Report # ANM-112N-05-06, July 2005
[25] M. Eboo, W. M. Steen, J. Clarck, Proc. Conf. Advances in Welding Processes, Harrogate, UK, 9-11 May 1978, pp. 257-265
[26] H. Staufer, M. Rührnößl, G. Miessbacher: "LaserHybrid welding and LaserBrazing: state of the art in technology and practice by the examples of the Audi A8 and VW-Phaeton", Fronius International GmbH (2003)
[27] ALUWELD (IWT 30909): "Innovative welding of aluminium alloys – Friction Stir Welding and Hybrid Laser Welding", 2004-2005 – collective research project funded by IWT (Flanders)
[28] ARCLASER (Convention n°816943): "Soudage hybride arc-laser de métaux pour une flexibilité et productivité accrues", 2009-2011 – collective research project funded by DG06 (Walloon Region)
[29] C. Wiesner et al.: "Joining and Near-Net Shape Manufacturing processes", presentation at www.specialmetalsforum.com/doc/download/7

[30] http://lyle.smu.edu/rcam/rcamweb/fswrp.htm
[31] H. Aydın, A. Bayram, I. Durgun: "The effect of post-weld heat treatment on the mechanical properties of 2024-T4 friction stir-welded joints", Materials and Design 31 (2010), pp. 2568-2577
[32] Kh. A. A. Hassan, A. F. Norman, D. A. Price, P. B. Prangnell: "Stability of nugget zone grain structures in high strength Al-alloy friction stir welds during solution treatment", Acta Materialia 51 (2003), pp. 1923-1936
[33] A. Scialpi, M. De Giorgi, L. A. C. De Filippis, R. Nobile, F. W. Panella: "Mechanical analysis of ultra-thin friction stir welding joined sheets with dissimilar and similar materials", Materials and Design 29 (2008), pp. 928-936
[34] N. J. Teh: "Small joints make a big difference", Connect No. 143, July/August 2006, p. 1
[35] T. Nishihara, Y. Nagasaka: "Development of Micro-FSW", Proceedings of the 5th International Symposium on Friction Stir Welding, Metz, France, 14-16 Sept. 2004
[36] A. P. Reynolds: "Mechanical and Corrosion Performance of TGA and Friction Stir Welded Aluminum for Tailor Welded Blanks: Alloys 5454 and 6061", Trends in Welding Research 1998, Pine Mountain, GA, pp. 563-567
[37] G. S. Frankel, Z. Xia: "Localized corrosion and stress corrosion cracking resistance of friction stir welded aluminum alloy 5454", Corrosion 55 (2) (1999), pp. 139-150
[38] D. A. Wadeson, X. Zhou, G. E. Thompson, G. Scamans, L. D. Oosterkamp: "Corrosion control of Friction Stir Welded AA5754 aluminium alloy", 207th ECS Meeting, MA2005-01, May 15-May 20, 2005, Quebec City, Canada
[39] http://www.fronius.com/cps/rde/xbcr/SID-57BBD94F-00273BC2/fronius_international/7042_cmt_the_new_revolution_in_digital_gma_welding_85643_snapshot.zip
[40] A. Scialpi et al.: "Mechanical analysis of ultra-thin friction stir welding joined sheets with dissimilar and similar materials", Materials and Design 29 (2008), pp. 928-936
[41] P. L. Threadgill et al.: "Friction stir welding of aluminium alloys", International Materials Reviews, (2009)
[42] D. Fersini et al.: "Fatigue behaviour of Al2024-T3 friction stir welded lap joints", Engineering Fracture Mechanics 74 (2007), pp. 468-480
[43] P. A. Colegrove et al.: "Development of the Trivex™ Friction Stir Welding Tool for making lap welds". In: Fifth International Symposium on friction stir welding (2004), Metz, France
[44] R. Nandan et al.: "Recent Advances in Friction Stir Welding – Process, Weldment Structure and Properties", Progress in Materials Science 53 (2008), pp. 980-1023
[45] G. Shannon, Industrial Laser Solutions, April 2009, pp. 11-14
[46] wim.vanhaver@bil-ibs.be
[47] Kallee et al.: "A preliminary recommendation on harmonising welding procedure specifications to accelerate the industrialisation of friction stir welding", Eureka project EUROSTIR®, TWI, 2003
[48] Midling O. T., Morley E. J., Sandvik A.: "Friction stir welding", European Patent Specification 0 752 926 B1
[49] Thomas W. M., Nicholas E. D., Needham J. C., Murch M. G., Temple-Smith P. and Dawes C. J.: "Improvements relating to friction welding", European Patent Specification 0 615 480 B1
[50] Iain J. Smith, Daniel D R Lord: "FSW Patents – A Stirring Story", poster during 7th International FSW Symposium, 20-22 May 2008, Awaji, Japan
[51] Iain J. Smith, Intellectual Property Manager, The Welding Institute, Granta Park, Great Abington, Cambridge, CB21 6AL, United Kingdom
[52] http://www.twi.co.uk/binary/FSWPatents.xls